NASA CR 54366
CER65VAS-REB12a

REVIEW OF LITERATURE

SECONDARY ELECTRON EMISSION

by

R. E. Bunney

prepared for

NATIONAL AERONAUTICS AND SPACE ADMINISTRATION

December 31, 1964

GRANT Na G-570

Technical Management
NASA Lewis Research Center
Cleveland, Ohio
Electric Propulsion Office
John Ferrante

Fluid Dynamics and Diffusion Laboratory
College of Engineering
Colorado State University
Fort Collins, Colorado

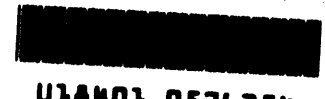

U18401 0576354

SECONDARY ELECTRON EMISSION

by

R. E. Bunney

SUMMARY

This report has been two-fold in purpose:

1. To review the available literature on secondary electron emission and to consolidate the general results of previous experiments with adaptability to the present research underway at Colorado State University.

2. To consolidate under one cover the basic theories of secondary emission and to attempt to trace the connections between them noting the deficiencies of each.

Due to the large number of independent publications on this subject, review articles have been utilized to the utmost. For the basic theories however, the original publications were consulted. The bibliography lists all of the articles reviewed, however many of them were not credited specifically in the report as the review articles were the principle references cited.

It is realized that many publications have been omitted entirely. However, most of these serve as refinements of the basic theories and should be included only in reports of broader scope than is outlined under (2) above. Thus, the theory as presented in this report is not complete in all aspects, however it compares approaches of the principal investigators and considers the deficiencies of each. Special emphasis has been placed on quantum theory as the author believes that this approach is the best method of gaining physical insight into the mechanism of secondary emission, whereas classical theories give empirical information only.

INTRODUCTION

The phenomenon of secondary emission has been actively investigated since its original observation by Austin and Starke in 1902. Many theories have been formed since that time and much experimental evidence has been gathered on their behalf. These theories range from relatively simple empirical treatments to highly complex quantum mechanical investigations with side investigations into surface phenomena, crystal formation, diffusion theory and others.

First investigations of the secondary emissions process indicates a very straightforward approach. Primary electrons bombard the surface of a material where, by certain physical mechanisms, electrons are caused to leave the material. One need merely to measure the number of so-called "secondary electrons" per second from a unit area on the surface as a function of their energy (E), and their direction (θ), i.e., measure $j(E,\theta)$; and construct a theory to satisfy these results. This was the emphasis of the early investigators; however, to completely understand the mechanism of secondary emission within the material more advanced and complicated approaches must be made. One author [4] diagrams the scheme of secondary emission as is shown in Fig. 1.

This process is roughly as follows: (1) The primary electron beam impinges upon the surface of the material where it interacts with the surface barrier and is split into two parts, a) those which are reflected and b) those which penetrate the surface; (2) The electrons penetrating the surface interact with the nuclei and electrons of the material and are thus distributed by elastic collisions with the nuclei and energy is lost through interaction with the electrons. The collisions cause the beam to be split again into various directions, some of which are back toward the surface. These reflected primaries will also produce secondaries, part of which will escape into free space. (3) The interactions of the primary electrons and the material

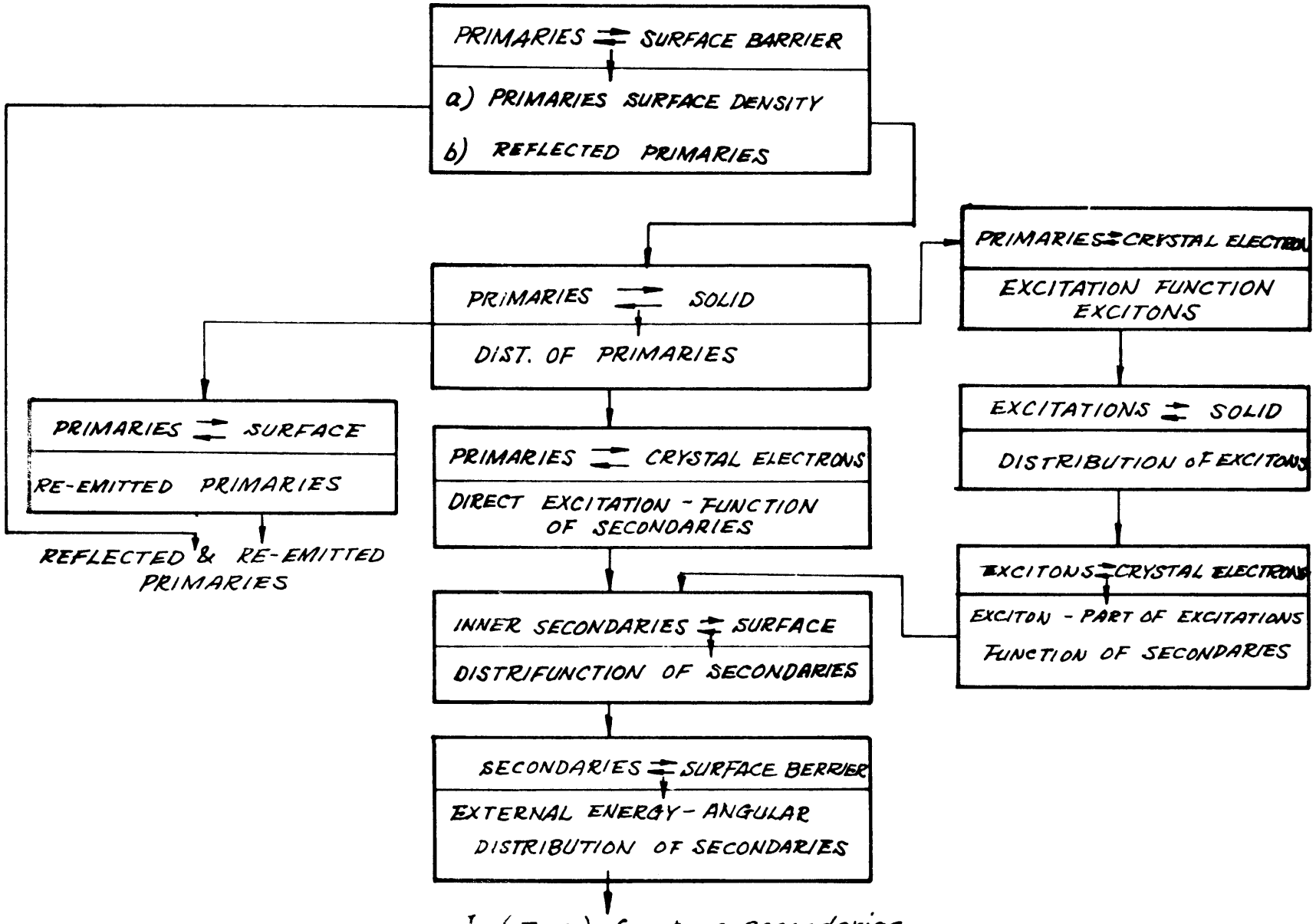

Fig. I Scheme of the secondary-emission process.

electrons will cascade through the material each causing further interactions or scattering of which a finite number of electrons will eventually reach the surface and escape.

I. Experimental Results

A. Measurement Results - The problems involved in measurement of properties of secondary emission are essentially the same as those encountered in electron optics. The electrons are emitted over the entire solid angle, therefore it is necessary to collimate the secondaries and then focus them for detection. Another technique is the use of a retarding field. In this method, the electrons when emitted from the material are subjected to a retarding field prior to being collected. Therefore, only those electrons with sufficient energy to overcome this field arrive at the collector. An inherent problem of this method is subtracting the effects of tertiary electrons at the collector surface. If, however, the collector is large relative to the emitter and the energy of the tertiary electrons is sufficiently small, their effect is negligible. This type of device is shown in Fig. 2. If the energy distribution is given by F(E), the secondary current is

$$i_s = \int_{ev_s}^{\infty} F(E)dE \tag{1}$$

so

$$F(E) = -\frac{di_s}{d(E_s)} \tag{2}$$

The device in Fig. 2 measures all electrons emitted into the sphere. It is possible to segment this sphere in order to determine angular distributions. Other methods have been devised to measure secondary emission energy distributions. Two of these use magnetic fields. These devices are diagrammed in Figs. 3 and 4. In the former, the secondary electrons are

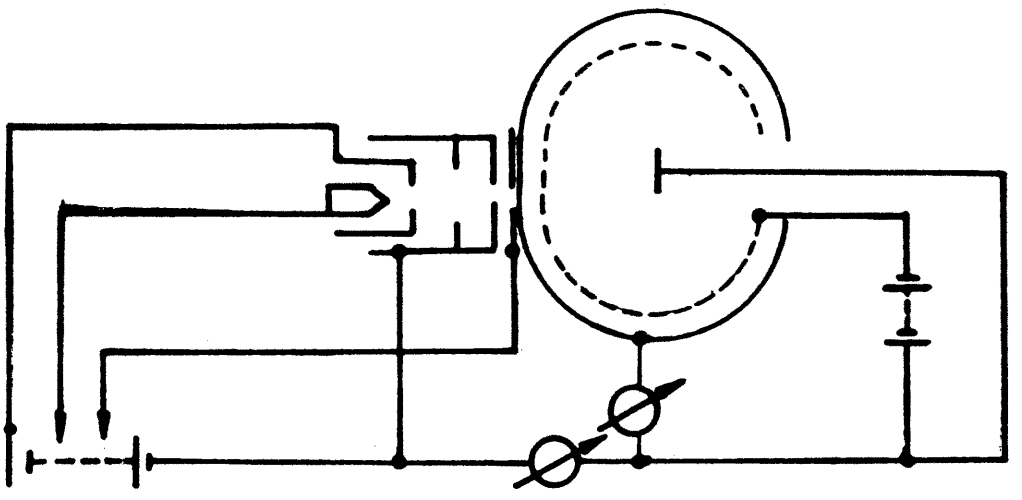

Fig. 2 Device to measure secondary emission by retarding field method [4]

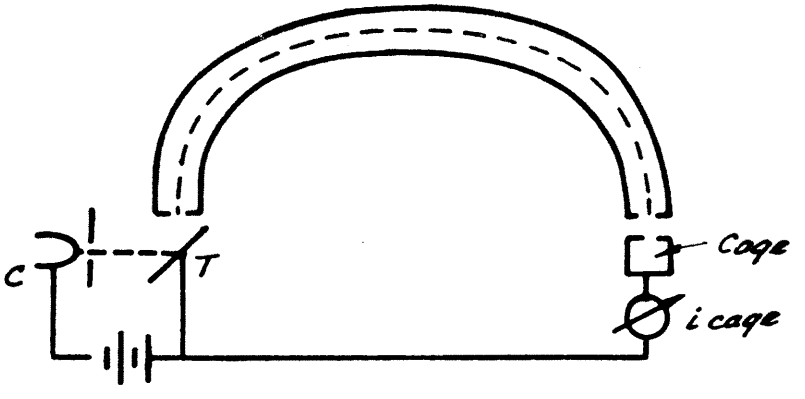

Fig. 3 Device to measure secondary emisson by transverse magnetic field method

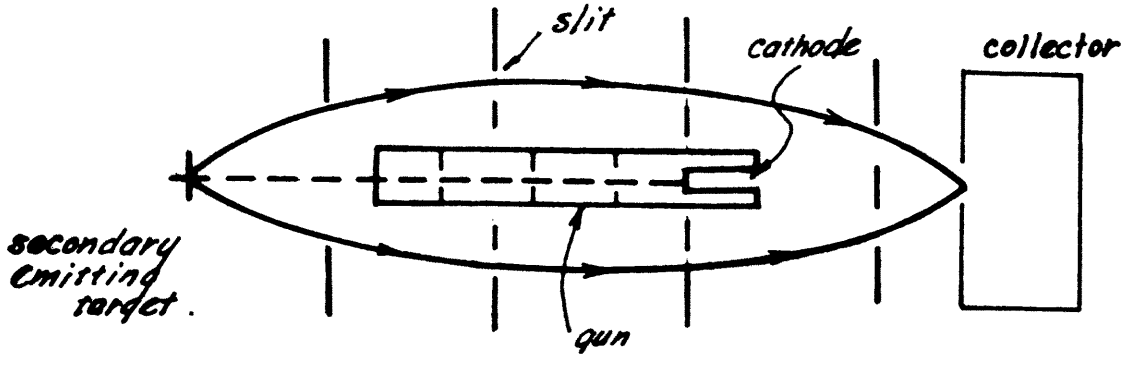

Fig. 4. Device to measure secondary emission by longitudinal magnetic field method [3]

deflected by a transverse homogeneous magnetic field forcing the electrons into a circular path similar to mass spectroscopic methods. Then, if B = Magnetic field, v = velocity of the particle and r = radius of the path;

$$B \cdot \frac{e}{m} \cdot r = v \tag{3}$$

The current at the collector as a function of B is given by

$$i_c = \phi(v)\, \Delta v \tag{4}$$

where $\phi(v)$ = velocity distribution of the secondary electrons. The velocity interval Δv determined by the collector aperature Δr by the relation

$$\Delta v = B \frac{e}{m} \Delta r \tag{5}$$

then, eliminating Δv from (3) and (4)

$$\phi(v) = \frac{i_c}{vf} \tag{6}$$

where $f = \frac{\Delta r}{r}$ is a constant of the apparatus. The main problems involved with this device are the required complexity and size.

The apparatus shown in Fig. 4 uses a longitudinal magnetic field. This device uses the principle that if a point source emits electrons with the same energy all at the same angle to the lines of force of a homogeneous magnetic field, the electrons will focus again at a point. The distance from the image point to the point source is proportional to the velocity of the electrons and inversely proportional to the magnetic field. This device is then a velocity filter in the same sense as the previous one.

A transverse electric field has been used by Harrower [30] for measuring the energy distributions of secondary electrons. This device uses a 127.2^0 cylindrical electrostatic condenser. The electron beam is focused on a slit after deflection. The energy distribution is obtained from the current at the collector divided by the electric field E.

B. Precautions to be Taken During Measurement - The most important points to be observed during measurement are:

1) The secondary electrons must not be subjected to stray magnetic or electric fields from the point of emission to the collector.

2) Space charge in the field free region must be avoided at all cost unless of course it is desirable to determine the effects of such a condition.

3) The contact potentials of the electrodes must be known.

4) All measurements must be made in vacuum such that the mean-free-path is long compared to the vessel. Scattering of the secondary electrons by a residual atmosphere will result in questionable results.

5) The condition of the emitter surface is of prime importance. Here, cleanliness is definitely a virtue. Impurities absorbed on the surface even in monomolecular layers may falsify the results through variations in the work function.

C. Energy Spectrum - If the number of secondary electrons with energy between E and $E + \Delta E$ is plotted against E, a typical spectrum results. This spectrum is shown in Fig. 5. As is shown, this curve may be divided into three distinct regions. The first of these (I) is the region of the primary energy E_p. These are generally considered to be the elastically reflected primaries. The second region falls between approximately 50 ev energy and E_p. This region has the characteristic shape of the spectrum of an electron beam passed through a thin film. These are generally assumed to be composed of inelastically reflected and rediffused primaries. Last, the region of the curve below 50 ev (III) represents true secondary electrons emitted from the material surface. It is these electrons that are of primary interest here. It should be pointed out however, that not all electrons with energies < 50 ev are secondaries. It is entirely possible for some rediffused primaries to fall in this energy range but this is offset by the equal possibility of secondaries having energies > 50 ev.

D. Yield - The yield, defined as the ratio of the secondary current to the primary current, i.e., $\delta = \frac{i_s}{i_p}$, as a function of primary energy (E_p)

is probably the most investigated phenomenon of secondary emission. The plot of δ vs E_p is shown in Fig. 6 and is the same general shape for all materials. It is assumed that the primaries are incident normal to the surface. Alterations to this curve due to primary electron impingement at other than normal incidence will be discussed later. For low E_p, δ is much less than unity and increases to a maximum $\delta(max) > \delta = z$ for pure metals as some $E_p = E_p(max)$ at a few hundred ev and then slowly decreases as E_p is further increased. Since these curves are so similar authors often specify only $\delta(max)$ and $E_p(max)$ when reporting results of experimentation. Impurities in the metal or adsorbed on the surface greatly affect the results of this measurement. Much effort has been expended in producing cleaner surfaces to determine δ more accurately. Some investigators [3] have utilized extensive baking processes. This method of surface decontamination is effective to gain reproducible values of δ, however the data is somewhat questionable in many cases due to the possibility of recrystallation and surface oxidation. Bruining [1] and others have attempted to overcome this deficiency by using thin films. Recently some researchers [3] have used single crystals of the material of interest contending that these represent the highest form of purity possible. Even if clean surfaces could be obtained, the yield would be radically affected by surface irregularities. Therefore, the data obtained on the yield will vary from author to author. Table 1 represents what is believed to be the best available results. The values of $\delta(max)$ are accurate to approximately 10 percent, however due to the difficulty in determining the peak for a wide maximum, therefore the values of $E_p(max)$ may vary greatly from those presented.

E. Correlation of $\delta(max)$ and Work Function - McKay [3] has attempted to correlate the maximum yield and work function (Fig. 7). He admits that, since the surface conditions of these materials and crystal orientation was not known, the result has a certain amount of unreliability. However, this approach does show certain interesting relationships. As seen from Fig. 7, there appears to be a tendency for materials with high work functions

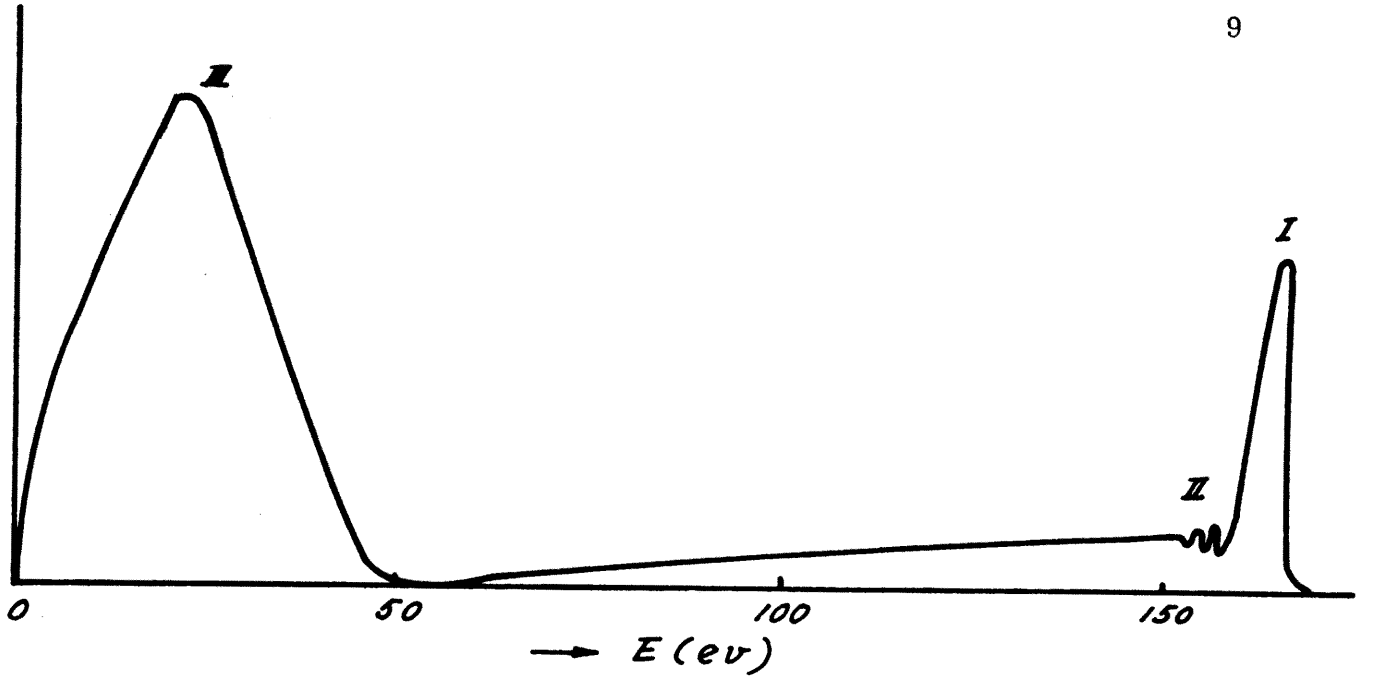

Fig. 5 Typical Energy distribution of secondary electrons [3]

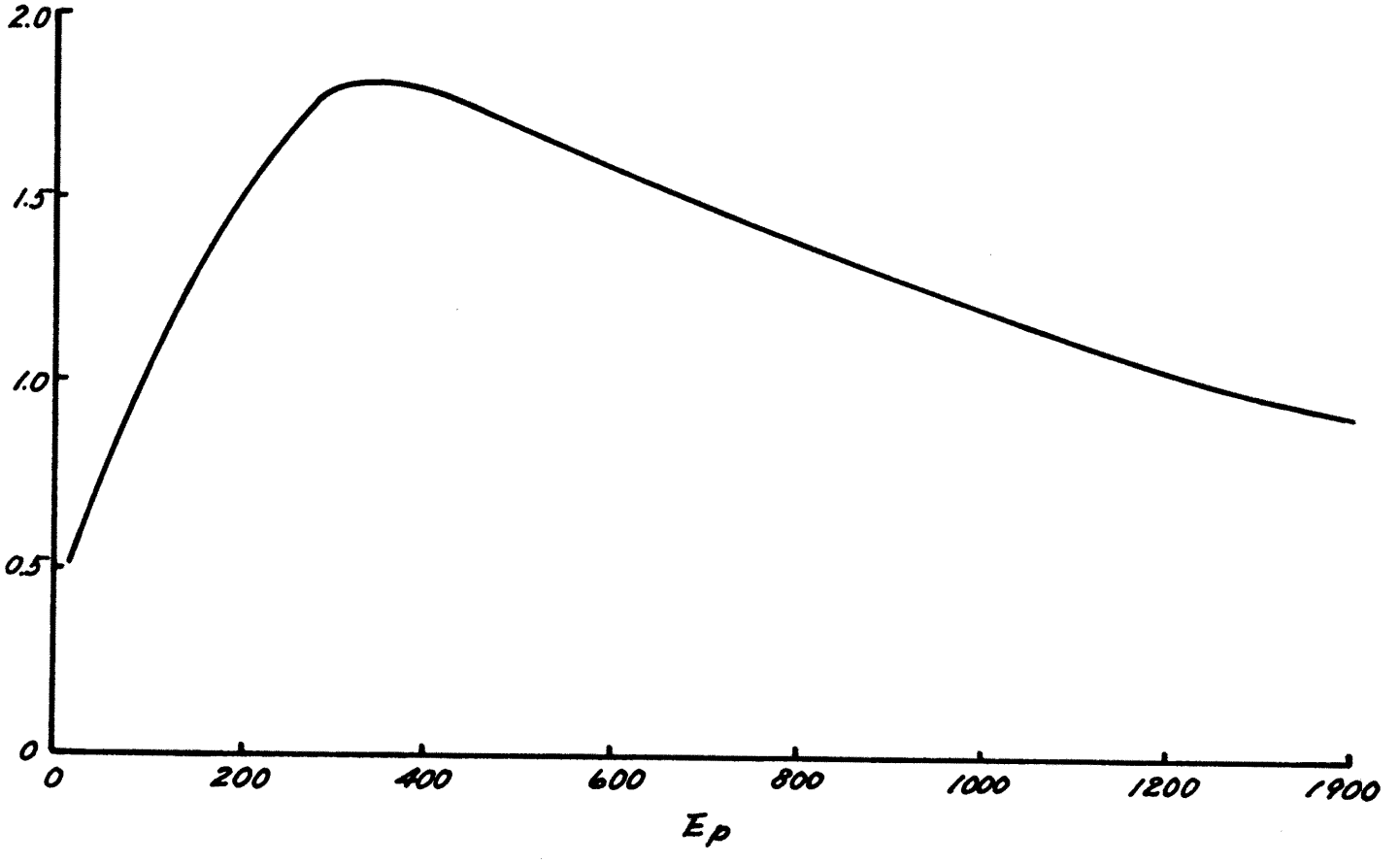

Fig. 6 Typical yield vs. primary energy curve [3]

to have high yields, however the inference should not be made that increasing the work functions will increase the yield. Often the inverse statement would be more reliable. In fact, as McKay points out, nearly as reliable data may be obtained by plotting δ(max) against the density of the target. Bruining performed this correlation and found that δ(max) had a tendency to increase with the density of the materials. Sternglass attempted also to correlate δ(max) with the position of metals within the periodic system of elements. He found that the yield rises in each horizontal line from the alkalies to the multivalent metals.

F. Normalized Yield - If for a given set of δ vs E_p curves, each δ is divided by δ(max) and each E_p divided by the respective E_p(max), the curves are said to be normalized. From this normalization a unique data pattern results. Baroody [52] first demonstrated this to show that the dependence of the yield on primary energy was the same for all metals. Presented in this form, the curves for different metals lie in a narrow range so that the representation is nearly a universal yield curve for all metals, (Fig. 8). This phenomenon will be considered in more detail in the theory section of this report.

G. Effects of Temperature on Secondary Emission - Most investigators agree that true secondary emission in metals is independent of the temperature of the emitter surface. Certain complications do occur however, since changes in temperature will change the density of gas adsorbed and could possibly change the crystal structure of the surface. Also, for high enough temperature, there should be contributions due to Richardson electrons. This should be contrasted with the effect of temperature on the secondary emission of insulators. Evidence indicates that there is an inverse relation between temperature and yield.

H. Angular Distribution of Secondary Electrons - Considering only electrons with energy < 50 ev, i.e., neglecting reflected primaries, researchers agree that most secondaries emerge normal to the surface and the number decreases with increasing angle of emergence. This indicates a

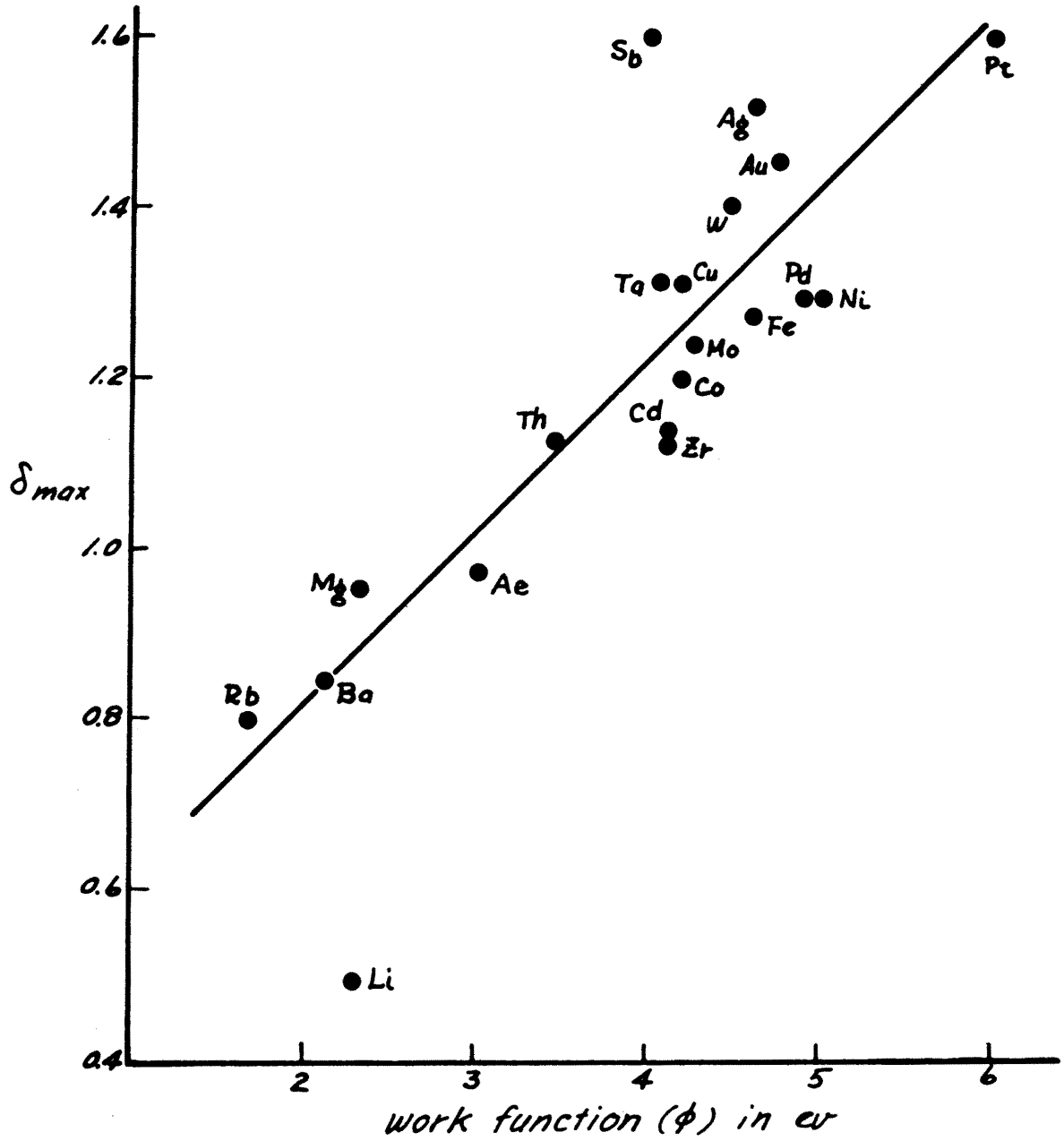

Fig. 7. Relation between δ_{max} and work function of different targets [3]

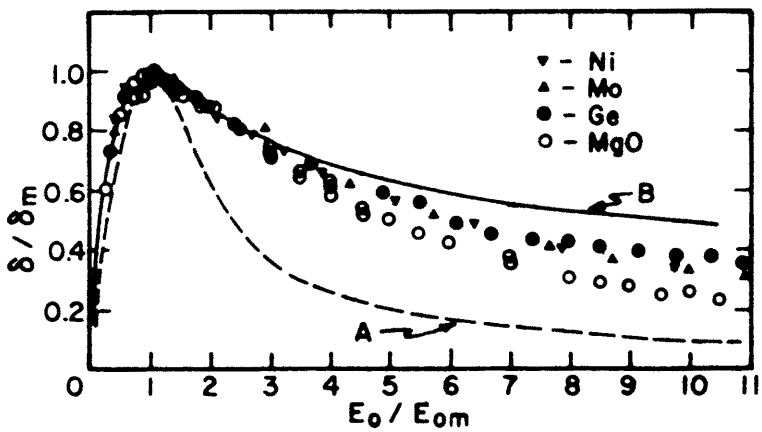

Fig. 8 Reduced yield curves for Ni;[20] Mo;[20] Ge;[23] and MgO.[46] Curve A represents Baroody's equation (6.10) Curve B represents Eq. (7.3) for n = 1.35.

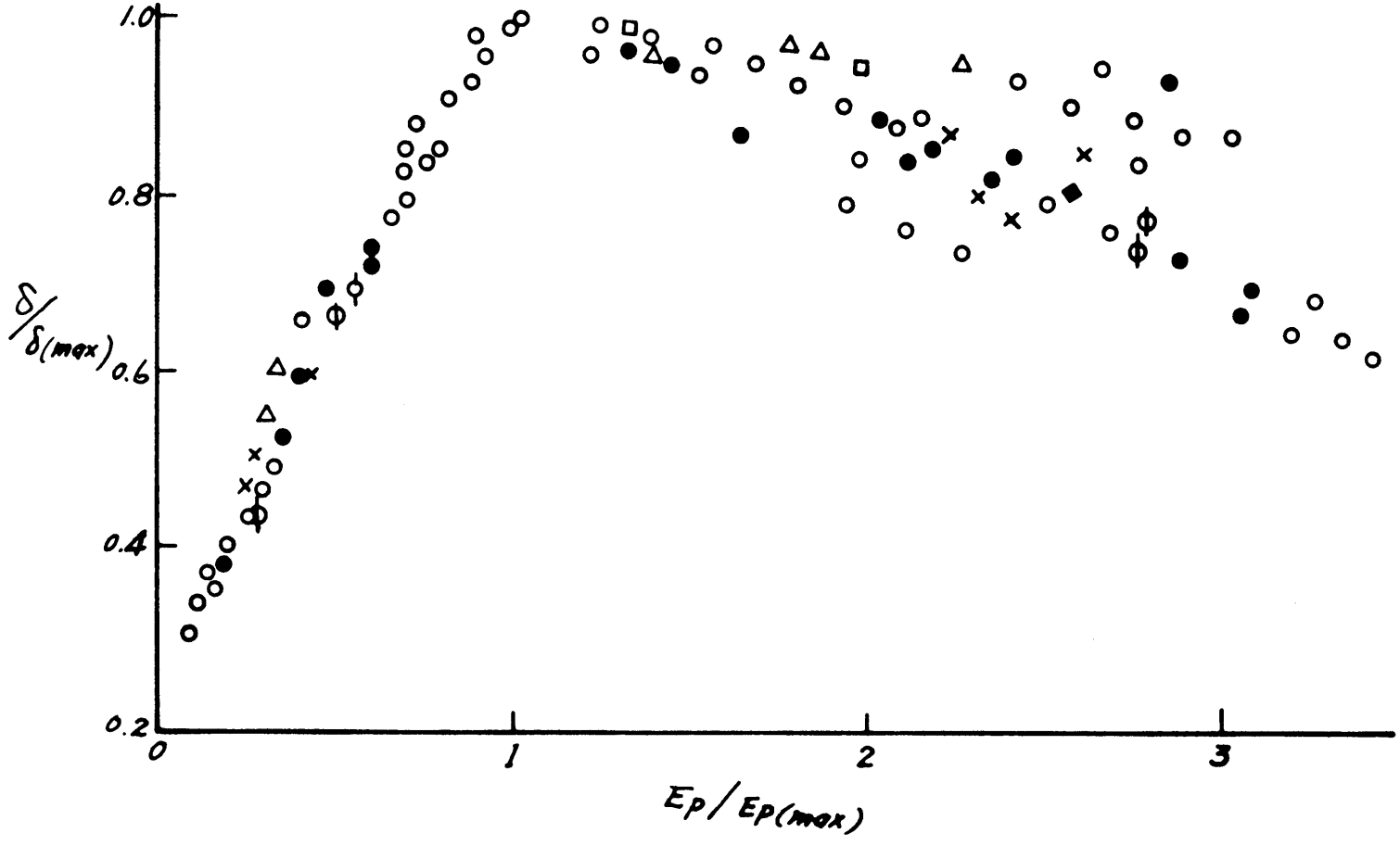

Fig 8a Typical normalized yield for different metals

Table 1. Maximum Secondary Emission Yields of Various Clean Metals. (Partial Table from K. G. McKay, Advances in Electronics, Academic Press, Vol. 1, p. 68, 1948.

Element	δ(max)	V_p(max) Volts
A_g	1.5	800
A_ℓ	1.0	300
A_n	1.46	800
B_a	0.83	400
B_ℓ	0.6	200
C	1.0	300
C_d	1.1	400
C_o	1.2	600
C_s	0.72	400
C_u	1.3	600
F_e	1.3	200
K	0.7	350
Li	0.5	85
Mg	0.95	300
M_o	1.25	375
N_b	1.2	375
N_i	1.3	550
P_d	1.3	250
P_t	1.6	800
R_b	0.9	350
T_h	1.1	800
T_i	0.9	280
W	1.4	600
Z_r	1.1	350

cosine law distribution. This relationship may vary for very low primary energies. This could be caused by variation of penetration depths and reflected beam density respectively. Faris [76] has derived an angular distribution relationship which depends upon the ratio of the propogation constant of the electron within the surface to that in free space. When this ratio approaches zero the distribution function reduces to a direct cosine law. This relation appears to be independent of the angle of incidence of the primary beam whereas, as will be shown later, the total yield is not. The cosine law distribution is not surprising since most electrons emitted at large angles of emergence are required to traverse a longer path length within the material and therefore, are more likely to be scattered or absorbed than those emitted normal to the surface.

I. Effect of Angle of Incidence of Primary Electrons [3] - The effect of oblique angle of incidence may be seen in Fig. 9 where R is the average range of a primary electron into the material. For primaries striking the surface at other than normal incidence, their penetration depth normal to the surface is only R cos θ while at normal incidence it is R. Therefore, secondaries produced at the end of the path have much less chance of being absorbed before reaching the surface and will in general have greater energy for penetrating the barrier at the interface than those coming from a greater depth or those produced by a primary beam normal to the surface. Bruining [1] has shown experimentally that for low primary velocities, i.e., for low penetration, there is very little variation in the yield with angle of incidence. He has also shown that a rough etched surface shows no angle of incidence dependence which is not too surprising due to the inhomogeneity of the orientation of the surface normal. Bruining derived the expression

$$\delta_\theta = \delta_o e^{\alpha x_m (1-\cos\theta)}$$

where

δ_θ = yield at angle of incidence = θ

δ_o = yield at angle of incidence = 0

x_m = mean depth of liberation of electrons

α = coefficient of electron absorption

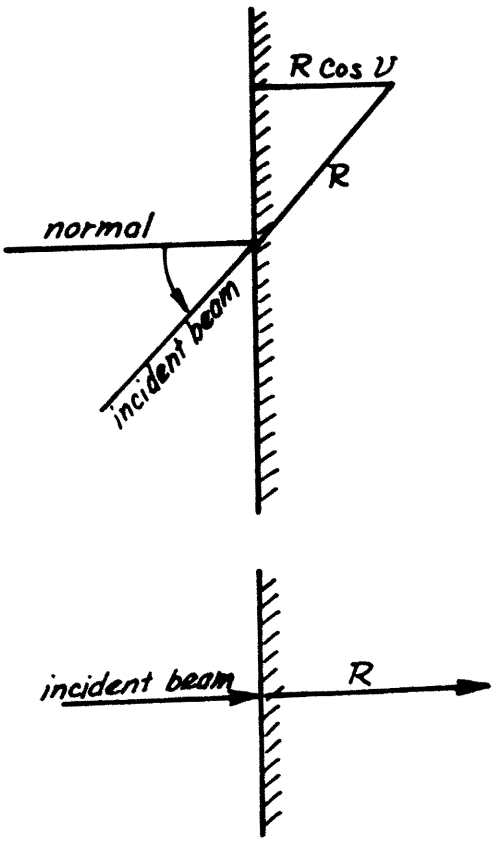

Fig. 9 Dependence of path length on the angle of incident primary electrons. [3]

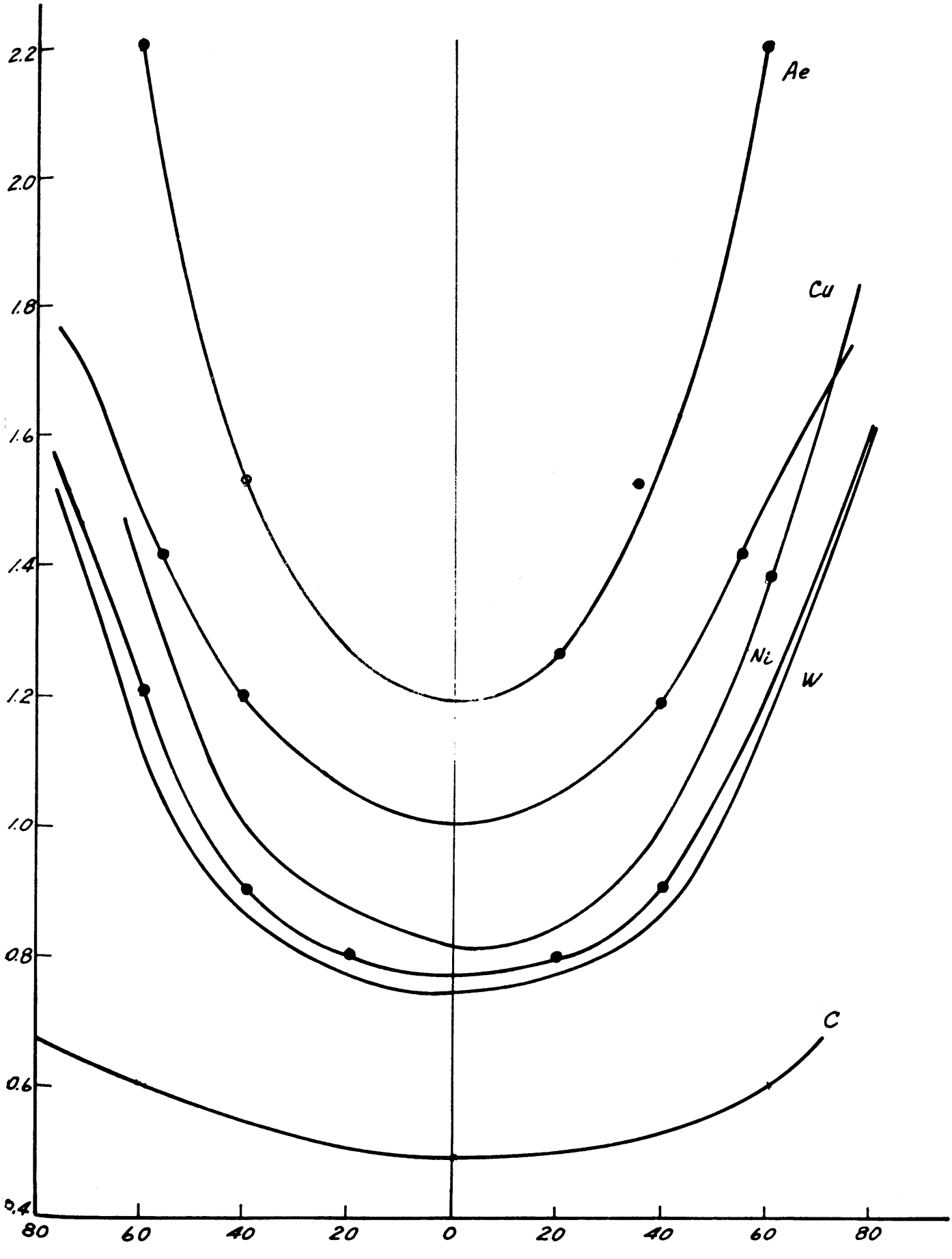

[1]

Fig. 10 Secondary emisson yield vs. angle of incidence primary electrons

by assuming an exponential absorption-with-distance relationship (see theory). This law would indicate a maximum at $\theta = \pi / 2$ since there is no absorption of secondaries. However, as McKay [3] points out, there is a broader maximum at a much higher E_p than for primaries incident at $\theta = 0$. This is attributed to the scattering of primary electrons into the surface of the material thus producing some secondary absorption.

J. Effect of Primary Current on Yield - It has been confirmed by many investigators under widely varying conditions that the yield is independent of the primary current density. Theoretical consideration confirm these results.

K. Surface Effects - As was indicated earlier, the condition of the surface has great bearing on secondary emission. Considerable experimental evidence indicates that a rough or porous surface lowers the secondary electron yield. At least one author [3] compares a rough surface to a series of holes or wells. A secondary electron, produced in the bottom of the well can get trapped on the sides and hence be prevented from being emitted at the surface.

Such a surface may be prepared artificially for investigation by covering the target with carbon soot either smoked on or prepared from a colloidal system or, by evaporating various metals on the surface through a rare gas atmosphere so that metallic agglomerates are formed before striking the target surface. Bruining [1] shows that the reduction in yield occurs when the carbon granules are approximately 30^0A in diameter.

Much investigation has been performed to determine the effects of depositing metals on the target surface [3]. Most results show a decrease in the work function, with a maximum occurring coincidentally with the attainment of an optimum layer thickness for minimum work function. Sixtus and Trelaar obtained the relation $\delta = e^{A-b\phi}$, (where A and b are constants for a given metal) for the dependence of the yield on the work function. This equation appears to be a good representation in agreement with most experimental data and theories. The work function however, plays a relatively minor role. McKay showed that an adsorbed layer of

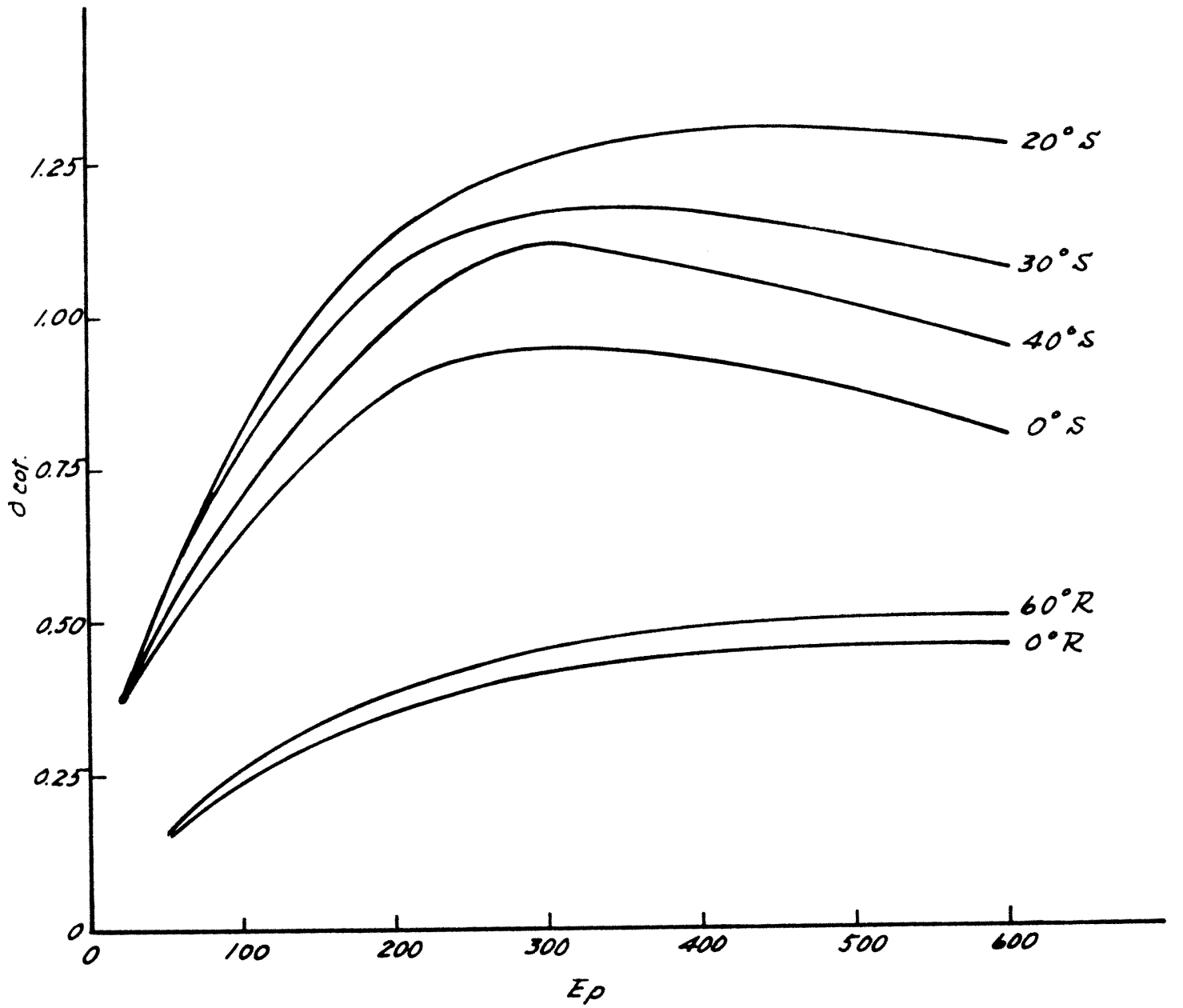

Fig. 11 Typical secondary emission δ vs. Ep for different angles of incidence
S = smooth surface, R = Rough surface [2]

sodium on tungsten increased the yield by 60 percent while decreasing the work function by a factor of 2. This roughly agrees with Trelors results of $\left(-\frac{\partial}{\partial\phi}\right)(\ell n\ \delta max) \sim 0.12\ ev^{-1}$. However, in thermionic emission a similar decrease in the work function would increase the current by a factor of 10. It therefore, seems unlikely that high yields can be obtained by uniquely varying the work function of the material.

Becker and Nichols [3] demonstrated the dependence of the effect on the yield of the orientation of the exposed crystal face. The magnitude of this effect may be estimated by assuming Trelor's result for variation of the work function for tungsten and using Nichol's data showing that the work function varies from 4.35 volts for the (111) crystal direction to at least 4.65 for the (110) direction. This gives a variation in δmax, of approximately 3 percent. Other researchers have done extensive work on this problem and all report that any given face of a crystal exhibits a characteristic yield. However, care should be taken when trying to correlate this information to experimental results, as a given substance need not necessarily exhibit all crystalline faces to the surface with equal probability. On the contrary, unless the experiment is precisely designed to locate a given lattice plane, the probability of the surface being inhomogeneous as to orientation of crystal faces is high.

The last topic to be covered under surface effects is that of adsorbed gas. We would expect a similar effect for adsorbed gas as was found for metals deposited on the surface. However, an adsorbed gas layer may also contribute significantly to the yield. Data reveal that monoatomic layers of adsorbed gas on target surfaces probably have a yield of approximately 0.02 for $E_p \sim 200$ volts, thus indicating that the variation for layers of this thickness are primarily due to the variation of the work function. Most reports attempt to correlate yield as a function of heat treatment. This data is usually unreliable as secondary effects may alter the emission mechanism, i.e., alter the crystal structure. Also, when gas layers are being removed it is extremely difficult (if not impossible)

to distinguish thickness and uniformity of remaining layers. Finally, the surface may become oxidized which will give unreliable data as oxygen on the surface will give erratic results due to the formation of an electrical double layer. Further, heating of the surface will not eliminate this problem either as oxygen may not be removed by heat treating alone.

L. Range of Primary Electrons - The range of the primary electron is defined as the distance into the material at which the average energy per unit path length $\frac{-dE_p}{dx}$ vanishes. Early investigators assumed Whiddington's law (see theory) and fast electrons to measure the range. These results were introduced into empirical theories as an attempt to approximate experimental data. Recently Young [73, 74] studied the penetration of primary electrons of energy $0.5 \text{ ev} < E_p < 11 \text{ kev}$ in $A\ell$. His results are shown in Fig. 12. These results confirm the Whiddington law for $E_p > 8.5$ kev. However, for $E_p < 8.5$ kev he found that the range was proportional to $E_p^{1.3}$ and thus proved that Whiddington's law was not valid in this range. Similar measurements on $A\ell_2O_3$ films concur with the above results. He found that for energies $0.3 \text{ kev} < E_p < 7.25$ kev the range was given by

$$R = 0.0115\, E_p^{1.35} \tag{8}$$

Other investigators [75] found that for $A\ell_2O_3$, the range was proportional to $E_p^{1.66}$. Therefore, in the range of interest, we must conclude that Whiddington's law is invalid in that the exponent on the primary energy must be replaced by a number on the order 1.5.

M. Time Lag of Secondary Emission - The secondary emission process as defined earlier consisted of penetration of the surface by a primary electron, the production of secondary electrons and the rediffusion of these secondary electrons back to the surface. It is only reasonable to assume that there is a finite time interval between the initial primary electron striking the surface of the material and the emission of the first secondary electron. One also expects a time interval between the time the first and last secondary, caused by a single primary, is emitted from

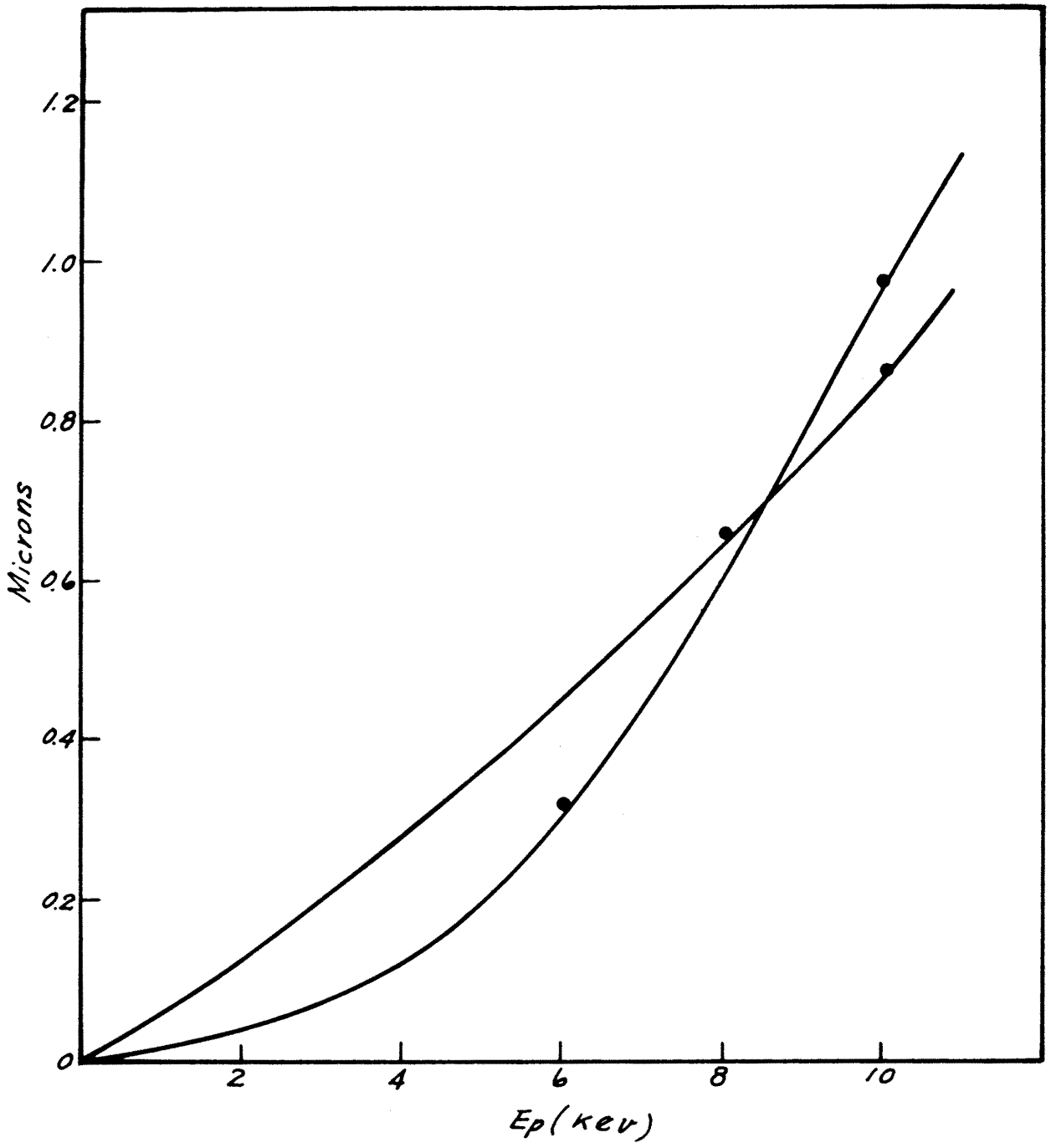

Fig. 12. Practicle range (R) Vs electron energy in aluminum [4]

the surface. Most authorities [2] have found that the upper limit of this time lag is of the order of magnitude of 10^{-11} sec. with perhaps 10^{-12} or 10^{-13} sec. being more realistic.

N. Secondary Electron Emission at the Melting Point and Curie Point - There appears to be little or no change occurring in the yield of the Curie point. The data available with regard to the melting point indicates that the yield increases; however, the results are inconclusive and incomplete. This may be one area for further investigation.

O. Backscattering of Primary Electrons [2] - The number of back-scattered electrons per incident primary η has been investigated by many researchers. Results indicate that for primary energies > 2 kev, that η varies with the atomic number Z. For energies < 2 kev and $Z \leq 30$ Sternglass [54] showed that η is nearly independent of Z and elements with $Z \gtrsim 30$, η decreases with decreasing primary energy. Thus, for $E_p < 2$ kev and $Z \geq 30$, η may fall below that of those with $Z \lesssim 30$. Sternglass then argues that on the basis of inelastic scattering theory an element of high Z may have a smaller number of electrons available for inelastic scattering than an element of low Z.

P. Fine Structure of the Velocity Distribution in Metals [2] - In addition to the general shape of the curve for the energy distribution, Haworth [70] finds secondary maxima for $_{42}Mo^{96}$ at 11, 24, and 26 ev. These maxima are thought to be associated with the emission of auger electrons. Lander and Hagstrum [39] have observed and investigated this phenomenon.

II. Theoretical Considerations

A. Semi-Empirical Theory [2] - Several investigators have attempted to treat the theory of secondary emission empirically. It is found that although these theories give good agreement with experiment they all have major deficiencies, particularly in explaining the true

mechanism of the secondary electron emission process. This theory also cannot predict the magnitude of the yield for a given material and does not provide a basis for a discussion of the energy distribut ion of the secondary electrons. Hence, for the purposes of this report these theories will be grouped together as the semi-empirical theory.

These investigators basically start from the expression for the yield

$$\delta = \int n(x, E_o)\, f(x)\, dx \tag{9}$$

where $n(x, E_o)$ is the average number of secondaries produced per incident primary in a layer of thickness dx at the depth x in the material. $f(x)$ is the probability of escape from the surface. Usually, the following assumptions are made:

a) That a definite distinction between the production mechanism and the emission processes may be made, i.e., that these processes are completely independent phenomena.

b) That only the number of secondaries need be considered and the energy distribution of the interanl secondaries may be completely ignored.

c) The escape mechanism is described by an exponential law without giving any consideration to the physical process involved.

d) The number of secondaries is proportional to the energy loss per unit path length of the primary electron.

Then, from the above assumptions

$$f(x) = Be^{-\alpha x}$$

$$n(x, E_o) = -\frac{1}{\epsilon}\frac{dE}{dx} \tag{10}$$

where α = absorption coefficient and B and $\frac{1}{\epsilon}$ are the proportionally constants.

So (9) may be written

$$\delta = -\frac{B}{\epsilon}\int \left(\frac{dE}{dx}\right) e^{-\alpha x}\, dx \tag{11}$$

All the semi-empirical theories involve variations of this relation.

Power Law[2] - This law assumes that

$$\frac{dE}{dx} = -\frac{A}{E^{n-1}} \tag{12}$$

which can be integrated to

$$E^n(x) = E_p^n - Anx \tag{13}$$

This expression is the celebrated Whiddington's law for the case $n = 2$.

The range of the particle may be found by setting $E^n(x) = 0$ or,

$$R = \frac{E_p^n}{An} \tag{14}$$

For purposes of integration, substitute

$$y^n = \alpha(R-x) \tag{15}$$

Then,

$$\delta = \left(\frac{B}{\epsilon}\right)\left(\frac{An}{\alpha}\right)^{1/n} e^{-\alpha R}\int_0^{y_m} e^{y^n}\, dy \tag{16}$$

where $y_m^n = \alpha R$, i.e., where $x = 0$.

Since we are interested in the dependence of δ on E_p, introduce

$$r^n = \alpha R = \alpha\frac{E_p^n}{An} \tag{17}$$

so

$$\delta = \left(\frac{B}{\epsilon}\right)\left(\frac{An}{\alpha}\right)^{1/n} e^{-r^n}\int_o^r e^{y^n}\, dy \tag{18}$$

$$= \left(\frac{B}{\epsilon}\right)\left(\frac{An}{\alpha}\right)^{1/n} Gn(r)$$

Let $r = r_m$ be the value of r at the point that the yield is maximum, i.e., $\delta = \delta max$. Then, by maximizing (18), it can be easily shown that

$$\delta max = \left(\frac{B}{\epsilon}\right)\left(\frac{An}{\alpha}\right)^{1/n}\left(\frac{1}{nr_m^{\,n-1}}\right)$$

$$= \frac{B}{\epsilon}\left(\frac{An}{\alpha}\right)^{1/n} G_n(r_m) \qquad (19)$$

Thus, by division and substitution from (17) that $\frac{r}{E_p} = \frac{r_m}{E_{p(max)}}$

$$\frac{\delta}{\delta max} = nr_m^{\,n-1}\, Gn\left(r_m E_p / E_{p(max)}\right) \qquad (20)$$

$$= \frac{Gn(r_m E_p / E_{p(max)})}{Gn(r_m)}$$

which eliminates many of the unmeasurable constants. This theory shows that for a given value of n all materials demonstrate the same reduced yield curves. This says that $\delta/\delta max$ is a universal curve. For the particular case used by Bruining and Baroody, $n = 2$, i.e., they assumed Whiddington law, and found r_m to be 0.92 so

$$\delta/\delta_m = 1.85\, G_2\left(0.92\, E_p/E_{p(max)}\right) \qquad (21)$$

This curve is plotted in Fig. 13. It is obvious that there is a large discrepancy for values of E_p/E_{pmax} greater than 1. This would indicate that perhaps the value $n = 2$ was too high.

Young, doing experiments on the range of electrons in $A\ell_2 0_3$ (see experimental results) derived the expression (8)

$$R = 0.0115\, E_p^{1.35}$$

comparing this result with Eq. 14 indicates that perhaps n should be more of the order of 1.35. The curve of this assumption is also plotted in Fig. 13. It is noted that there is far better agreement with theory using this value of n.

Theory Including Primary Scattering [2] - Young [73, 74] predicts that primary scattering is important and that the end points of the individual primary paths are evenly distributed throughout the target. From this assumption he concluded that the energy dissipation is linear, i.e.,

$$-\frac{dE}{dx} = \frac{E_p}{R} \tag{22}$$

Then, making this substitution into Eq. 11,

$$\delta = \frac{B}{\epsilon} \frac{E_p}{R} \int_0^R e^{-\alpha x} \, dx$$

$$= \frac{B}{\epsilon} \frac{E_p}{\alpha R} (1 - e^{\alpha R}) \tag{23}$$

Assuming the energy-range question

$$R = \frac{E_p^n}{An} ,$$

$$\alpha R = \frac{\alpha}{An} E_p^n = z^n \tag{24}$$

Then,

$$\delta = \frac{B}{\epsilon} \frac{E_p}{\frac{\alpha}{An} E_p^n} \left[1 - e^{-\alpha R}\right]$$

$$= \frac{B}{\epsilon} \left(\frac{An}{\alpha}\right)^{1/n} \frac{1}{z^{n-1}} \; 1 - e^{-z^n}$$

$$= \frac{B}{\epsilon} \left(\frac{An}{\alpha}\right)^{1/n} g_{n(z)} \tag{25}$$

and, by a similar treatment as before,

$$\frac{\delta}{\delta_m} = \frac{g_{n(z_m E_p / E_{p(max)})}}{g_{n(z_m)}} \tag{26}$$

where $z_m = z$ for which $g_{n(z)}$ reaches a maximum using Young's exponent for E_p of $n = 1.35$ gives the curve shown in Fig. 13 for Young's theory.

Calculation of the Parameters - The equations used above yield good results with experiment; however, one must be able to calculate the parameters α, B, A and G.

The parameter A may be determined immediately from the experimental-range-energy relationships (14). The quantity r_m may be determined by maximizing the equation obtained from (18)

$$G_n(r) = e^{-r^n} \int_0^r e^{y^n} \, dy \tag{27}$$

for a given value of n. Also, if the range-energy relations are known for the primaries, then (17) may be used as

$$r_m^n = \alpha R_m$$

Then $\frac{1}{\alpha}$ may be determined. The value $\frac{\epsilon}{B}$ can be determined from the relationship

$$\frac{\epsilon}{B} = \left(E_{pmax} / r_m \delta_m\right) G_n(r_m) \tag{28}$$

which follows from Eqs. (17) and (19).

Sternglass Theory [2] - Sternglass [54] argues that after reaching a given depth in the target, the primaries will appear to diffuse at random. This characteristic depth λ_m corresponds to a distance for which the total angle of deflection is approximately $\frac{\pi}{2}$ relative to the direction of the incident primaries. Thus, the distance λ_m is the momentum loss mean-free-path and dependent upon E_p. He then simplifies the theory by replacing x in Eq. (11) by this distance λ_m, i.e., he assumes that all secondaries are produced at one depth in the material.

He then includes backscattering into his theory by introducing the parameters λ, defined as the number of electrons per primary electron with energies greater than 50 ev, and k defined as the mean fractional energy of these electrons with respect to the primary energy. Then,

$$\delta = \frac{B}{\epsilon}\,(1 - \eta k)\, e^{-\lambda_m \alpha} \int \frac{dE}{dx}\, dx$$

$$= \frac{B}{\epsilon}\,(1-\eta k) e^{-\lambda_m \alpha} E_p \tag{29}$$

Next, Sternglass considers the Bethe expression

$$-\frac{dE}{dx} = (2\pi N e^4/E) \sum_{n,\ell} Z_{n,\ell}\, \ell n \left[\frac{2E}{I_{n,\ell}}\right] \tag{30}$$

where N is the number of atoms per unit volume, Zn, ℓ is the number of electrons in the shell n, ℓ and $I_{n', \ell}$ is the binding energy of the electrons in the shell n, ℓ.

Using the approximation

$$\frac{1}{y}\, \ell ny \simeq 0.62 y^{-1/2} \tag{31}$$

(which is valid within 10 percent for $2.4 < y < 47$)

then

$$-\frac{dE}{dx} = 0.62 \left(\frac{2\pi N e^4}{E}\right) \sum_{n,\ell} Z_{n,\ell} \left[\frac{2E}{I_{n,\ell}}\right]^{1/2}$$

$$= E^{-1/2}\, (\sqrt{2}\ 0.62)\, (2\pi\, N\, e^4)\, \Sigma \frac{Zn,\ell}{In,\ell^{1/2}} \tag{32}$$

and, upon integration

$$\alpha \lambda_m = \beta\, E_p^{1/2} \tag{33}$$

so

$$\delta = \frac{B}{\epsilon}\,(1 - \eta k)\, E_p\, e^{-\beta E p^{1/2}} \tag{34}$$

where β contains the term $\sum_{n,\ell} \left(Z_{n,\ell} / I_{n,\ell}^{1/2}\right)$

Thus, Sternglass concludes that the inner atomic shells play an important role in secondary emission.

Now,

$$\delta_m = \frac{B}{\epsilon}\,(1 - \eta k)\, E_{p(max)} e^{-\beta\ E_{p(max)}^{1/2}} \tag{35}$$

or, $E_{p(max)}^{1/2} = \frac{2}{\beta}$ (36)

so finally,

$$\frac{\delta}{\delta_m} = \frac{E_p}{E_{p(max)}} \exp\left\{2\left[1 - \left(\frac{E_p}{E_{p(max)}}\right)^{1/2}\right]\right\} \tag{37}$$

which also agrees very well with experimental data.

Baroody Theory - Baroody [52] utilizes the Sommerfield model and considers the classical interaction with a free electron gas. Due to the small temperature dependence he can then treat the lattice electron available for reaction as a completely degenerate Fermi-Dirac gas. Considering the primary to move with constant velocity in a straight line, to interact with a lattice electron of negligible speed he can write the momentum transfer perpendicular to the primary path as

$$\Delta p = \int_{-\infty}^{\infty} \frac{e^2 \rho \, dt}{(\rho^2 + v^2 t^2)} = \frac{2e^2}{v\rho} \tag{38}$$

where

ρ = impact parameter

v = velocity of primary

t = time measured from instant of closest approach.

Now, in momentum space for Fermi-Dirac statistics, all states lying within a sphere of radius p_o are filled. p_o is defined by the Eq.

$$E_f = \frac{p_o^2}{2m} \tag{39}$$

where E_f is the fermi energy.

Thus, for the conduction electron at ρ, the effect of passing a primary is a shift of the center of the momentum-space sphere from the origin by an amount Δp. The number of secondaries produced per unit volume at ρ having $p > \mu p_o$ is the volume of the displaced sphere lying outside $\frac{2}{h^3} \mu p_o$ where $2/h^3$ is the density in phase space. Let G be this number then, for $\mu > 1$,

$$G(S) = \frac{\pi p_o^3}{6h^3 S}\left[3(\mu^2-1)^2 - 8(\mu^3-1)S + 6(\mu^2+1)S^2 - S^4\right] \quad (\mu-1 \leq S \leq \mu+1)$$

$$= \frac{8\pi p_o^3}{3h^3} \qquad S \geq \mu+1 \qquad (40)$$

where

$$S = \frac{\Delta p}{p_o}$$

Now, from above

$$2\pi\rho\, d\rho = -\frac{8\pi e^4}{v^2 p_o^2}\frac{dS}{S^3} \qquad (41)$$

Then

$$N(\mu) = \frac{8\pi e^4}{v^2 p_o^2}\int_{\mu-1}^{mv/p_o} G(S) S^{-3}\, dS \qquad (42)$$

where

$$N(\mu) = \frac{32\,\pi^2\, e^4\, p_o}{3h^3 v^2(\mu^2-1)} \qquad (43)$$

where, since μ is the momentum distribution, the differential $-\frac{dN}{d\mu}$ gives the internal momentum distribution.

We can also write

$$N(\mu) = \frac{B E_p^{1/2}}{W(\mu^2-1)} \qquad (44)$$

where

E_p = primary energy;

W = kinetic energy of the secondaries; and

$$B = \frac{160\,\pi^2 (6)^{1/2} m^{3/2} e^{7/2}}{3h^3} = 2.95 \times 10^8 \text{ ev}^{1/2} \text{ cm}^{-1} \qquad (45)$$

If μ_o is the minimum μ for escape from metals and $W \sim 10^2$ ev, then $N(\mu_o) \sim 10^7$ cm^{-1} Now, considering the case for singly scattered secondaries let δ be the number of secondary electrons leaving the surface having undergone a single elastic collision. The probability of this in the depth r and r + dr is given by

$$P = e^{-\sigma r}\frac{dr}{d\ell} \qquad (46)$$

where the inverse mean free path is $(\ell + \lambda) / \ell\lambda$. Integration over r gives the probability per unit solid angle

$$P(\Omega) = \frac{1}{4\pi\sigma\ell} \tag{47}$$

Let q denote the cosine of the angle with respect to the outward normal to the surface. Then, the probability of scattering into dq is

$$P(dq) = \frac{dq}{2\ell\sigma} \tag{48}$$

Let N(q, z) be the number of secondaries produced per unit path length at depth z with enough energy to escape at angle $\cos^{-1}q$. So, by also including factors for absorption and scattering

$$\delta_1 = (2\ell\sigma)^{-1} \int_0^1 \int_{-\infty}^{\infty} N(q, z) e^{-\sigma 3/q} \, dzdq \tag{49}$$

but

$$N(q, z) = N\left(\frac{\mu_o}{q}\right) ; \quad z = \frac{BE_p^{1/2} q^2}{W(\mu_o^2 - q^2)} \tag{50}$$

where

$\mu_o^2 = (E_p + \phi) / E_p$ (~ 1.5 to 2.0)

ϕ = work function of the material.

Assuming $-\frac{dW}{dz}$ inversely proportional to W, i.e.,

$$W^2 = W_p^2 - az \tag{51}$$

Then we can write

$$\delta_1 = \frac{BE_o^{1/2}}{2\ell\sigma} \int_0^1 \int_0^{W_p^2/a} \frac{q^2 e^{-\sigma z/q} \, dzdq}{(W_o^2 - az)^{1/2}(\mu_o^2 - q^2)} \tag{52}$$

changing variable to let $q^{-1/2} = \omega$,

$$\delta_1 = \frac{2BE_p^{1/2}}{\ell\sigma^{3/2}a^{1/2}} \int_1^{\infty} \frac{F(H\omega) \, d\omega}{(\mu_o^2\omega^4 - 1)\omega^4} \tag{53}$$

where

$$F(x) = e^{-x^2} \int_0^x e^{t^2}\, dt \tag{54}$$

and

$$H = (\omega_p^{\,2}\ \sigma/a)^{1/2} \tag{55}$$

and $F(H, \omega)$ has a maxima at $H\omega = 0.92$ and the remaining factors are largest for $\omega = 1$ and decrease in value rapidly for larger values of ω. Thus, for $H \sim 1$, δ_1 can be approximated by

$$\delta_1 \sim \frac{2BE_p^{1/2}}{\ell\, \sigma^{3/2} a^{1/2}}\ F(H) \int_1^{\infty} \frac{d\omega}{(\mu_o^{\,2}\omega^4 - 1)\omega^4} \tag{56}$$

which is accurate to about one percent.

Next, Baroody considers the case for multiplying scattered secondaries. For $\ell << \lambda$, the electrons move to the surface by means of a diffusion process. Then, for a primary current of unit density, the production of secondary electrons between μ and $\mu + d\mu$ per unit volume per unit time is given by

$$\frac{2BE_p^{\,1/2}\ \mu\, d\mu}{(W_o^{\,2} - az)^{1/2}\ (\mu^2 - 1)^2} \tag{57}$$

If all secondary electrons for which $\mu > \mu_o$ could leave the surface upon arrival, diffusion theory gives the secondary current density as

$$i_s = \int_0^{W^2/a} \int_{\mu_o}^{\infty} \frac{2BE_p^{\,1/2}\ e^{-3/L}\ \mu\, d\mu\, dz}{(W_o^{\,2} - az)^{1/2}\ (\mu^2 - 1)^2} \tag{58}$$

where

$$L = \left(\frac{\lambda\, \ell}{3}\right)^{1/2}$$

The actual momentum (μp_o) must exceed μ_o/μ. Thus the equation above must be multiplied by the corresponding fraction of forward solid angle $(\mu - \mu_o)/\mu$.

Then,

$$\delta = \frac{2BE_p^{1/2} L^{1/2}}{A^{1/2}} F\left[(W_o^2/AL)^{1/2}\right] \int_{\mu_o}^{\infty} \frac{(\mu - \mu o)\, d\mu}{\mu_o(\mu^2 - 1)^2} \tag{59}$$

where $F(x)$ is defined above.

To consider the variation of the secondary emission with primary energy, Baroody refers to Bruining's equation

$$\delta = K \left(\frac{A}{\alpha}\right)^{1/2} F\left[\left(W_o^2 \frac{\alpha}{A}\right)^{1/2}\right] \tag{61}$$

Assuming $\lambda << \ell$, this gives the same result as the above equations. Bruining shows that $F(x) = F(x)_{max}$ for $x = 0.92$ so that

$$(W_o)_{max} = 0.92 \left(\frac{A}{\alpha}\right)^{1/2} \tag{62}$$

Then

$$\frac{\delta}{\delta_{max}} = 1.85\, F\left\{0.92\, \frac{W}{W_{o\,max}}\right\} \tag{63}$$

This is the familiar expression derived earlier in the semi-empirical theory.

Baroody divides the velocity distribution of the emitted secondaries into two parts:

a) Normal energy distribution - The expression

$$E_p^{1/2} (\mu_o \operatorname{ctnh}^{-1} \mu_o - 1) \tag{64}$$

is used to calculate the fraction of emitted secondaries for which the normal energy $(\frac{1}{2} m v_z^2)$ is greater than the energy. This is the fraction of the emitted secondaries which would escape if the work function were greater by an amount E, namely

$$\frac{\mu_1 \operatorname{ctnh}^{-1} \mu_1 - 1}{\mu_o \operatorname{ctun}^{-1} \mu_o - 1} \tag{65}$$

where

$$\mu_1^2 = 1 + (\phi + E)/E_o = \mu_o^2 + (\mu_o^2 - 1)\, E/\phi \tag{66}$$

b) Total energy distribution - from above, the number of electrons leaving the metal with kinetic energy greater than $\epsilon\phi$ is proportional to

$$Q_1(\mu_1) = \int_{\mu_1}^{\infty} (\mu - \mu_o)(\mu^2 - 1)^{-2}\, d\mu \tag{67}$$

where

$$\mu_1^2 = \mu_o^2 + (\mu_o^2 - 1)\,\epsilon \tag{68}$$

The corresponding fraction of secondaries is given by

$$P(\epsilon) = Q(\mu_1)/Q(\mu_o) \tag{69}$$

and

$$\frac{dp(\epsilon)}{d\epsilon} = \frac{(\mu_o^2-1)(\mu_1-\mu)}{2\mu_1(\mu_1^2-1)^2 Q(\mu_o)} \tag{70}$$

By substitution of the proper values, the energy of the greatest number of secondaries is approximately 0.7 of the work function.

To find the angular distribution of the secondaries, consider the following: according to the refraction law, an electron incident on the inside at an angle β with the normal will emerge at an angle θ with the normal given by

$$\sin\theta = \mu \sin\beta\,(\mu^2 - \mu_o^2)^{1/2} \tag{71}$$

where the electrons have the momentum μp_o. For given β, all electrons emerging at angles less than θ are those for which

$$\frac{\mu}{(\mu^2 - \mu_o^2)^{1/2}} < \frac{\sin}{\sin\beta} \tag{72}$$

or

$$\mu^2 > \frac{\mu_o^2 \sin\theta}{\sin^2\mu - \sin^2\beta} \tag{73}$$

for $\beta \leq \theta$ and zero outside the range.

Assuming that the number of electrons incident in range $d\beta$ is proportional to the corresponding solid angle, the number of electrons emerging for angles less than θ is proportional to

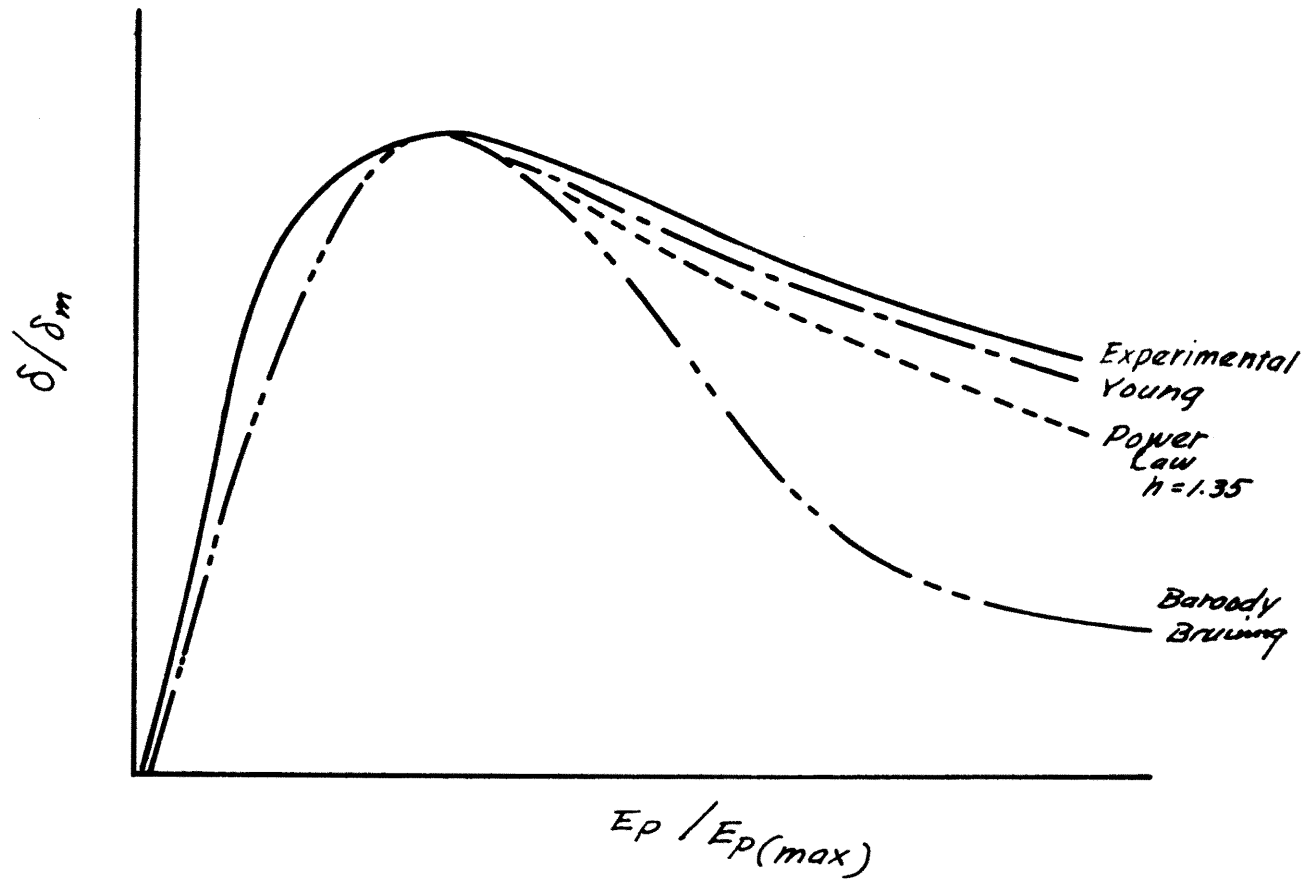

Fig. 13 Comparison of various theories for reduced yield

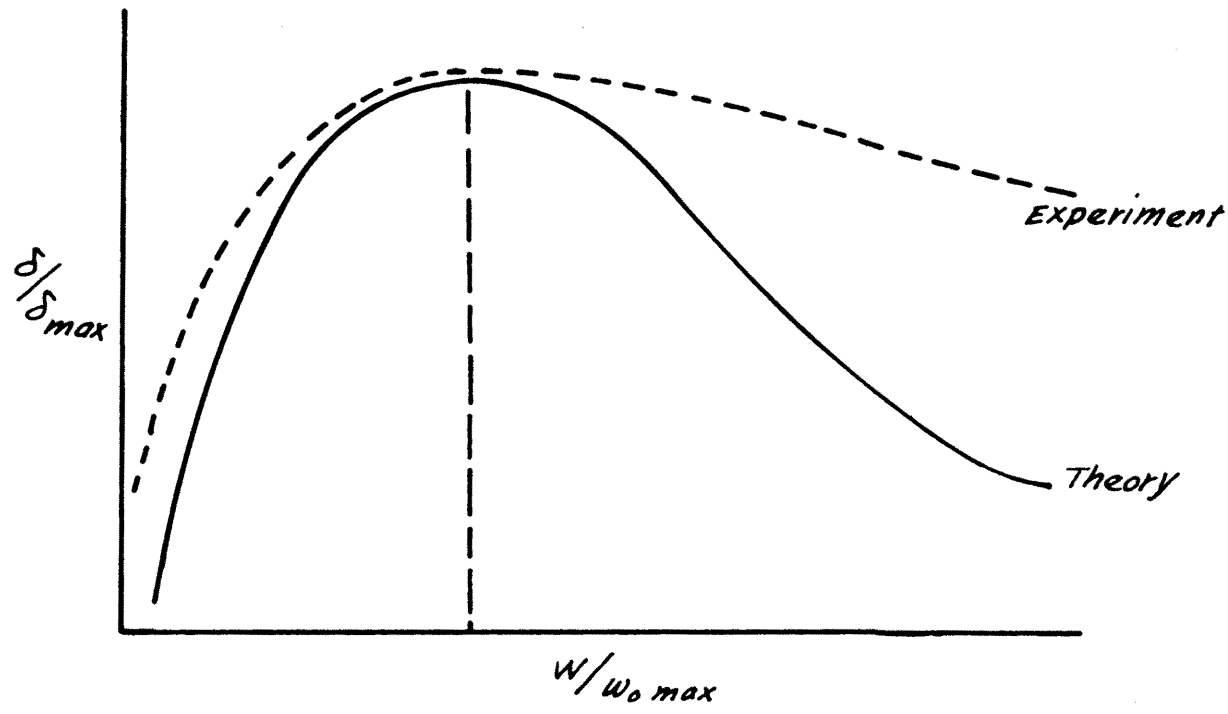

Fig. 14 Typical reduced yield curve comparing the theory of Baroody with experiment.

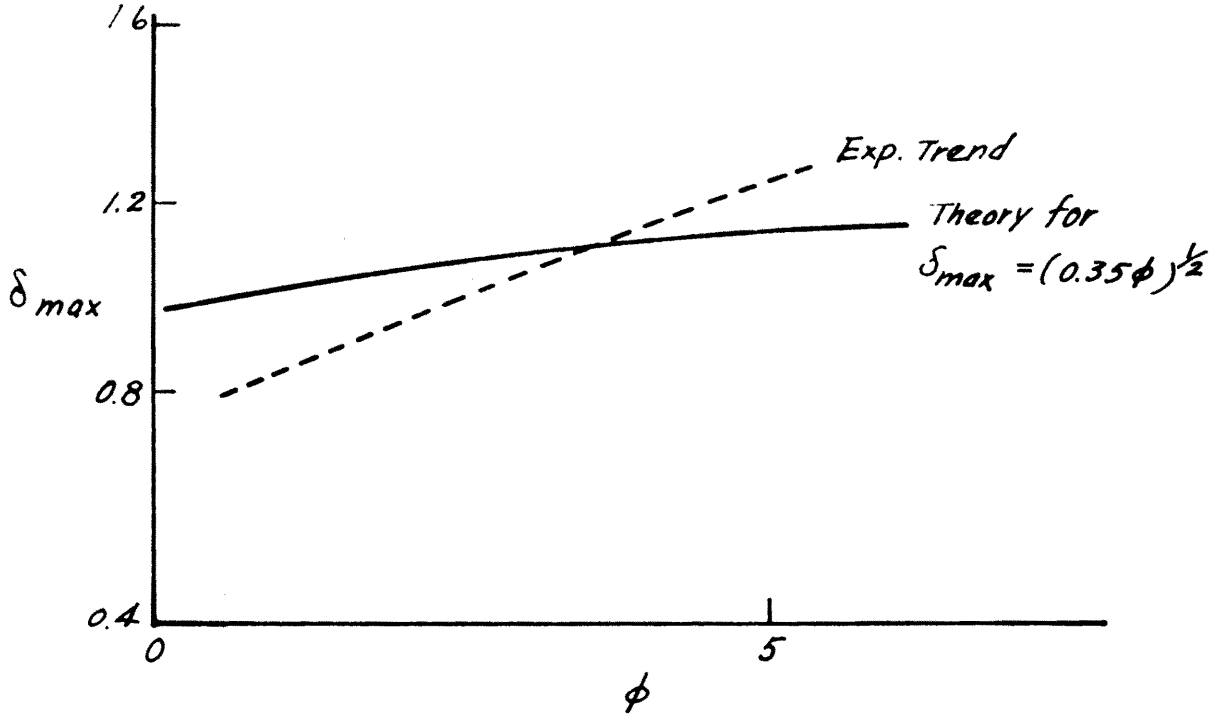

Fig. 15 Comparison of theory of Baroody to experiment for δ_{max} vs. work function.

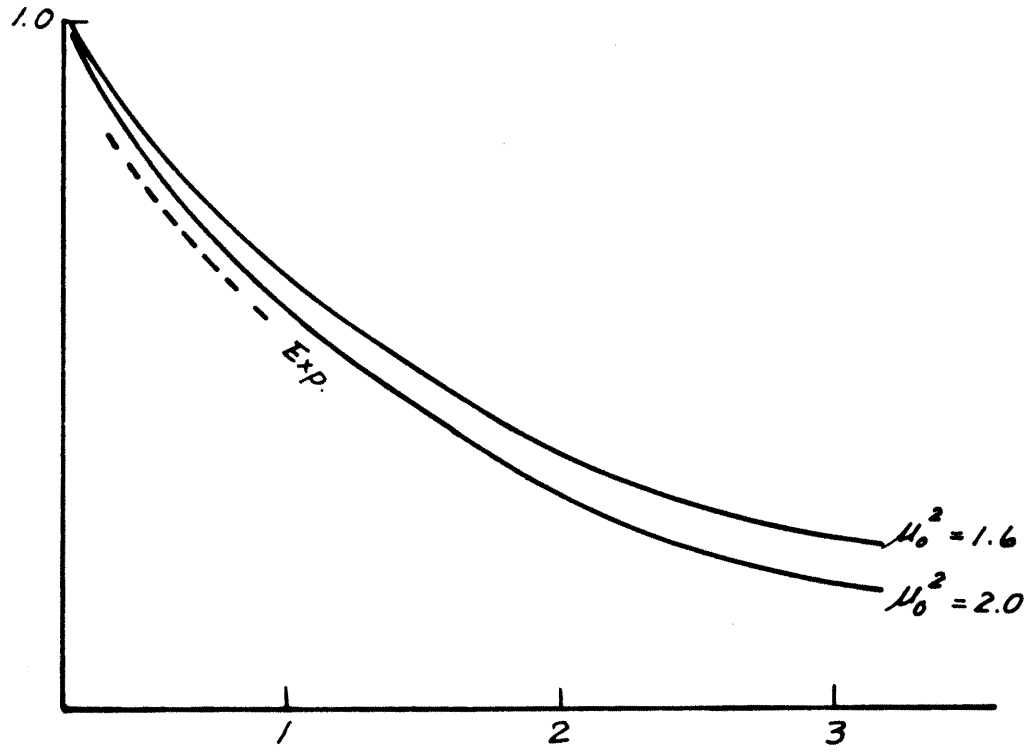

Fig. 16. Comparison of experimental curves with those for different values of μ_0^2

$$\int_0^{\theta} \frac{(\sin^2\theta - \sin^2\beta)\sin\beta \, d\beta}{\left[(\mu_o^2 - 1)\sin^2\theta + \sin^2\beta\right]} \tag{75}$$

which is approximately $\cos\theta$ in the range of interest.

Fig. (13) through (16) correlate the experimental data with the results of this theory.

III. Quantum Mechanical Theories

Earlier theories have given approaches which adequately predict the experimental points without regard to the physical processes involved. This section will cover the important theories, whereby, to obtain feeling for the physical phenomena of secondary emission, the interaction probabilities and potentials are considered. This, of course, may be accomplished only through quantum mechanical formulation. Due to its complexity, most of the mathematical detail of this section has been relegated to an appendix.

A. Woolridge Theory [62] - One of the first to consider secondary emission quantum mechanically, Woolridge based his theory on the following assumptions:

1. Bound valence electrons
2. Incident primary forces are independent of restraint forces.
3. Lattice electrons are considered distinguishable.
4. Lattice has simple cubic structures.

From the last assumption, the unperturbed eigenfunctions may be written as Bloch functions of the type:

$$U_k(r)\, e^{i(k \cdot r)} \tag{76}$$

where $U_k(r)$ contains the periodicity of the lattice and may be written in the form

$$U_k(r) = \sum_m \beta_m(k)\, e^{2ki(m \cdot r)/\ell} \tag{77}$$

where ℓ is the lattice spacing and each component of m is a positive or negative unit vector. The unperturbed eigenfunction for a free electron is given by

$$e^{i(K \cdot R)} \tag{78}$$

Thus, the unperturbed wave function for a system of two particles, one free and one bound in a periodic lattice is

$$\psi_{k,K}(t) = \frac{1}{\Omega} U_k(r)\, e^{i\left[(\vec{K} \cdot \vec{R}) + \vec{k} \cdot \vec{r}\right]}\, e^{i(E_K + E_k)\, t} \tag{79}$$

Assuming the coulomb interaction potential,

$$V = \frac{e^2}{|\vec{R} - \vec{r}|}, \tag{80}$$

then, one can write,

$$A_{k'K'} = \int \psi_{k,K}(t)\, \frac{e^2}{|\vec{R} - \vec{r}|}\, \psi_{k.K}(t)\, d\tau\, dt \tag{81}$$

where dt is the time differential element and $d\tau$ the space differential element dXdYdZdxdydz and $|A_{k'K'}|^2$ is the interaction probability. By integrating,

$$A_{k'K'} = \frac{4\pi e^2}{\Omega^2 S^2}\, \frac{e^{i\hbar \epsilon t} - 1}{i/\hbar} \sum_{m,n} \int e^{i(\vec{S} + \vec{s} + 2\pi i \vec{\rho}/\ell) \cdot r}$$

$$\times \rho^*_m(k)\, \rho_n(k)\, d\tau_r \tag{82}$$

where

$$S = |\vec{K} - \vec{K}'|, \quad s = |\vec{k} - \vec{k}'|, \quad \vec{\rho} = \vec{m} - \vec{n}. \tag{83}$$

For $A_{k',K'}$ to be non zero, it is necessary that

$$\vec{S} + \vec{s} + 2\pi i \vec{\rho}/\ell = 0 \tag{84}$$

This is the law of conservation of momentum. For free electron case, $\rho_{mn} = 0, 0, 0$ and the expression reduces to the classical conservation of momentum expression. Hence, this will be one of the system constraints, i. e., that momentum is conserved in the form of Eq. (84).

The probability amplitude;

$$|A_{k'K'}|^2 \left(\frac{1-\cos \epsilon t}{t^2}\right) \left| \sum_{m,n} \int \beta_m(k)\, \beta_n(k)\, e^{i\left(\vec{S}+\vec{s}+\frac{2\pi\vec{\rho}}{\ell}\right)} - r^2 \, d\tau_r \right| \tag{85}$$

involves the product of two terms leading to the conditions that

$$\vec{S}+\vec{s}+\frac{2\pi i\vec{\rho}}{\ell} = 0$$

as before and

$$\epsilon t = t\left[(E_k+E_K) - (E_{k'}+E_{K'})\right] = 0 \tag{86}$$

or, that energy is conserved as a second restriction on the system. These two restrictions define a six-dimensional k', K' space within which the state specified by k' and K' (specified as k and K at time t = 0) will be non-zero. Considering $\frac{1-\cos \epsilon t}{(\epsilon t)^2}$ to be a slowly varying function, i.e., nearly constant, the number of lattice electrons available for collision, i.e., the number at time t which have their wave functions in the range $d\tau_{k'}$ around k', may be determined. This expression is found to be

$$dN = \frac{2e^4 t^2}{\pi \Omega \hbar^2}\left[S_\rho^{1/4}\, F(\epsilon_\rho t) \left| \sum_m \beta_{\rho+m}(k)\, \beta^*_m(k') \right|^2\right] d\pi_{k'} \tag{87}$$

where

$$\vec{\rho}+\vec{m} = \vec{n}. \quad F(\epsilon_\rho t) = 2(1-\cos\epsilon\rho t)/(\epsilon\rho t)^2. \tag{88}$$

Since these expressions are derived from a two-particle model it becomes necessary to consider the actual case, i.e., to expand it into a many particle model. Let N_p and $N_\ell(k)$ be the numbers of primary and lattice electrons respectively. Let $\rho_p = N_p/\Omega$ and $\rho_\ell(k) = N_\ell(k)/\Omega$. Then, if the primary current density is J_p (Elect. cm^{-2} sec^{-1}) and if the primary electron velocity is v,

$$\rho_p = \frac{J_p}{v} \tag{89}$$

but

$$v = \frac{hK}{m} \tag{90}$$

so

$$\rho_p = \frac{J_p m}{Kh} \tag{91}$$

Then, the above expression must be multiplied by $N_\ell = \rho_\ell \Omega$ and $N_p = J_p m\Omega / Kh$ for the total number variation; thus

$$dN = \Sigma\, dN_p = J_p\, \Omega\, t\, \frac{2me^4}{\pi h^3}\; \rho_\ell(k)\, \frac{1}{K}\left[S_\rho^{1/4}\, F(\epsilon\, \rho t)\right] \left| \sum_M \beta_{\rho+m}^{(k)}\; \beta_m^{*(k')} \right|^2 d\tau_{k'} \qquad (92)$$

which must be evaluated for any given ρ.

Using the conservation restrictions, a spherical surface of radius R and surface element $d\sigma$ and geometrical arguments (see appendix), Woolridge shows that the rate of transition is given by

$$\frac{dN_p}{dt} = \Omega\, \frac{16\pi m^2 e^4}{h^4}\; \rho_\ell(k) \frac{J_p \frac{2R}{K}\, \rho}{\left[\left(\frac{2\pi\rho}{\ell}\right) \cdot \left(\frac{2\pi\rho}{\lambda} + 2k\right)\right]} \left| \sum_m \beta_{\rho+m}(k)\, \beta_m^*\left(k + \frac{2\pi\rho}{\ell}\right) \right|^2 \qquad (93)$$

where for large K, $\frac{2R}{K} \sim 1$ and the transition rate is independent of the primary energy; a result verified by experimental result.

Woolridge then shows (by work of P. M. Morse, Phys. Rev. 35, 1311 (1930)) that using only the values $\rho = 0, 0, \pm 1$; $\rho = 0, \pm 1, 0$; $\rho = \pm 1, 0, 0$ a good first approximation of the problem may be found. This approximation is

$$\frac{dN_\rho}{dt} = \Omega\, \frac{16\pi m^2 e^4}{h^4}\; \rho_\ell(k)\, J_p \frac{|b_p(k)|^2}{\left[\left(\frac{2\pi\rho}{\ell}\right) \cdot \left(\frac{2\pi\rho}{\ell} + 2k\right)\right]^2}\; F_\rho(k, K) \qquad (94)$$

where

$$F_\rho(k, K) = \left[1 - \frac{\left(k + \frac{2\pi\rho}{\ell}\right)^2}{K^2} - \frac{2K \cdot \left(k + \frac{2\pi\rho}{\ell}\right)}{K^2}\right]^{1/2} \qquad (95)$$

and

$$b_p(k) = \sum_m \beta_{\rho+m}(k)\, \beta_m^*(k) \qquad (96)$$

From here, by use of Fermi statistics and the exclusion principle, he shows that the average energy absorbed by a lattice electron from a primary electron is given by

$$E_o = \left(\frac{h^2}{2m}\right) \left(\frac{2\pi}{\ell}\right)^2 \qquad (97)$$

and that the production of secondaries fall off rapidly when

$$E_p \lesssim E_o + E_{max} \tag{98}$$

quoting as an example Silver, for which $E_o \sim 25$ ev and $E_{max} \sim 5$ ev he expects the secondary emission to drop off rapidly when the bombarding energy (inside the metal) drops below 25 or 30 ev.

Free Electron Approximation - From the expression for dN_ρ, utilizing the born approximation rather than the exclusion principle, and assuming $|\vec{k}| << |\vec{K}|$, the expression

$$\frac{1}{\rho_\ell J_p} \frac{1}{\Omega t} (dN_o)_{t_o t} = \frac{e^4}{m^2 v^4} (\sec^4 \alpha + \csc^4 \alpha) 4 \cos \alpha \, d\omega \tag{99}$$

may be obtained. This is the Rutherford scattering formula, which should be expected from these conditions.

This equation divides the primary beam into two groups:

1) Electrons which after collision differ only slightly in direction from the primary beam. For purposes of calculation these are assumed to remain in the primary beam.

2) Electrons which are scattered into states of lower energy and which move away at angles greater than 45^0.

If one calculates the rate at which electrons are produced in the second group with energies and direction which make it possible for them to escape from the back side of the target, a rough estimate of secondary emission may be obtained from the free electron approximation. This result is given by

$$\frac{N_1}{N_o} = \frac{4 |b_1(k)|^2 - \left(\frac{E_p}{E_o}\right)^2}{\left(\frac{E_p}{\omega_a}\right)^{1/2} - 1} \tag{100}$$

where it has been assumed that ρ and K coincide so that $|\rho| = 1$ and $\omega_a = E_p \cos^4 \alpha_{max}$. From this relation and from experimental results, Woolridge concludes that when electrons of a few hundred electron-volt energy travel through metal, they lose energy principally by the production of

secondaries corresponding to the expansion for which $\rho \neq 0$ until their energy becomes too small to produce further secondaries (for Ag, $\sim$ 25 ev). For the remainder of their path, the rate of energy loss is probably determined by "free electron" scattering.

Limitations and Applicability of Results - To compare the theoretical transition rate with experimental results, one would like to consider some averaging process over all lattice points to eliminate the k dependence. However, it is obvious that for a given direction of ρ there will exist a few electrons such that their momentum, direction and magnitude will require that

$$\left(\frac{2\pi\rho}{\ell}\right) \cdot \left(\frac{2\pi\rho}{\ell} + 2k\right) = 0 \tag{101}$$

For such electrons, k apparently lies on the surface of a Brillouin zone. It then appears that the transition rate assigns a definite probability of transition of these electrons into a new state

$$\vec{K} = \vec{k} + \frac{2\pi\vec{\rho}}{\ell} \tag{102}$$

It is easily shown however, that such a transition is forbidden, i.e., the approximation is not valid. If, however, it is assumed that $\vec{k} \cdot \vec{\rho} = 0$, then for $\rho = 1$

$$\frac{dN_p}{dt} = \frac{16\pi\Omega m^2 e^4}{h^4} \rho_\ell J_p \left(\frac{|b_{\rho\pi}|^2}{\frac{2\pi}{\ell}}\right) 4 F_\rho (K) \tag{103}$$

where now it is accurate enough to write

$$F_\rho (K) = \left[1 - \frac{\left(\frac{2\pi}{\ell}\right)^2 + \frac{2ME_F}{h^2}}{K^2} - \frac{2\vec{K} \cdot \left(\frac{2\pi\vec{\rho}}{\ell}\right)}{K^2}\right]^{1/2} \tag{104}$$

Woolridge interprets this equation as follows: A current of primary electrons of number J_p per cm^2 per sec and of momentum $\hbar K$ travels through a simple cubic lattice of principal axes (1, 0, 0), (0, 1, 0) and (0, 0, 1). Corresponding to each of the six directions ρ = (1, 0, 0), (-1, 0, 0)... a group of secondary electrons is produced at a rate given by $da\rho/dt$. The average

energy of a secondary electron is

$$E_{av} = E_F + \frac{\hbar^2}{2m}\left(\frac{2\pi}{\ell}\right)^2 \tag{105}$$

where E_F is the mean Fermi energy of the lattice Electrons and $\frac{\hbar^2}{2m}\left(\frac{2\pi}{\ell}\right)^2$ is the average energy lost by a primary electron in producing one secondary electron. For a given ρ, the secondaries all have their directions bunched around the direction of ρ. If $\frac{2\pi}{\ell} >> k$, the spread of energies will be small. Finally, due to the approximations, the equations become invalid for $S_{min} \to 0$. But, this occurs regardless of the condition $\vec{k} \cdot \vec{\rho} = 0$ for large K. Therefore, it is possible to predict that the yield will decrease for high primary energies in agreement with experimental results.

Application of Results - Utilizing (103) and (104) from the previous section along with their subsequent interpretation and with the conclusion that primary energy is lost principally through secondary electron production and, assuming an inhomogeneous surface, Woolridge derives an expression for the reduced yield

$$\frac{\delta}{\delta_\infty} = \left\{1 - \exp\left[\frac{\frac{1}{2}\left\{1 - (W_a/(E_o+E_F))^{1/2}\right\}}{\delta_\infty}\left(\frac{E_p}{E_o}\right) - 1\right]\right. \tag{106}$$

$$\left. + \frac{1}{2}\left\{1 + \left(\frac{W_a}{E_o + E_F}\right)^{1/2}\right\}\int_0 \frac{\frac{1}{2}\left\{1 - (W_a/(E_o + E_F)^{1/2}\right\}\left(\frac{E_p}{E_o} - 1\right)}{\frac{E_p}{E_o} - \frac{\frac{1}{2}\left\{1 - (W_a/(E_o + E_F))^{1/2}\right\}}{\delta_\infty}} e^{-v}\, dv\right. \tag{107}$$

where

$$\delta_\infty = \frac{96\pi\, m^2 e^4}{h^4}\,\rho_\ell\,\frac{|b_1|^2}{\left(\frac{2\pi}{\ell}\right)^4}\,\frac{\frac{1}{2}\left\{1 - \frac{W_a}{(E_o + E_F)}\,1/2\right\}}{\gamma} \tag{108}$$

γ = absorption coefficient of the material

Thus, if δ_∞ is known the δ vs E_p curves may be plotted.

This expression has been derived for a simple cubic lattice structure. However, most materials of interest possess either a body centered or a face centered cubic structure. This correction may be made by the approximation that

$$\ell_o = 0.9\ell \tag{109}$$

where

$$E_o = \frac{h^2}{2m}\left(\frac{2\pi}{\ell_o}\right)^2$$

Comparison of Theory and Experiment - The figures shown are examples of the experimental-theory correlation. It is seen that except for cesium and barium, the agreement between theory and experiment is within 50 percent. The curves for copper and silver are excellent probably because these metals exhibit a yield which is practically constant over a wide range of primary energies. For all other metals correlated, (except for C_s and B_a) the theoretical curve is always appreciably below the experimental curves. This may be eliminated by considering the yield decrease at high primary energies and primary reflection at low energies.

The apparent incompatability of experiment and theory in the instances of Cs and Ba is too large to be explained by either of the above causes. It is felt that perhaps the theory breaks down for these elements. This is possibly due to non-negligible Rutherford scattering, or due to the large volume of these elements in relation to their small yield. It is also possible that these discrepancies arise from ignoring the conduction band interactions.

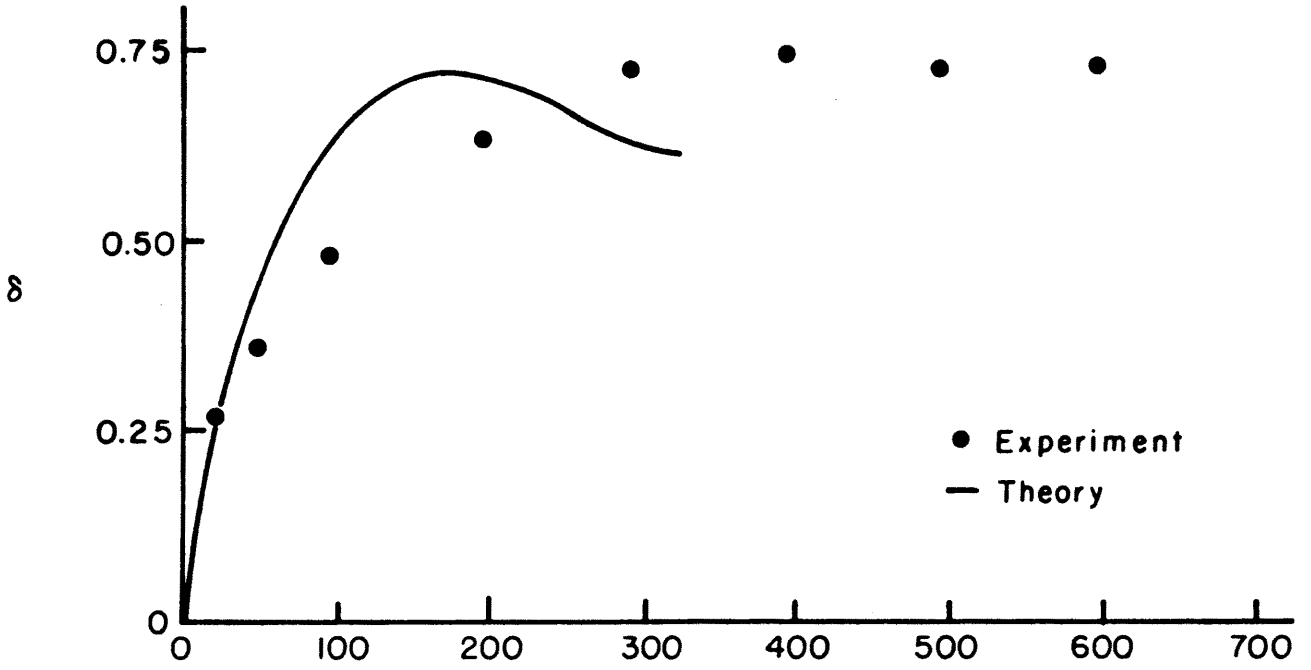

Fig 17 δ vs E_p for Cesium

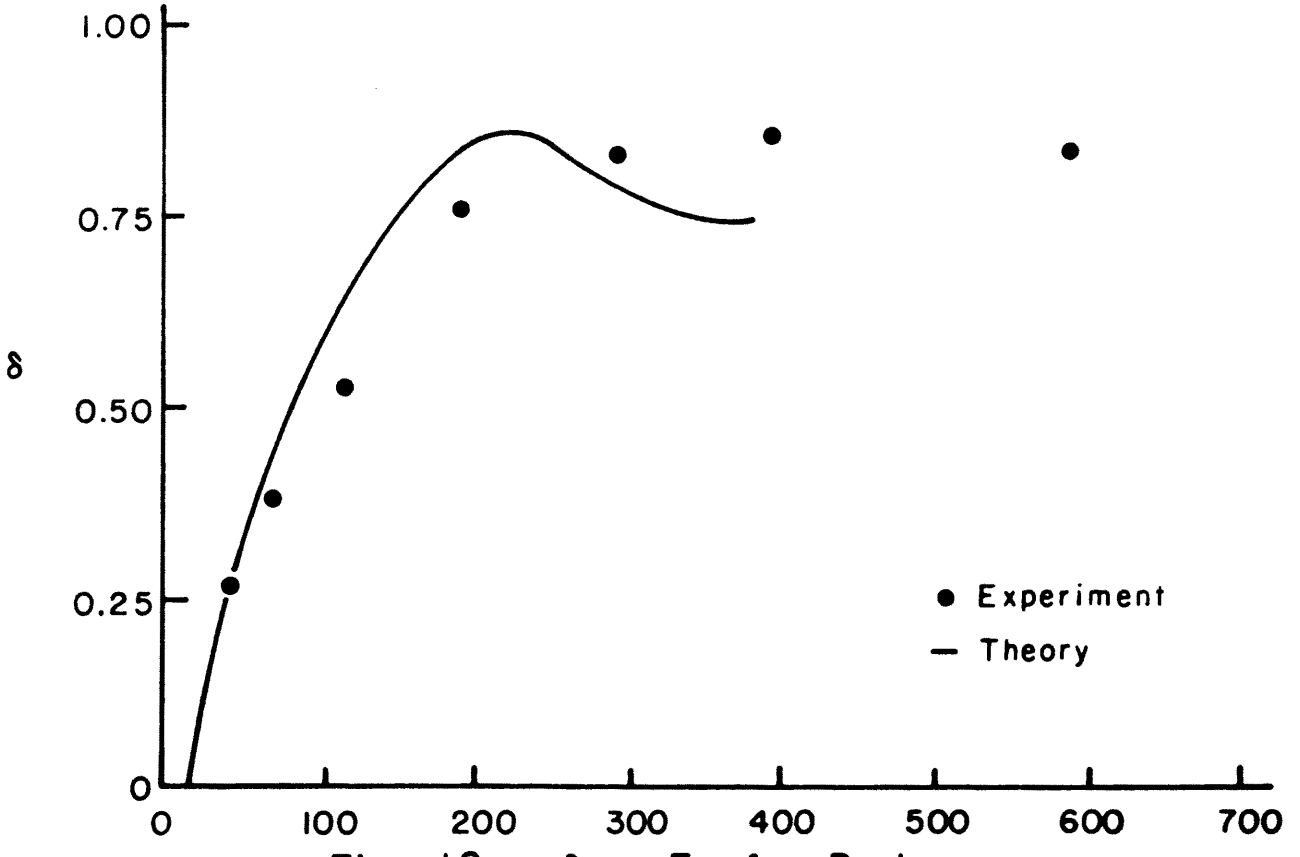

Fig 18 δ vs E_p for Barium

ALL EXPERIMENTAL POINTS COME FROM BRUINING AND DeBAER

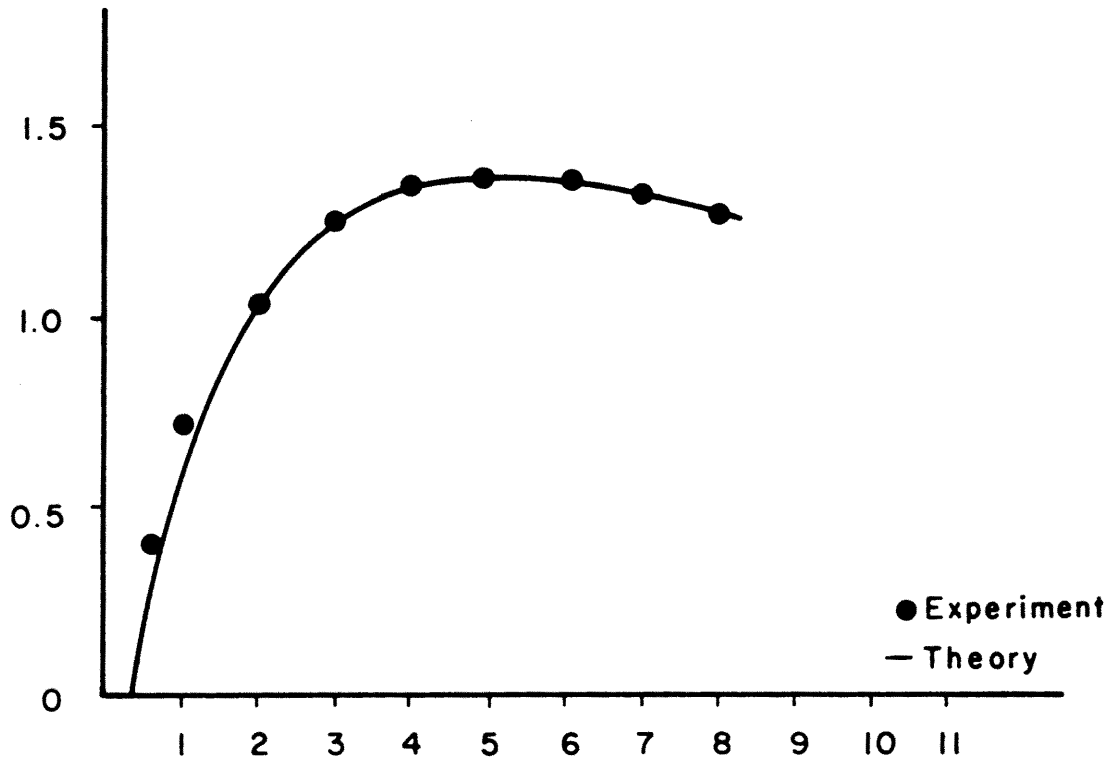

Ep vs S for Copper

Fig 19

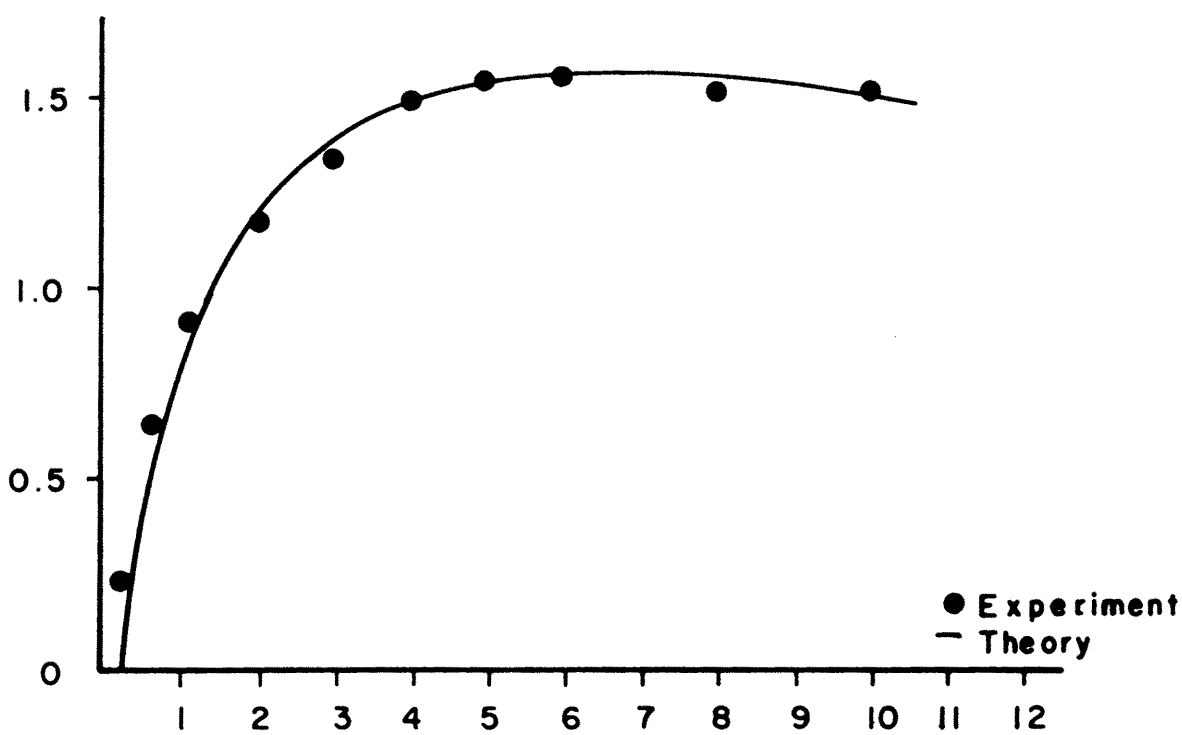

S vs Ep for Silver

Fig 20

B. Theory of Van Der Ziel and Dekker [41] - These authors have extended Woolridge's theory in an attempt to resolve some of the deficiencies and made an attempt to justify his work as being a portion of a more general theory. The main deficiency that they attempt to remove is that of the impossibility of obtaining secondary emission from a free gas due to the conservation of momentum.

They begin by questioning the coulomb interaction potential

$$U = \frac{e^2}{|\vec{R} - \vec{r}|} \tag{111}$$

in this general theory. They suggest, for example a better approach might be to consider the conduction electrons along with the positive ion cores as a plasma. For their arguments in this work, however, they do concede to the assumption of the coulomb potential being valid and attempt to consolidate the theories of Baroody and Woolridge into a basic theory.

The Fundamental Process - Considering a free primary electron of wave vector $\vec{K}$ and of energy $\frac{\hbar^2 K^2}{2m}$ and wave function $e^{i\vec{K}\cdot\vec{R}}$ and a lattice electron with wave vector $\vec{k}$ and wave function $\psi_k(r)$ and considering no interaction, they write the wave function of the system as

$$u_o = e^{i(\vec{K}\cdot\vec{R})}\psi_k(r)e^{-\frac{i}{\hbar}Et} \tag{112}$$

where

$$E = E(k) + \frac{\hbar^2}{2m} K^2 \tag{113}$$

Because of the interaction, transitions are such that the state $\vec{k}$ is transformed into the state $\vec{k}'$ and the state $\vec{K}$ into $\vec{K}'$. Thus, the transition rate must be computed for the solution to the problem, i. e., the transition rate $P(K, k \rightarrow K', k')d\Omega'$ for which the primary electron is scattered into a solid angle $d\Omega'$ around K' and for which the lattice electron is scattered into the state k'. By the usual methods, the wave function for this system at time t may be expanded into

$$U(t) = \sum_{k'}\sum_{K'} A_{kK'}(t)\, e^{i(\vec{K}\cdot\vec{R})}\psi_{k'}(r)\, e^{-\frac{i}{\hbar}E't} \tag{114}$$

where

$$E' = E(k') + \hbar^2/2m \tag{115}$$

Then, assuming a coulomb interaction

$$A_{k'K}(t) = i^{1/2} \int_R \int_r \int_o^t e^{i(\vec{K}-\vec{K}')\cdot\vec{R}} \frac{e^2}{|\vec{R}-\vec{r}|} \psi_k(r)\, \psi_{k'}^*(r)$$

$$x e^{-i(E-E')\,t/\hbar}\, dt\, dr\, dR \tag{116}$$

As before, use Bethe's relationship

$$\int \frac{e^2}{|\vec{R}-\vec{r}|} e^{i(\vec{K}-\vec{K}')\cdot\vec{R}}\, dR = \frac{4\pi e^2}{q^2} e^{i\vec{q}\cdot\vec{r}} \tag{117}$$

where $\vec{q} = \vec{K} - \vec{K}'$

By substitution, this leads to the transition probability amplitude

$$|A_{k',K'}(t)|^2 = \frac{16\pi^2 e^4}{q^4} \frac{2\left\{1 - \cos\left[(E'-E)\,t/h\right]\right\}}{(E'-E)^2} |I|^2 \tag{118}$$

where

$$I = \int e^{i\vec{q}\cdot\vec{r}}\, \psi_k(r)\, \psi_{k'}^*(r)\, dr \tag{119}$$

Large values of t in the transition probability lead to processes for which energy is conserved.

By standard procedures it is possible to derive the transition rate as

$$P(K, k \rightarrow K', k')\, d\Omega' = \frac{4m^2 e^4 K'}{h^4 q^4 K} |I|^2\, d\Omega' \tag{120}$$

The basic theories now vary from this expression only in the manner in which I is evaluated.

Assuming free lattice electrons should lead to Baroody's conclusions; the nearly free approximation should lead to results similar to Woolridge and tightly bound electron to those of Rudberg and Slater [69].

Weakly Bound Lattice Electrons - This assumption allows the lattice electrons to be described by Block functions of the form

$$\psi_k(r) = e^{i(\vec{k}\cdot\vec{r})}\, U_k(r) \tag{121}$$

where $U_k(r)$ contains the periodicity of the lattice and may be expanded by Fourier series as

$$U_k(r) = \sum_{n_1 n_2 n_3 = 0} C_n(k) e^{i(\vec{n} \cdot \vec{r})} \tag{122}$$

where

$$\Sigma_n \left| C_n(k) \right|^2 = 1 \tag{123}$$

Here,

a) $\frac{n}{2\pi}$ is a vector of one of the points in the reciprocal lattice.

b) $\frac{An}{2\pi}$ represents a vector of integral components if A is one of the lattice constants.

c) For a body centered lattice, those coefficients are zero for which the sum of the components of $\frac{An}{2\pi}$ is odd.

d) For a face centered cubic lattice only those coefficients do not vanish for which <u>all</u> components of $\frac{An}{2\pi}$ is odd.

e) A lattice electron may be considered completely free if either $n = 0$ or the coefficient is zero, i.e., if $C_{ooo}(k') = 1$ and $C_n(k) = 0$.

Then,

$$I = \Sigma_n C_n(k) \int e^{i(\vec{q} + \vec{k} - \vec{k}' + \vec{n}) \cdot \vec{r}} dr \tag{124}$$

which equals unity if

$$\vec{q} + \vec{k} - \vec{k}' + \vec{n} = 0 \tag{125}$$

or,

$$\vec{K} + \vec{k} + \vec{n} = \vec{C}_n = \vec{k}' + \vec{K} \tag{126}$$

and is negligible otherwise. This represents the conservation of momentum for the system. Then, for a particular n,

$$P_n(Kk \rightarrow K'k') d\Omega' = \left| C_n(k) \right|^2 \frac{4\pi^2 e^4 K'}{h^4 q^4 K} d\Omega' \tag{127}$$

Now, $P_n >> 1$ for $q << 1$, however, from the conservation of energy

$$q_{min} = \frac{2m}{\hbar^2} \frac{E(k) - E(k)}{K + K} \simeq \frac{m}{\hbar^2} \frac{E(k') - E(k)}{K} << 1 \tag{128}$$

which holds for $K >> k$ and $K >> 1$.

Also, from the conservation of momentum equation, the transitions for which

$$k' \simeq k + n \qquad n \neq 0$$

and (129)

$$K + k = K' + k' \qquad n = 0$$

are the only ones allowable.

Transitions Defined by $n = 0$ - In momentum state, define a polar coordinate system with K as the Z-axis and θ and ϕ as the polar angles defining K', then

$$q^2 = K^2 + K'^2 - 2\,KK' \cos\theta \tag{130}$$

or,

$$qdq = -\,K'\,Kd\,(\cos\theta)$$

and it follows that

$$d\Omega' = \frac{qdq}{KK'}\,d\phi \tag{131}$$

Substituting this into the transition rate expression and integrating gives

$$P_n(k, k') = \int\int_{K-K'}^{K>>K-K'} |C_n(k)|^2\,\frac{4m^2e^4K'}{\hbar^2 q^4 K}\,\frac{qdq}{KK'}\,d\phi \simeq |C_n(k)|^2\,\frac{4\pi e^4}{E^2_{kk'}} \tag{132}$$

where

$$E_{kk'} = E(k') - E(k)$$

and it is noted that P_n is independent of the energy of the primary particle except for the assumption $K>>k$. Since $E^2_{kk'}$ is in the denominator and $|C_n(k)|^2$ in the numerator, the number of these processes decrease for increasing n. It is also worth noting that the above expression is nearly identical with Woolridge's result.

Since k is usually smaller than $|n|$, the momenta of the secondaries are strongly influenced by the direction of n. The magnitude of this influence may be estimated by

$$E(k) \simeq \frac{\hbar^2 k^2}{2m} \tag{133}$$

then

$$E_{kk'} = \left(\frac{\hbar^2}{2m}\right)(n^2 + 2k \cdot n)$$

$$= \left(\frac{\hbar^2}{2m}\right)(n^2 + 2k_n n) \qquad (134)$$

So that for a given $|n|$ and $|k|$, the transition probability is maximum when k and n are in opposite directions and minimum when n and k are parallel. Thus, for a given n all those lattice electrons for which the components of k along n has value between k_n and $k_n + dk_n$ will gain energy between $E_{kk'}$ and $E_{kk'} + dE_{kk'}$. Denoting this group by $N(E_{kk'})\, dE_{kk'}$, the distribution loss is given by

$$P_n(\text{total})\, E_{kk'} dE_{kk'} = v_n < |C_n(k)|^2 > \frac{4\pi e^4}{E^2_{kk'}} N(E_{kk'})\, dE_{kk'} \qquad (135)$$

where v_n = the number of vectors n that have the same $|n|$, $< |C_n(k)| >$ = a suitable average to account for the fact that not all electrons in $N(E_{kk'}) dE_{kk'}$ have the same $C_n(k)$. Then, it is easily shown that the total energy loss of the primary path per unit path length is

$$-\left(\frac{dEp}{dx}\right)_n = \frac{8\pi e^4 Nm}{h^2 n^2} v_n < |C_n(k)|^2 >$$

$$= \frac{4\pi e^4 N}{E_o} v_n < |C_n(k)|^2 > \qquad (136)$$

which is independent of the energy of the primary particles. The above equation however, is only a rough approximation since by using the average value E_o, the higher probability of the smaller energy losses has not been considered. Similarly, the production of secondaries may be approximated by

$$P_n(k') \simeq \frac{4\pi e^4 N}{E_o^2} v_n < |C_n(k)|^2 > \qquad (137)$$

Transition Defined by $n = 0$ - This case corresponds to the Sommerfeld model of a metal. Due to the conservation of momentum lattice electrons gain momentum perpendicular to the wave vector $\vec{K}$ of the primary electron. Thus, if $\vec{K}$ is perpendicular to the surface, the lattice electrons gain momentum parallel to the surface. This led Woolridge to neglect this case. However, Baroody has shown that, by scattering, this case may still be included. Thus, it is not at all obvious that the case $n = 0$ should be neglected.

Suppose the wave vectors of a lattice electron and a primary electron are known. Then, the momentum law requires that $\vec{K} + \vec{k} = \vec{C}_o = \vec{K}' + \vec{k}'$. Introducing a polar coordinate system with C_o as the Z-axis and the angles θ and ϕ define K', then

$$k'^2 = K'^2 + C_o^2 - 2 C_o K' \cos\theta \tag{138}$$

and, by differentiation

$$-d(\cos\theta) = \frac{k'dk'}{K'}\left(\frac{2}{C_o} - \frac{\cos\theta}{K'}\right) \simeq \frac{k'dk'}{KK'}$$

so

$$d\Omega' \simeq \frac{k'dk'}{KK'}\, d\phi \tag{139}$$

which is valid for K>>k.

Substitution leads to the number of transitions per unit time whereby k is scattered into a state between k' and k'+ dk' to

$$P_o(k')\,dk' = \frac{4m^2e^4k'dk'}{\hbar^4 K^2}\int_o^{2\pi} \frac{d\theta}{|\vec{k}'-\vec{k}|^4} \tag{140}$$

where

$$C_o(k) = 1$$

For $k' >> k$, the integral reduces to $2\pi / k'^4$. This is equivalent to Baroody's assumption k = 0 for the momentum transfer process. For N free electrons,

$$P_{o(tot)}(k')dk' = \frac{8\pi m^2 e^4 N}{h^4 K^2}\,\frac{dk'}{k'^3} = \frac{\pi e^4 N}{E_p}\,\frac{dE_{k'}}{E^2_{k'}} \tag{141}$$

where

E_p = primary energy

$E_{k'}$ = energy loss in any one transition.

The assumption k'>>k is usually not allowed because the transition probability $|\vec{k}' - \vec{k}|$ is most often small. This problem may be circumvented as follows: multiply $P_o(k')dk'$ by the number of lattice electrons that may be scattered into states k' by an increase of momentum $\hbar|\vec{k}'-\vec{k}|$. If α is the angle

between $\vec{k}$ and $\vec{k}'$ and this number is equal to $k^2 dk \sin\alpha \, d\alpha / 2\pi^2$. Integration of this expression over α and ϕ then yields,

$$P_{o(tot)}(k')dk' = \frac{8m^2e^4}{\pi\hbar^4K^2} k'dk' \int_0^{k_m} \frac{k^2dk}{(k'^2 - k^2)^2} \tag{142}$$

where k_m is the wave number of an electron at the top of the Fermi distribution. Integration over k gives

$$P_{o(tot)}(k')dk = \frac{2me^4}{\pi\hbar^2 Ep} k'dk' \left[\frac{k_m}{k'^2 - k_m^2} - \frac{1}{2k'} \log\left(\frac{k'+k_m}{k'-k_m}\right) \right] \tag{143}$$

Putting $k_m^3 = 3\pi^2 m$ and forming an expansion in terms of k_m/k' this expression reduces to Eq. (141).

To obtain the distribution of energy losses, introduce $E_{kk'} = \hbar^2(k'^2 - k^2)/2m$ as variable instead of k' in Eq. (142) and integrate over k, thus

$$P_{o(tot)}(E_{kk'})dE_{kk'} = \frac{\pi e^4 N}{Ep} \frac{dE_{kk'}}{E^2_{kk'}} \qquad E_{kk'} > E_m$$

$$= \frac{\pi e^4 N}{Ep} \left[1 - \left\{ 1 - \left(\frac{E_{kk'}}{E_m} \right)^{3/2} \right\} \right] \frac{dE_{kk'}}{E^2_{kk'}} \qquad E_m > E_{kk'} \tag{144}$$

The total energy loss per unit path length is given by

$$-\left(\frac{dEp}{dx}\right)_{n=0} = \frac{\pi e^4 N}{Ep} \left[\frac{8}{3} - \log 4 + \log \frac{Ep}{E_m} \right] \tag{145}$$

which may also be written

$$-\left(\frac{dEp}{dx}\right)_{n=0} = \frac{\pi e^4 N}{Ep} \log\left(2\frac{Ep}{E_i}\right) \tag{146}$$

where

$$E_i = 8 E_m e^{-8/3} = 0.55 E_m \tag{147}$$

The Approximation of Strongly Bound Electrons - For strongly bound electrons, the wave functions are nearly identical to the atomic wave functions. This means that the wave function of a lattice point defined by the vector r_i is appreciable only in the range $|\vec{r} - \vec{r}_i|$ of order of the atomic nucleus. Thus, since $q \sim q_{min}$,

$$e^{i\vec{q}\cdot\vec{r}} = \left[1 + i\vec{q}\cdot(\vec{r}-\vec{r}_i)\right] e^{i(\vec{q}\cdot\vec{r}_i)} \tag{148}$$

So, using the orthogonality of $\psi_k(r)$ and $\psi_{k'}(r)$ leads to

$$|I^2| = \left|\int\left\{\vec{q}\cdot(\vec{r}-\vec{r}_i)\right\}\psi_k(r)\,\psi_{k'}^*(r)\,dr\right|^2 = q^2\,|L_{kk'}|^2 \tag{149}$$

where $|L_{kk'}|^2$ is the optical transition probability and is zero unless the reduced wave vector is the same before and after transition.

The number of transitions $P(kk')$ may then be written

$$P(kk') = \frac{4\pi me^4}{\hbar^2 Ep}\,|L_{kk'}|^2 \log\frac{q_{max}}{q_{min}} \tag{150}$$

where

$$q_{min} = K - K' = mE_{kk'}/h^2K \tag{151}$$

and

$$q_{max} = K$$

Thus,

$$P(kk') = \frac{4\pi me^4}{\hbar^2 Ep}\,|L_{kk'}|^2 \log\frac{2Ep}{E_{kk'}}$$

$$= \frac{2\pi e^4}{Ep}\,\frac{f_{kk'}}{E_{kk'}} \log\frac{2Ep}{E_{kk'}} \tag{152}$$

where

$$f_{kk'} = \frac{2m}{h^2}\,E_{kk'}\,|L_{kk'}|^2 \tag{153}$$

Then, the distribution of energy losses suffered by the primary may be written

$$P(E_{kk'})\,dE_{kk'} = \text{Const}\;f_{kk'}N(E_{kk'})\,\frac{dE_{kk'}}{E_{kk'}} \tag{154}$$

where $N(E_{kk'})dE_{kk'}$ is the number of transitions giving rise to energy losses in the defined range. The energy loss per unit path length may be derived as

$$-\left(\frac{dEp}{dx}\right) = \frac{2\pi e^4}{Ep}\,N_a \sum_{k'}\sum_{k} f_{kk'} \log\frac{2Ep}{E_{kk'}} \tag{155}$$

Introducing the atomic number Z through the equation

$$Z' \log E'_i = \sum_{k'}\sum_{k} f_{kk'} \log E_{kk'} \tag{156}$$

the above may also be written

$$-\left(\frac{dEp}{dx}\right) = \frac{2\pi e^4}{Ep} N_a Z' \log\left(\frac{2Ep}{E_i}\right) \tag{157}$$

All of the above approximations should apply to those energy bands for which it is most fitting, allowing of course for a certain amount of overlapping. For instance, the free electron approximation would be expected to hold reasonably well for the valence electrons of the alkali metals whereas for valence electrons of other metals a combination of $n = 0$ and $n \neq 0$ would probably be more suitable. The contribution of the innermost electronic shells to the production of secondaries and to the energy losses suffered by the primaries is probably best described by the tight binding approximation.

Van Der Ziel's Theory [38] - Dekker and Van Der Ziel [41] unified some of the existing theories, however, due to the use of the coulomb interaction energy, this unification has many of the same difficulties of the previous works. Some of these difficulties are:

a) In a single collision between a primary and lattice electron the probability $P(E_{kk'})\, dE_{kk'}$ of an energy loss between $E_{kk'}$ and $E_{kk'} + dE_{kk'}$ becomes infinite for $E_{kk'} \longrightarrow 0$.

b) The probability $P(k')dk'$ of a transition of a lattice electron to an energy state having an absolute value of the wave vector between k' and $k' + dk'$ becomes infinite at the Fermi level.

c) The rate of energy loss $\left(\frac{dEp}{dx}\right)$ due to the lattice electron for a primary electron of energy Ep varies as $E_p^{-1} \log\left(\frac{Ep}{E'_o}\right)$ for very small E'_o.

In this work, Van Der Ziel attempts to correct this deficiency by use of a screened coulomb interaction, i.e., by use of

$$V(R, r) = \frac{e^2}{|\vec{R} - \vec{r}|} e^{-\lambda|\vec{R}-\vec{r}|} \tag{158}$$

where λ is determined by the properties of the electron gas and is estimated $\lambda \simeq 10^8\ cm^{-1}$ for a metal.

It is assumed that the metal is a cube of volume 1 cm^3 and that the primary beam has the intensity 1 electron per cm^2 per sec. and that energy is conserved in the process, i. e.

$$h^2K^2/2m + E = h^2K'^2/2m + E'. \tag{159}$$

Then, from Van Der Ziel and Dekker's work,

$$P(K, k \rightarrow K', k')\, d\Omega' = \frac{m^2(K'/K)}{4\pi^2\hbar^4} J^2 |I|^2 d\Omega' \tag{160}$$

where

$$J = \int V(R, r)\, e^{i\vec{q}\cdot(\vec{R} - \vec{r})} dR \tag{161}$$

$$I = \int \psi_k(r)\, \psi_{k'}{}^*(r)\, e^{i\vec{q}\cdot\vec{r}}\, dr$$

which has been shown to be valid for any arbitrary interaction V(R, r). Then, by substituting V(R, r),

$$J = \frac{4\pi e^2}{q^2+\lambda^2} \tag{162}$$

and

$$P(K, k \rightarrow K - k') = \frac{4m^2e^4}{\hbar^4(q^2+\lambda^2)^2} |T|^2 d\Omega' \tag{163}$$

For the case $\lambda \rightarrow 0$, then V(R, r) reduces to the coulomb potential and P(Kk → K'k) goes to Dekker and Van Der Ziel's solution. To evaluate the production of secondaries, (I) must be evaluated in terms of weakly and strongly bound lattice electrons independently.

Weakly Bound Lattice Electrons - For weakly bound lattice electrons, $\psi_k(r)$ is in the form of the Bloch function $U_k(r)e^{i\vec{k}\cdot\vec{r}}$ which may be expanded by Fourier series since $U_k(r)$ contains the periodicity of the lattice to

$$\psi_k(r) = \Sigma_n C_n(k)\, e^{i(\vec{n}+\vec{k})\cdot\vec{r}}$$

and

$$\psi_k(r) = \Sigma_m C_m(k')\, e^{i(\vec{m}+\vec{k})\cdot\vec{r}} \tag{164}$$

which then yields for I,

$$I = \sum_n \sum_m C_n(k)\, C_m{}^*(k') \tag{165}$$

if $\vec{C} = \vec{K} + \vec{k} + \vec{n} - \vec{m} = \vec{K'} + \vec{k'}$ (momentum law) and zero otherwise;

$-h(n - m) = -\hbar p$ is the momentum absorbed by the lattice.

For a given $\hbar p$

$$P_p(K, k \rightarrow K', k')\, d\Omega' = \left|\sum_m C_{m+p}(k)\, C_m^*(k')\right|^2 \times \frac{4m^2e^4(K'/K)}{h^4(q^2+\lambda^2)^2}\, d\Omega' \qquad (166)$$

where

$$|\vec{K} - \vec{K'}| = |\vec{k'} - \vec{k} - \vec{p}| \qquad (167)$$

Introducing a polar coordinate system with $\vec{C}_p = (\vec{K}+\vec{k}+\vec{p})$ as the Z-axis. Then, since $C_p \simeq K$ if $K \gg |k+\rho|$

$$d\Omega' = \frac{k'dk'}{C_pK'}\, d\phi = \frac{k'dk'}{KK'}\, d\phi \qquad (168)$$

so that

$$P_p(k')dk' \frac{4m^2e^4}{\hbar^4K^2}\, k'dk' \int_0^{2\pi} \frac{d\phi}{(|\vec{k'}-\vec{k}+\vec{p}|^2+\lambda^2)^2} \left|\sum_m C_{m+p}(k)C_m^*(k')\right|^2 \qquad (169)$$

Now, have two cases for momentum $-\hbar p$ taken up by the lattice, a) $p \neq 0$, and b) $p = 0$. For $\lambda = 0$, these cases reduce to Woolridge's and Baroody's theory respectively.

Comparing the cases $p \neq 0$ and $p = 0$,

$$\left|\sum_m C_{m+p}(k)\, C_m^*(k')\right| \ll 1 \qquad (p \neq 0)$$

$$\simeq 1 \qquad (p = 0) \qquad (170)$$

Then $p \neq 0$ has smaller probability than for $p = 0$. For $\lambda = 0$ this is offset by the factor $|\vec{k'} - \vec{k} - \vec{p}\,|^{-4}$ has a sharp maximum around $k' \simeq (k + p)$, but for $\lambda = 0$ this is no longer true. The unimportance of $p \neq 0$ is further strengthened by the fact

$$\left|\sum_m C_{m+p}(k)\, C_m^*(k')\right| = 0 \quad \text{for} \quad k' = k + p \qquad (171)$$

Thus, Woolridge's mechanism is unimportant for the screened potential and it is sufficient only to consider the case $p = 0$ (Baroody's mechanism).

Assuming $k' >> k$,

$$P(k')\, dk' = \frac{8\pi m^2 e^4}{h^4 K^2} \frac{k' dk'}{(k'^2+\lambda^2)^2} \tag{172}$$

and the rate of energy loss between $E_{kk'}$ and $E_{kk'} + dE_{kk'}$ occurs as

$$P(E_{kk'})\, dE_{kk'} = \frac{\pi\, Ne^4}{Ep} \frac{dE_{kk'}}{(E_{kk'} + E_o)^2} \tag{173}$$

where

N = conduction electron density

$$E_o = \frac{h^2}{2m} \lambda^2$$

$$Ep = \frac{h^2}{2m} K^2$$

$$E_{kk'} = E' = \frac{h^2}{2m} k'^2 = \text{energy loss.} \tag{174}$$

The rate of energy loss is therefore

$$-\frac{dEp}{dx} = \int_o^{Ep} E_{kk'}\, P(E_{kk'})\, dE_{kk'}$$

$$= \frac{\pi Ne^4}{Ep} \left[\log\left(\frac{Ep + E_o}{E_o} \right) - \frac{Ep}{Ep + E_o} \right] \tag{175}$$

which, for $Ep >> E_o$ may be written

$$-\frac{dEp}{dx} = \frac{\pi Ne^4}{Ep} \log \frac{Ep}{\epsilon E_o} \tag{176}$$

where ϵ = base of natural logarithms.

The number of states in k space from which an electron may be scattered into a new state k' by an increase in momentum $h/(k'-k')$ is

$$2 \cdot 2\pi k^2 dk \sin\theta\, d\theta / 8\pi^3$$

where θ is the angle between k and k'. Then, the number of transitions per unit time may be written

$$P(k, k')\, dkdk' = \frac{8m^2 e^4 k' dk' k^2 dk}{\pi \hbar^4 K^2 \left[(k^2 + k'^2 + \lambda^2)^2 - (2kk')^2 \right]} \tag{177}$$

integrating this with respect to k between $k = 0$ and $k = k_m$ corresponding to the wave vector magnitude at the Fermi level gives

$$P_{tot}(k')\,dk' = \frac{4m^2e^4k'dk'}{\pi\hbar^4K^2}\left\{-\frac{1}{4k'}\log\left[\frac{(k'+k_m)^2+\lambda^2}{(k'-k_m)^2+\lambda^2}\right]\right.$$

$$\left.= \frac{1}{2\lambda}\tan^{-1}\left(\frac{2k_m\lambda}{k'^2+\lambda^2-k_m^2}\right)\right\}\frac{2k'k_m}{(k_m^2+k'^2+\lambda^2)}$$

Considering the log term as being a function of and making a series expansion gives

$$P(E')\,dE' \simeq \frac{\pi Ne^4}{Ep}\,\frac{dE'}{(E'+E_o)^2} \qquad (179)$$

where

$$E' = \left(\frac{h^2}{2m}\right)k'^2$$

Substituting

$E_{kk'} = \frac{\hbar^2}{2m}(k'^2-k^2)$ as the new variable of integration,

$E_o = \left(\frac{\hbar^2}{2m}\right)\lambda^2$ as a constant,

one can then integrate to get

$$P(E_{kk'})dE_{kk'} = \frac{\pi Ne^4dE_{kk'}}{Ep}\,\frac{3}{4E_oE_m}\left[1-\left(\frac{E_{kk'}+E_o}{2(E_oE_m)^{1/2}}\right)\tan\left(\frac{2(E_oE_m)^{1/2}}{E_{kk'}+E_o}\right)\right] \qquad (180)$$

for $E_{kk'} \geq E_m'$ and

$$P(E_{kk'})dE_{kk'} = \frac{\pi Ne^4dE_{kk'}}{Ep}\,\frac{3}{4E_oE_m}\left\{1-\left(\frac{E_{kk}+E_o}{2(E_oE_m)^{1/2}}\right)\tan\left(\frac{2(E_oE_m)^{1/2}}{E_{kk'}+E_o}\right)\right.$$

$$-\left(1-\frac{E_{kk'}}{E_m}\right)^{1/2}\left[1-\left(\frac{E_{kk'}+E_o}{2\left[E_o(E_m-E_{kk'})\right]^{1/2}}\right)\right.$$

$$\left.\left.\tan^{-1}\left(\frac{2\left[E_o(E_m-E_{kk'})\right]^{1/2}}{E_{kk'}+E_o}\right)\right]\right\} \qquad (181)$$

for $E_{kk'} \leq E_m$.

Thus, $P(E_{kk'}) \rightarrow 0$ if $E_{kk'} \rightarrow 0$ so that the previous infinity at this value has been eliminated. Further, this relationship shows the maximum value for $E_{kk'} \lesssim E_m$ observed by Rudberg and Slater who could only theoretically treat the free electrons as bound.

For the case $\lambda = 0$,

$$-\frac{dEp}{dx} = \frac{\pi Ne^4}{Ep} \log\left(\frac{Ep}{E'_o}\right) \tag{182}$$

as before.

Strongly Bound Electrons - As before, $\psi_k(\pi)$ in this case strongly resembles the atomic wave function whereby the approximation

$$e^{i(\vec{k}\cdot\vec{r})} = \left[1 + i\vec{q}\cdot(\vec{r}-\vec{r}_i)\, e^{i\vec{q}\cdot\vec{r}_i}\right] \tag{183}$$

and, by making use of the orthogonality of $\psi_k(r)$ and $\psi_{k'}(r)$ leads to

$$|I|^2 = q^2\left|\int \frac{1}{q}\,\vec{q}\cdot(\vec{r}-\vec{r}_i)\;\psi_k(r)\;\psi^*_{k'}(r)dr\right|^2 = |L_{kk'}|^2 q^2 \tag{184}$$

whereby substitution yields

$$P(K, k \rightarrow K', k') = \frac{4m^2e^4K'/K}{\hbar^4}\;|L_{kk'}|^2\;\frac{q^2}{(q^2+\lambda^2)^2}\;d\Omega' \tag{185}$$

choosing K as the Z-axis of a Polar coordinate system

$$d\Omega \simeq \frac{qdq}{KK'}\,d\phi \tag{186}$$

and integrating with limits $\phi = 0$ to $\phi = 2\pi$ and $q_{min} = m\frac{E_{kk'}}{\hbar^2 K}$ to $q_{max} = K$ gives

$$P(k, k') = \frac{4\pi me^4}{\hbar^2 Ep}\;L_{kk'}{}^2\left[\frac{1}{2}\log\frac{4Ep(Ep+E_o)}{E^2_{kk'}+4E_pE_o} - \frac{1}{2}\left(\frac{4E_oEp}{E^2_{kk'}+4E_oE_p} - \frac{E_o}{E_o+Ep}\right)\right] \tag{187}$$

For $Ep >> E_o$ and $E'^2_{kk} >> 4E_oEp$, this expression reduces to that found for the ordinary coulomb potential

$$P(k, k') = \frac{4\pi me^4}{\hbar^2 Ep}\;L_{kk'}{}^2\log\frac{2Ep}{E_{kk'}} \tag{188}$$

which occurs at the deeper-lying bound electrons. If, however, $Ep >> E_o$ and $E^2_{kk'} << 4E_oEp$, this reduces to

$$P(k, k') = \frac{4\pi me^4}{\hbar^2 Ep} L_{kk'}{}^2 \frac{1}{2} \log \frac{Ep}{\epsilon E_o} \tag{189}$$

Thus, the screened potential does not vary the theory for tightly bound lattice electrons significantly.

III. Theories of Miscellaneous Phenomena

A. The Cascade Theory - This theory concerns the secondary electrons introduced by previously formed secondaries diffusing back toward the surface of the material. The interaction between these electrons was shown earlier to be of the form of a screened coulomb potential and since the yield is essentially temperature independent, the electron-phonon interactions are negligible. The basic equation describing this process is

$$\frac{\partial N}{\partial t}(r, \Omega, E, t) + v \cdot \Delta N(r, \Omega, E, t) = -\frac{vN(r, \Omega, E, t)}{\lambda(E)}$$

$$+ S(r, \Omega, E, t) + \int dE' \int \frac{v'N(r, \Omega', E', t)}{\lambda(E')} F(\Omega', E', \Omega, E, d, \Omega') \tag{190}$$

where

$N(r, \Omega, E, t)$ = number of electrons as a function of r

Ω = unit vector in direction of velocity v

E = Energy

t = time

$\lambda(E)$ = mean free path of electron of energy E.

$F(\Omega', E', \Omega, E)$ = probability for an electron initially in the state Ω', E' is found after scattering in the state Ω, E.

$S(r, \Omega, E, t)$ = Source function = density of internal secondaries produced by the bombarding primaries.

Neglecting the exclusion principle, the normalization is obtained by

$$\int_o^{E'} dE' \int F(\Omega', E', \Omega, E)\, d\Omega = 2 \tag{191}$$

where the 2 represents the fact that for each electron in the cascade there are two after the scattering. For the case of normal incidence of primaries and for $\frac{\partial N}{\partial t} = 0$, and transforming to a polar coordinate system the above may be greatly simplified. Expanding N, F and S into spherical harmonics, thus,

$$N(z, \cos\theta, E) = \Sigma_\ell \left(\frac{2\ell+1}{4\pi}\right) N_\ell (z, E)\, P_\ell (\cos\theta)$$

$$S(z, \cos\theta, E) = \Sigma_\ell \left(\frac{2\ell+1}{4\pi}\right) N_\ell (z, E)\, P_\ell (\cos\theta) \qquad (192)$$

$$F(\Omega', E, \Omega, E) = F(\cos\phi, E, E') = \Sigma_\ell \left(\frac{2\ell+1}{4\pi}\right) F_\ell (E', E)\, P_\ell (\cos\theta) \qquad (193)$$

where ϕ = angle between Ω' and Ω.

Introducing

$$\psi_\ell = \frac{vN_\ell}{\lambda(E)} \qquad (194)$$

then, the following set of simultaneous integro-differential equations are obtained;

$$\psi_\ell = \lambda(E)\left[\left(\frac{\ell}{2\ell+1}\right)\frac{\partial \psi_{\ell-1}}{\partial z} + \left(\frac{\ell+1}{2\ell+1}\right)\frac{\partial \psi_{\ell+1}}{\partial z}\right]$$

$$+ \int_{-\infty}^{\infty} dE' F_\ell (E', E)\, \psi_\ell (z, E') + S_\ell (z, E) \qquad (195)$$

the solution of which is beyond the scope of this report.

B. Relation to Photoeffect - Since the production of secondary electrons and photoelectrons are both caused by lattice excitations there could be a similarity between them. Let the material be described by the dielectric constant $\epsilon = (n + ik)^2$. Then the intensity of a monochromatic wave in this material is

$$I(x, \omega) = I(\omega) e^{-2\frac{\omega k(\omega)}{c} x} \qquad (196)$$

For the case $x << \frac{c}{2\omega k(\omega)}$;

$$T(x,\omega) = I(\omega)\left(1 - 2\frac{\omega k(\omega)}{c} x\right) \qquad (197)$$

considering a disk of thickness $d << \frac{c}{2\omega k(\omega)}$, the energy

$$2\, I(\omega)\, \frac{\omega k(\omega)}{c}\, d \tag{198}$$

is absorbed for each unit surface area per sec. If this wave is composed of quanta $\hbar\omega$, the number of photo electrons $S_L(\omega)$ excited by $I(\omega)$ per cm^2 per sec in the disk is given by

$$S_L(\omega) = \frac{2d}{\hbar c}\, k(\omega)\, I(\omega) = \frac{2d}{\hbar c}\, \frac{n(\omega)\, k(\omega)}{|\epsilon(\omega)|^2}\, \frac{|\epsilon(\omega)|^2}{n(\omega)}\, I(\omega) \tag{199}$$

If $j_L(E, \theta, \omega)$ = current density of external photo electrons in the state (E, θ).

$I(\omega)$ = incident radiation energy, then

$$j_L(E, \theta, \omega) = h_L(E, \theta, \omega)\, S_L(\omega) = \frac{2d}{\hbar c}\, f_L(E, \theta, \omega)\, \frac{|\epsilon(\omega)|^2}{n(\omega)}\, I(\omega) \tag{200}$$

where

$$f_L(E, \theta, \omega) = h_L(E, \theta, \omega)\, \frac{n(\omega)k(\omega)}{|\epsilon(\omega)|^2} \tag{201}$$

which may be determined if the optical constants $n(\omega)$ and $k(\omega)$ are known.

From Fermi theory,

$$-\frac{dEp}{dx} = \frac{4e_o^2}{v_p^2} \int_o^\infty \omega\, \frac{n(\omega)k(\omega)}{|\epsilon(\omega)|^2}\, x\, K_o(x) K_1(x) d\omega \tag{202}$$

where

$$x = \frac{r_{min}}{v_p}\, \omega$$

$v_{min} \sim 10^{-8}$ cm

$K_o(x), K_1(x)$ = modified Bessel functions

and is valid for $\beta^2 \epsilon << 1$

If above is the energy losses of the electron caused by emission, then the number of quanta $\hbar\omega$ absorbed per unit path length in $d\omega$ is

$$\frac{4e_o^2}{\hbar \pi v_p^2}\, \frac{n(\omega)k(\omega)}{|\epsilon(\omega)|^2}\, x\, K_o(x) K_1(x) d\omega \tag{203}$$

which for any length d, one electron will emit

$$\frac{4e_o^2}{\hbar \pi v_p^2}\, \frac{n(\omega)k(\omega)}{|\epsilon(\omega)|^2}\, x K_o(x)\, K_1(x) d\omega \tag{204}$$

quanta $\hbar\omega$ per cm^2 per sec.

Assuming

$$j_S(E, \theta, \omega) = h_L(E, \theta, \omega)\, S_E(\omega) \tag{205}$$

Then

$$j_S(E, \theta) = \frac{4e_o^2 d}{\hbar \pi v_p^2} \int_o^\infty f_L(E, \theta, \omega)\, x K_o(x) K_1(x) dx \tag{206}$$

whereby if $f_L(E, \theta, \omega)$ is known the external secondary current density may be determined.

C. Angular Distribution of Secondaries - Faris [78] has approached this problem from diffusion theory. His argument starts from the expression for the density of excited electrons

$$(z) = \frac{\tau}{2L} \int_o^\infty \left[e^{-|\vec{z}-\vec{z}'|/L} - e^{-|\vec{z}+\vec{z}'|/L} \right] q(z')dz' \tag{207}$$

where

$L = \sqrt{\frac{\ell N \tau}{3}}$ = diffusion length

τ = mean lifetime of the excited electrons

v = mean velocity of excited electrons

ℓ = total mean free path of the excited electrons.

He next assumes

$$q(z') = q\ (\text{const});\ z' < z_{max} \tag{208}$$
$$= 0 \text{ otherwise}$$

and shows for $z < z_{max}$

$$(z) = \frac{\tau q}{2} \left[2 - \left[2e^{-z/L} - (e^{z/L} - e^{-z/L})\, e^{-z_{max}/L} \right] \right] \tag{209}$$

and for $z < z_{max}$

$$(z) = \frac{\tau q}{2}\, e^{-z/L} (e^{z_{max}/L}\, e^{-z_{max}/L} - 2) \tag{210}$$

He then states the probability that an electron will make its last collision at depth z and will arrive at the surface in the solid angle $d\Omega$ at the angle θ to the normal at

$$n(z, \theta) - dz\, d\Omega = K\rho(z) e^{-z \sec \theta/\ell}\, dz\, d\Omega \tag{211}$$

So by the integration,

$$\sigma(\theta)d\Omega = \int_0^{\infty} (z)\, e^{-z \sec/\ell}\, dz\, d\Omega$$

$$= \frac{\tau q}{2} (e^{\beta} + e^{-\beta} - 2) \int_{\beta L}^{\infty} e^{-z/L}\, e^{-z \sec/L}\, dz$$

$$= \tau q \frac{2}{L} (1 - e^{-\beta}) \cos^2\theta \qquad (212)$$

where $L >> \ell$ and $z_{max} = \beta L$.

Assuming the medium extends to infinity in all directions, and maintaining the same source distribution, Faris approaches this problem in a different manner. He then states that for this case

$$\rho(z) = \frac{\tau}{2L} \int_0^{z_{max}} \left[q e^{-|z - z'|/L} \right] dz' \qquad (213)$$

which, upon integrating

$$\rho(z) = \frac{\tau q}{2} (2 - e^{-z/L} - e^{z/L - z_{max}/L}) \qquad (z < z_{max})$$

$$= \frac{\tau q}{2} e^{-z/L} (e^{z_{max}/L} - 1) \qquad (z > z_{max}) \qquad (214)$$

and proceeds to show that the angular distribution of the secondaries as they arrive at the surface is

$$\sigma(\theta) = A_1\, \tau q \left(\frac{\ell}{L}\right)^2 (1 - e^{-\beta}) \left[\cos^2\theta + \frac{1}{2} \cos\theta \right] \qquad (215)$$

where, by using the relationship

$$k \sin\theta = k' \sin\theta \qquad (216)$$

The distribution becomes

$$\sigma(\theta) = K \left[\sqrt{1 - \frac{k'^2}{k} \sin^2\theta'} + \frac{1}{2} \right] \left(\frac{k'}{k}\right)^2 \cos\theta \qquad (217)$$

where k and k' are the propogation vectors inside and outside the surface respectively. When $\left(\frac{k'}{k}\right)^2$ approaches unity, the distribution inside and outside the surface is identical.

SUMMARY

To briefly summarize, the early theories were strictly empirical to attempt to explain experimental results. These theories are probably still sufficient to predict within experimental error results obtained from measurements taken of secondary emission. The difficulties arise from these theories when one attempts to explain the physical processes involved.

In this vein, Woolridge and others have developed and modified a quantum mechanical theory which appears at best only to approximate experimental results under the most rigid conditions and most general assumptions. However, these theories probably can not be greatly improved until more is known about the general solution to the many-body problem.

To summarize the starting points of these theories and some of the properties of them, a translation by D. Winder from the Encyclopedia of Physics 21 p. 284-85 (1956) is included.

APPENDICES

APPENDIX A

Mathematical Treatment of Quantum Theory

A. Woolridge Theory [62]

1. General Treatment - Assume Bloch functions for the lattice unperturbed eigenfunctions of the form

$$U_k(r)e^{i(\vec{k}\cdot\vec{r})} \tag{A-1}$$

for which

$$U_k(r) = \Sigma_m \beta_m(k)\, e^{2\pi i\left(\frac{\vec{m}\cdot\vec{r}}{\ell}\right)} \tag{A-2}$$

where

ℓ = lattice spacing

$\vec{m}$ = vector for which each component is a positive or negative unit vector,

and, from normalization,

$$\Sigma \int U_k^*\ U_k\, d\tau = 1 \tag{A-3}$$

Assuming the free electron unperturbed eigenfunction, the unperturbed time independent wave function for a system of two particles, one free and one bound is given by

$$\psi_{k,\,k}(\vec{r}) = \frac{1}{\Omega}\ U_k(\vec{r})\ e^{i\left[(\vec{K}\cdot\vec{R}) + (\vec{k}\cdot\vec{r})\right]} \tag{A-4}$$

and the time dependent wave function

$$\psi_{k,\,k}(t) = \psi_{k,\,k}(\vec{r})\ e^{-\frac{i}{\hbar}\left[E_k + E_K\right]t} \tag{A-5}$$

where $\psi^*\,\psi\, d\tau_R d\tau_r\, dt$ is the probability of finding a primary electron (free electron) in the volume element of $d\tau_R = dXdYdZ$ at a position R and a lattice electron in the volume element $d\tau_r = dxdydz$ at the position r at a given time t. Ω is the normalization constant. If one has an interaction potential U, then $\int \psi^*\, U\, \psi\, d\tau_r\, d\tau_r\, dt$ is the probability of interaction of the two particles. Defining $A_{k',\,K'}$ as this interaction probability and assuming the coulomb potential

$$U = \frac{e^2}{\vec{R} - \vec{r}} \tag{A-6}$$

Then,

$$A_{k',K'} = \int \psi^*_{k,K}(t)\ U \psi_{k,K}(t)\ d\tau\, dt$$

$$= \frac{e^2}{\Omega^2} \int U_k^*(r)\, e^{-i\left[\vec{K}\cdot\vec{R} + \vec{k}\cdot\vec{r}\right]} e^{-\frac{i}{\hbar}\left[E_k + E_K\right]t} \frac{1}{|\vec{R}-\vec{r}|}\, U_{k'}(\vec{r})\, e^{i\left[\vec{K}\cdot\vec{R} + \vec{k}\cdot\vec{r}\right]}$$

$$\times\, e^{-\frac{i}{\hbar}\left[E_{k'} + E_{K'}\right]t}\, d\tau\, dt$$

$$= \frac{e^2}{\Omega^2} \int U_k^*(r)\, U_{k'}(\vec{r})\, \frac{e^{i(\vec{K}'-\vec{K})\cdot\vec{R} + (\vec{k}'-\vec{k})\cdot\vec{r}}}{|R-r|}\, e^{\frac{i}{\hbar}\epsilon t}\, d\tau\, dt \qquad (A\text{-}7)$$

where

$$\epsilon = (E_{k'} + E_{k'}) - (E_k + E_K)$$

$$= \frac{e^2}{\Omega^2} \left[\frac{e^{\frac{i}{\hbar}\epsilon t} - 1}{\frac{i}{\hbar}\epsilon}\right] \int \frac{e^{i\left[\vec{K}' - \vec{K}\right]\cdot\vec{R}}}{|\vec{R}-\vec{r}|}\, e^{i(\vec{k}'-\vec{k})\cdot\vec{r}}\, U_k^*(\vec{r})\, U_{k'}(\vec{r})\, d\tau_R\, d\tau_r \qquad (A\text{-}8)$$

But Bethe [72] has shown

$$\int \frac{e^{i(\vec{K}' - \vec{K})\cdot\vec{R}}}{|\vec{R}-\vec{r}|}\, d\tau_R = \frac{4\pi\, e^{i(\vec{K}' - \vec{K})\cdot\vec{r}}}{|\vec{K}' - \vec{K}|^2} \qquad (A\text{-}9)$$

Hence

$$A_{k',K'} = \frac{4\pi e^2}{\Omega^2 |\vec{K}' - \vec{K}|^2} \left[\frac{e^{\left(\frac{i}{\hbar}\right)\epsilon t} - 1}{\left(\frac{i}{\hbar}\right)\epsilon}\right] \int e^{i\left[(\vec{K}'-\vec{K}) + (\vec{k}' - \vec{k})\right]\cdot\vec{r}}\, U_k^*(\vec{r})\, U_{k'}(\vec{r})\, d\tau_r$$

$$= \frac{4\pi e^2}{\Omega^2 S^2} \left[\frac{e^{(i/h)\epsilon t} - 1}{(i/h)\epsilon}\right] \int e^{i(\vec{S}+\vec{s})\cdot\vec{r}}\, U_k^*(\vec{r})\, U_{k'}(\vec{r})\, d\tau_r \qquad (A\text{-}10)$$

But

$$U_k^*(\vec{r})\, U_{k'}(\vec{r}) = \sum_{n,m} \beta_n^*(k)\, \beta_m(k)\, e^{2\pi i\, \frac{(\vec{m}-\vec{n})}{\ell}\cdot\vec{r}}$$

$$= \sum_{n,m} \beta_n(k)\, \beta_m(k)\, e^{2\pi i \frac{\vec{\rho}}{\ell}\cdot\vec{r}} \qquad (A\text{-}11)$$

where $\vec{\rho} = \vec{m} - \vec{n}$

Thus,

$$A_{k',K'} = \frac{4\pi e^2}{\Omega^2 S^2} \left[\frac{e^{(i/\hbar)\epsilon t} - 1}{(i/\hbar)\epsilon}\right] \sum_{n,m} \int e^{i\left(\vec{S}+\vec{s}+\frac{2\pi\vec{\rho}}{\ell}\right)\cdot\vec{r}}\, d\tau_r \qquad (A\text{-}12)$$

and then, the amplitude of the wave is given by

$$|A_{k',K'}|^2 = \frac{1}{\Omega^4}\left(\frac{4\pi e^2}{S^2}\right)^2 \left[\frac{e^{(i/\hbar)\,\epsilon t}-1}{(i/\hbar)\,\epsilon}\right]\left[\frac{e^{-(i/\hbar)\,\epsilon t}-1}{(i/\hbar)\,\epsilon}\right]$$

$$\times \left|\sum_{mn}\int \beta_n^*(\vec{k})\,\beta_m(\vec{k})\,e^{i(\vec{S}+\vec{s}+\frac{2\pi\vec{\rho}}{\ell})\cdot\vec{r}}\,d\tau_r\right|^2$$

$$= \frac{2t^2}{\hbar^2\Omega^4}\left(\frac{4\pi e^2}{S^2}\right)\left(\frac{1-\cos\epsilon t}{\epsilon^2 t^2}\right)\left|\sum_{mn}\int \beta_n^*(k)\,\beta_m(k)\,e^{i(\vec{S}+\vec{s}+\frac{2\pi\vec{\rho}}{\ell})\cdot\vec{r}}\,d\tau_r\right|^2 \qquad (A\text{-}13)$$

If Ω is large, the range of $\vec{K}'$ will be such that $(1-\cos\epsilon t)/(\epsilon t)^2$ may be considered constant. If $\vec{K}'_\rho = \vec{K}'$ for a given $\vec{k}, \vec{K}$ and $\vec{k}'$ allowed by the conservation of momentum, then by integration

$$|A_{k',K'_\rho}|^2 = \frac{1}{\Omega^2}\,\frac{16\pi^2 e^4}{\hbar^2}\,\frac{1}{S_\rho^4}\left|\sum_{n,m}\beta_n^*(k)\,\beta_m(k)\right|^2 t^2\,F(\epsilon_\rho t) \qquad (A\text{-}14)$$

where

$$F(\epsilon_\rho t) = \frac{2(1-\cos\epsilon\rho t)}{(\epsilon_\rho t)^2}$$

Since $\vec{\rho} = \vec{m} - \vec{n}$, one can rewrite the above as

$$|A_{k',K'_\rho}|^2 = \frac{1}{\Omega^2}\,\frac{16\pi^2 e^4}{\hbar^2}\,\frac{1}{S_\rho^4}\left|\sum_m \beta^*_{\rho+m}(\vec{k})\,\beta_m(\vec{k})\right|^2 t^2\,F(\epsilon_\rho t) \qquad (A\text{-}15)$$

Summing over all ρ gives

$$|A_{k'}|^2 = \sum_\rho |A_{k',k'_\rho}|^2 = \frac{1}{\Omega^2}\,\frac{16\pi^2 e^4 t^2}{\hbar^2}\sum_\rho\left[\frac{1}{S_\rho^4}\,F(\epsilon_\rho t)\left|\sum_m \beta^*_{\rho+m}(k)\beta_m(k)\right|^2\right] \qquad (A\text{-}16)$$

Converting this to an integral will give the number of lattice electrons which at time t have their wave vectors in range $d\tau_{k'}$ around k'. Thus,

$$dN = \frac{\Omega}{8\pi^3}\,\frac{1}{\Omega^2}\,\frac{16\pi^2 e^4 t^2}{\hbar^2}\left[\frac{1}{S_\rho^4}\,F(\epsilon\rho t)\left|\sum_m \beta^*_{\rho+m}(\vec{k})\right|^2\right] d\tau_{k'} \qquad (A\text{-}17)$$

for two particles, or

$$dN_\rho = J_p\,\Omega\,t^2\,\frac{2me^4}{\pi\hbar^3}\,\rho_\ell(k)\,\frac{1}{K}\left[\frac{1}{S_\rho^4}\,F(\epsilon_\rho t)\left|\sum_m \beta^*_{\rho+m}(k)\,\beta_m(k)\right|^2\right] d\tau_{k'} \qquad (A\text{-}18)$$

For N particles where

$$\rho_\ell = \frac{N_\ell}{\Omega}$$

$$J_p = \frac{KhNp}{m\Omega}$$

which reduces the problem to evaluating dN_ρ for a given ρ.

From conservation of momentum equation

$$\vec{S} + \vec{s} + \frac{2\pi\vec{\rho}}{\ell} = 0$$

and conservation of energy

$$k'^2 + K'^2 = k^2 + K^2$$

we know the constraining relationships on the final states $\vec{k}'$ and $\vec{K}'$. From Fig. A. 1 and the requirement that $\alpha < \frac{\pi}{2}$, it can be shown

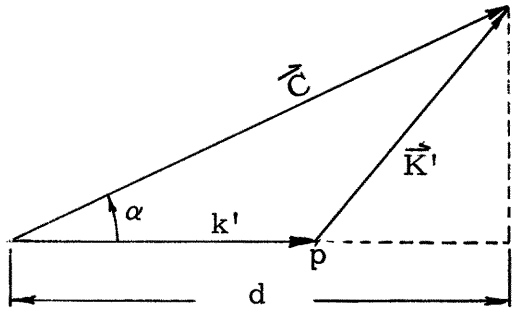

Fig. A. 1. Vector diagram of conservation of momentum. Principle $\vec{c} = \vec{k} + \vec{K} + \frac{2\pi\vec{\rho}}{\ell}$

that

$$k' = \frac{d}{2}\left[1 \pm (1 - \frac{D^2}{d^2})^{1/2}\right] \qquad \text{(A-19)}$$

where

$$\vec{c} = \vec{K} + \vec{k} + \frac{2\pi\vec{\rho}}{\ell}$$

$$D^2 = 2(c^2 - k^2 - K^2)$$

$$d = C \cos \alpha$$

If a sphere of radius

$$R = \left[\frac{1}{4}(C^2 - D^2)\right]^{1/2} \qquad \text{(A-20)}$$

is constructed with its center at the midpoint of C, then it is easily shown that P must lie on the surface of the sphere.

Now, to evaluate N_ρ, the above indicates splitting the problem into spherical coordinates by the substitution

$$d\tau_{k'} = dR\,d\sigma \tag{A-21}$$

where $d\sigma$ = spherical surface element.

Assume that t is large so $F(\epsilon\rho t)$ is much more varying than any other term. Then, all other terms may be considered constant and therefore one need only to evaluate

$$\int F(\epsilon t)\, dR = \int \frac{F(\epsilon t)\, d(\epsilon t)}{d(\epsilon t)} \tag{A-22}$$

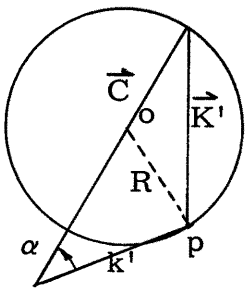

Fig. A. 2. Vector diagram of conservation of energy principle.

From Fig. A. 2.

$$k'^2 + K'^2 = 2R^2 + \frac{1}{2}\, C^2 = 2mE_{k'K'} / \hbar^2 \tag{A-23}$$

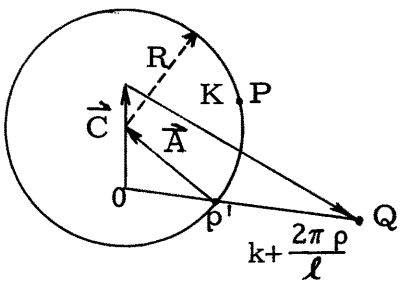

Fig. A. 3. Vector diagram showing the determination of S_{min}.

Or, from Fig. A.3.

$$2R^2 + \frac{1}{2}\ C^2 = \frac{2m}{\hbar^2}\ (h\epsilon + E_{k,K}) \tag{A-24}$$

Therefore

$$\frac{d(\epsilon t)}{dR} = \frac{2\hbar t R}{m} \tag{A-25}$$

so

$$\int F(\epsilon t)\, dR = \frac{m}{2\hbar t}\ \frac{1}{R} \int F(\epsilon t)\ d\,(\epsilon t) \tag{A-26}$$

where

$$\int F(\epsilon t)\, d(\epsilon t) = \int_{-\infty}^{\infty} \frac{2(1-\cos x)}{x^2}\ dx = 2\pi \tag{A-27}$$

Hence,

$$F(\epsilon t)\, dR = \frac{1}{t}\ \frac{\pi m}{\hbar}\ \ \frac{1}{R} \tag{A-28}$$

and

$$dN_\rho = J_p\ \Omega t\ \frac{2m^2e^4}{\hbar^4}\ \rho_\ell\,(k)\ \frac{1}{R}\ \frac{1}{K}\left[\frac{1}{S_\rho^4}\ \left|\sum_m \beta_{\rho+m}(k)\ \beta(k)\right|^2\right] d\sigma \tag{A-29}$$

In Fig. A.3., C is resolved into the components $\vec{K}$ and $\vec{k} + \frac{2\pi\vec{\rho}}{\ell}$. Defining

$$A = \frac{1}{2}\ \vec{C} - (\vec{k} + \frac{2\pi\vec{\rho}}{\ell})$$

$$= \frac{1}{2}\ (\vec{K} + \vec{k} + \frac{2\pi\vec{\rho}}{\ell}) - (\vec{k} + \frac{2\pi\vec{\rho}}{\ell}) \tag{A-30}$$

Then

$$A^2 = \frac{1}{4}\left[K^2 - 2\vec{K}\cdot(\vec{k} + \frac{2\pi\vec{\rho}}{\ell}) + (\vec{k} + \frac{2\pi\vec{\rho}}{\ell})^2\right] \tag{A-31}$$

but

$$R^2 = \frac{1}{4}\left[K^2 - 2\vec{K}\cdot(\vec{k} + \frac{2\pi\vec{\rho}}{\ell}) + k^2 - (\frac{2\pi\vec{\rho}}{\ell})^2 - 2\vec{k}\cdot\frac{2\pi\vec{\rho}}{\ell}\right] \tag{A-32}$$

Therefore

$$A^2 = R^2 + \frac{1}{2}\ \frac{2\pi\vec{\rho}}{\ell}\cdot\left[\frac{2\pi\vec{\rho}}{\ell} + 2\vec{k}\right] \tag{A-33}$$

Now, S is the length of the vector joining Q to a point P on the sphere so a possible minimum value of S is given by

$$S_{min} = A - R \tag{A-34}$$

If the primary electrons have high energy so that $\frac{2\pi\vec{\rho}}{\ell} << \vec{K}$ and $\vec{k} << \vec{K}$, then $R \sim \frac{1}{2}\ K$ so that

$$A \sim R + \frac{1}{4}\left[\frac{\frac{2\pi\vec{\rho}}{\ell}\cdot\left(\frac{2\pi\vec{\rho}}{\ell}+2\vec{k}\right)}{R^2}\right]R \tag{A-35}$$

or

$$S_{min} \sim \frac{1}{4}\,\frac{\frac{2\pi\vec{\rho}}{\ell}\cdot\left[\frac{2\pi\vec{\rho}}{\ell}+2\vec{k}\right]R}{R^2} \tag{A-36}$$

Since $\left|\frac{2\pi\vec{\rho}}{\ell}\right| << R$,

$$S_{min} << R.$$

Thus, $\frac{1}{S^4}$ is only important over a small portion of the sphere and the Fourier components in the expression for dN_ρ may be treated as constants. As a consequence, one must evaluate $\int \frac{d\sigma}{S^4}$. This is easily accomplished over the surface of the sphere as

$$\frac{d\sigma}{S^4} = \frac{4\pi R^2}{(A^2-R^2)^2} = \frac{16\pi R^2}{\left[\frac{2\pi\vec{\rho}}{\ell}\cdot\frac{2\pi\vec{\rho}}{\ell}+2\vec{k}\right]^2} \tag{A-37}$$

Thus, upon substitution

$$\frac{dN\rho}{dt} = \Omega\,\frac{16\pi m^2 e^4}{\hbar^4}\,\rho_\ell(\vec{k})\,\frac{J_p\left[\frac{2R}{K}\right]\rho}{\left[\frac{2\pi\vec{\rho}}{\ell}\cdot\left(\frac{2\pi\vec{\rho}}{\ell}+2\vec{k}\right)\right]}\left|\sum_m \beta^*_{\rho+m}(\vec{k})\beta_m(\vec{k})+\frac{2\pi\vec{\rho}}{\ell}\right| \tag{A-38}$$

where $\frac{dN\rho}{t}$ has been replaced by $\frac{dN\rho}{dt}$ to indicate the time rate of transitions. For large K, $\frac{2R}{K} \sim 1$ and $\frac{dN\rho}{dt}$ is independent of the primary energy.

For usually observed secondaries, $\vec{k}'$ and $\vec{K}$ have approximately opposite directions. Since $\vec{k}' \sim \vec{K} + \frac{2\pi\vec{\rho}}{\ell}$; $R \gtrsim \frac{1}{2}K$ for $|\vec{K}| > \left|\vec{k}+\frac{2\pi\vec{\rho}}{\ell}\right|$. Because $\vec{k}\cdot\vec{\rho}$ is inhomogeneous, one may choose $\vec{k} = \vec{0}$. Therefore, the expression for A is valid as long as $\left(\frac{2\pi\vec{\rho}}{\ell}\right)^2 / K^2 << 1$. This means that $\frac{1}{S^4}$ has a large value over only a small portion of the sphere and is a good approximation allowing the Fourier components in the integration to be considered constant and allows the approximation

$$\vec{k}' = \vec{k} + \frac{2\pi\vec{\rho}}{\ell} \tag{A-39}$$

A more detailed investigation shows that even when $\left|\vec{k}+\frac{2\pi\vec{\rho}}{\ell}\right| \sim \vec{K}$ and when $\vec{k}'$ and $\vec{K}$ do not have opposite directions the same assumptions on $\frac{1}{S^4}$

and the Fourier components hold. In this range, the factor $\left[\frac{2R}{K}\right]_\rho$ becomes important. Since only primary energies very much greater than the Fermi energy will be considered, $\frac{k^2}{K^2}$ may be neglected. Hence, one may write

$$F_\rho(\vec{k}, \vec{K}) = \left[\frac{2R}{K}\right]_\rho = \left[1 - \frac{(\vec{k} + \frac{2\pi\vec{\rho}}{\ell})}{K^2} - \frac{2\vec{K}\cdot(\vec{k} + \frac{2\pi\vec{\rho}}{\ell})}{K^2}\right]^{1/2} \qquad \text{(A-40)}$$

so

$$\frac{dN\rho}{dt} = \Omega \frac{16\pi m^2 e^4}{\hbar^4} \rho_\ell(\vec{k}) J_p \frac{|b_p(\vec{k})|^2}{\left[\left(\frac{2\pi\vec{\rho}}{\ell}\right)\cdot\left(\frac{2\pi\vec{\rho}}{\ell} + 2\vec{k}\right)\right]^2} F_\rho(\vec{k}, \vec{K}) \qquad \text{(A-41)}$$

where

$$b_p(k) = \sum_m \beta^*_{\rho-m}(\vec{k})\beta_m(\vec{k})$$

B. Free Electron Approximation - To calculate the production rate of electrons which are scattered into states of lower energy and which move away at 45^0, for normal incidence, one must merely integrate the Rutherford scattering formula, thus

$$\int_{\alpha=\frac{\pi}{4}}^{\alpha=\alpha_{max}} \frac{e^2}{m^2v^4}(\sec^4\alpha + \csc^4\alpha)\ 4\cos\alpha\ dw \qquad \text{(A-42)}$$

where α_{max} = angle at which the secondary beam is normal to the target surface.

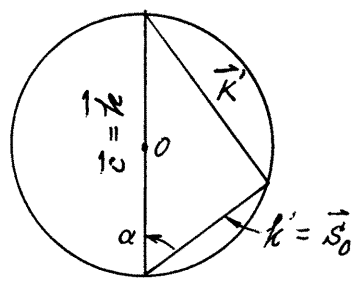

Fig. A. 4. Special case of momentum principle for which $\rho = 0$.

From Fig. A.4. it is clear that the energy of an electron scattered into an angle α is $E_p \cos^2\alpha$. Hence,

$$(E_p \cos^2 \alpha_{max}) \cos^2 \alpha_{max} = W_a \tag{A-43}$$

or

$$\cos^2 \alpha_{max} = \left(\frac{W_a}{E_p}\right)^{1/2} \tag{A-44}$$

Therefore, the rate of production of electrons which can escape from the back of the target is given by

$$\frac{1}{\rho_\ell}\frac{1}{J_p}\frac{1}{\Omega t}\int (dN_o)_{tot} = \frac{e^4}{E_p^2}\int_{\alpha=\frac{\pi}{4}}^{\alpha=\alpha_{max}} (\sec^4\alpha + \csc^4\alpha)\cos\alpha \, dw$$

$$\sim \frac{\pi e^4}{E_p^2}\left[\left(\frac{E_p}{W_a}\right)^{1/2} - 1\right] \tag{A-45}$$

where the approximation $W_a << E_p$ has been made and by letting $E_p^2 = \frac{m^2v^4}{4}$.

From the expression for the transition probability and assuming $\vec{\rho}$ and $\vec{k}$ to coincide in direction along one of the axes of the lattice, the number of forward electrons due to the "bound" term for which $|\vec{\rho}| = 1$ is given by

$$\frac{1}{\rho_\ell J_p}\frac{1}{\Omega t}(N_1) \sim \frac{16\pi m^2 e^4}{\hbar^4}\frac{|b_1(\vec{k})|^2}{\left(\frac{2\pi}{\ell}\right)^4} \tag{A-46}$$

where $E_p >> 0$. If $\frac{h^4}{m^2} = 4E_p^2/K^4$,

$$\frac{1}{\rho_\ell J_p}\frac{1}{\Omega t} N_1 = \frac{4\pi e^4 |b_1(\vec{k})|^2}{E_p^2 (2\pi/\ell \vec{K})^4} \tag{A-47}$$

or, since

$$\left(\frac{2\pi}{\ell \vec{K}}\right)^4 = \left(\frac{E_o}{E_p}\right)^2 \tag{A-48}$$

$$\frac{1}{\rho_\ell J_p}\frac{1}{\Omega t} N_1 \sim \frac{4\pi e^4 |b_1(\vec{k})|^2}{E_p^2 (E_o/E_p)^2} \tag{A-49}$$

and, by division

$$\frac{N_1}{N_o} = \frac{4|b_1(\vec{k})|^2 (E_p/E_o)^2}{\left[(E_p/W_a)^{1/2} = 1\right]} \tag{A-50}$$

C. Application of Results - For $\rho = 1$,

$$\frac{1}{\Omega}\frac{dN\rho}{dt} = \frac{16\pi m^2 e^4}{h^4} \rho_\ell J_p \frac{|b_\rho|^2}{\left(\frac{2\pi}{\ell}\right)4} F_\rho(\vec{K}) \tag{A-51}$$

where

$$F_\rho(\vec{K}) = \left[K^2 - \left(\frac{2\pi}{\ell}\right)^2 + \frac{2mEF}{\hbar^2} - 2\vec{K}\cdot\left(\frac{2\pi\vec{\rho}}{\ell}\right)\right]^{1/2} \frac{1}{K^2} \tag{A-52}$$

and $|b_\rho|^2 = |b_\rho(\vec{k})|^2$ averaged over all lattice electrons.

Assuming an inhomogeneous surface, the fraction of all the cyrstallites which have one of their six directions for $|\vec{\rho}| = 1$ within the solid angle dw making an angle θ with the normal to the target surface is $6\frac{d\omega}{4\pi}$. Thus, a volume element $d\Omega$ averaged over a time dt emits a number of secondaries dN at directions included within the solid angle $d\omega$ at an angle θ to the normal where

$$dN = \frac{16\pi m^2 e^4}{h^4} J_p \rho_\ell \frac{b_1^2}{\left(\frac{2\pi}{\ell}\right)4} F_1(K, \theta)\, 6\, \frac{d\omega}{4\pi}\, d\Omega\, dt \tag{A-53}$$

where, for normal incidence,

$$F_1(K, \theta) = \left[1 - \left(\frac{2\pi}{K\ell}\right)^2 + \frac{2mEF}{(\hbar K)^2} + \frac{4\pi}{K\ell}\cos\right]^{1/2} \tag{A-54}$$

If $d\Omega$ lies directly on the surface of the target, then the emitted secondaries are those for which their directions make angles of less than θ_{max} with the normal, where

$$(E_o + E_F)\cos^2\theta_{max} = W_a \tag{A-55}$$

and

$W_a = E_F(\max) + \phi$ (work function)

= normal component of energy which the electron must have to escape.

Also,

$$E_o = \left(\frac{\hbar^2}{2m}\right)\left(\frac{2\pi}{\ell}\right)^2 \tag{A-57}$$

The fraction of the secondaries which can escape is

$$f = \frac{\int_{\theta=0}^{\theta_{max}} F_1(K,\theta)\,\frac{d\omega}{4\pi}}{\int_0^{\pi} F_1(K,\theta)\,\frac{d\omega}{4\pi}} \tag{A-58}$$

which may be evaluated. The result may be expanded as

$$f = \frac{1}{2}\left\{1 - \left(\frac{W_a}{E_o+E_F}\right)^{1/2}\right\} + \frac{1}{4}\,\frac{2\pi}{\ell K}\left\{1 - \frac{W_a}{E_o E_F}\right\} + 0\left|\left(\frac{2\pi}{\ell K}\right)\right|^2 \tag{A-59}$$

where it can be easily shown that

$$\int_0^{\pi} F_1(K,\theta)\,\frac{d\omega}{4\pi} = 1 + 0\left(\frac{2\pi}{K}\right)^2 \tag{A-60}$$

Assuming the exponential absorption law

$$g(x) = f(x)e^{-\gamma x} \tag{A-61}$$

Then the expression for the yield is

$$\delta = \frac{96\pi m^2 e^4}{\hbar^4}\,\rho_\ell\,\frac{b_1^2}{\left(\frac{2\pi}{\ell}\right)4}\int_0^{\ell(E_p)} f(x)e^{-\gamma x}dx \tag{A-62}$$

where $\ell(Ep)$ is the distance the primary electrons travel into the material before they lose too much energy to produce secondary electrons.

When the bombarding energy is high,

$$f(x) = \frac{1}{2}\left\{1 - \left(\frac{W_a}{E_o+E_F}\right)^{1/2}\right\} \tag{A-63}$$

so

$$\delta_\infty = \frac{96\pi m^2 e^4}{h^4}\,\rho_\ell\,\frac{|b_1|^2}{\left(\frac{2\pi}{\ell}\right)4}\,\frac{1}{\gamma}\,\frac{1}{2}\left\{1 - \frac{W_a}{(E_o+E_F)^{1/2}}\right\} \tag{A-64}$$

or, by dividing,

$$\frac{\delta}{\delta_\infty} = \frac{\gamma \int_0^{\ell(E_p)} f(x) e^{-\gamma x} \, dx}{\frac{1}{2}\left\{1 - \frac{W_a}{(E_o + E_F)}1/2\right\}}$$

$$= \left\{1 - e^{\gamma \ell(E_p)}\right\} + \frac{1}{2}\left\{1 + \frac{W_a}{(E_o + E_F)}1/2\right\} \int_0^{\ell(E_p)} \frac{2\pi}{\ell K(x)} e^{-\gamma x} dx \qquad \text{(A-65)}$$

The number of secondaries produced by a primary electron traveling a distance dx into the target is given by

$$dn = \frac{96\pi m^2 e^4}{\hbar^4} \rho_\ell \frac{|b_1|^2}{\left(\frac{2\pi}{\ell}\right)^4} dx \qquad \text{(A-66)}$$

The energy lost by the primary is thus

$$-dE = E_o \, dn$$

$$= E_o \frac{96\pi m^2 e^4}{\hbar^4} \rho_\ell \frac{|b_1|^2}{\left(\frac{2\pi}{\ell}\right)^4} dx \qquad \text{(A-67)}$$

when the primary has penetrated a depth

$$\ell(E_p) = \frac{E_p - E_o}{-\left(\frac{dE}{dx}\right)} \qquad \text{(A-68)}$$

its energy is only E_o and it can produce no more secondaries, then, it can be shown that

$$\ell(E_p) = \frac{1}{2} \frac{\left\{1 - \frac{W_a}{E_o + E_F}\right\}^{1/2}}{\gamma \delta_\infty} \left\{\frac{E_p}{E_o} - 1\right\} \qquad \text{(A-69)}$$

where

$$E(x) = E_p, x \; E_o \frac{\gamma \delta_\infty}{\frac{1}{2}\left\{1 - \left(\frac{W_a}{E_o + E_F}\right)\right\}^{1/2}} \qquad \text{(A-70)}$$

or

$$\frac{E(x)}{E_o} = \frac{E_p}{E_o} - \frac{x\gamma\,\delta_\infty}{\frac{1}{2}\left\{1 - \left(\frac{W_a}{E_o+E_F}\right)^{1/2}\right\}} \tag{A-71}$$

Then, by combining equations

$$\frac{\delta}{\delta_\infty} = \left\{1 - \exp\left[\frac{\frac{1}{2}\left\{1 - \left(\frac{W_a}{E_o+E_F}\right)^{1/2}\right\}}{\delta_\infty}\left(\frac{E_p}{E_o} - 1\right)\right]\right.$$

$$\left. + \frac{1}{2}\left\{1 + \left(\frac{W_a}{E_o+E_F}\right)^{1/2}\right\}\int_o^{\frac{\frac{1}{2}\left\{1 - \left(\frac{W_a}{E_o+E_F}\right)^{1/2}\right\}\left(\frac{E_p}{E_o} - 1\right)}{\delta_\infty}} \frac{e^{-v}dv}{\left[\frac{E_p}{E_o} - \frac{\delta_\infty\, v}{\frac{1}{2}\left\{1 - \left(\frac{W_a}{E_o+E_F}\right)^{1/2}\right\}}\right]}\right\} \tag{A-72}$$

where

$$\frac{\ell K(x)}{2\pi} = \left(\frac{E(x)}{E_o}\right)^{1/2}$$

APPENDIX B

As a separate entity, the specific treatment of the work function ϕ of cesium on tungsten is treated here. The most complete article found is that of Chapter XII of NASA Technical Translation NASA TT F-73 which is included here in its entirety.

CESIUM ON TUNGSTEN

In 1923, Langmuir and Kingdon (Ref. 39), observed a large emission of thermal electrons from tungsten in cesium vapor of low density, even at relatively low temperatures of the tungsten. Thus, for $T = 690^0$ K(i. e., 417^0C, at which temperature the filament is still dark) and for a pressure of the cesium vapor corresponding to a temperature $t = 30^0$C, the density of the current was equal to $j = 10^{-4} \frac{a}{cm^2}$,

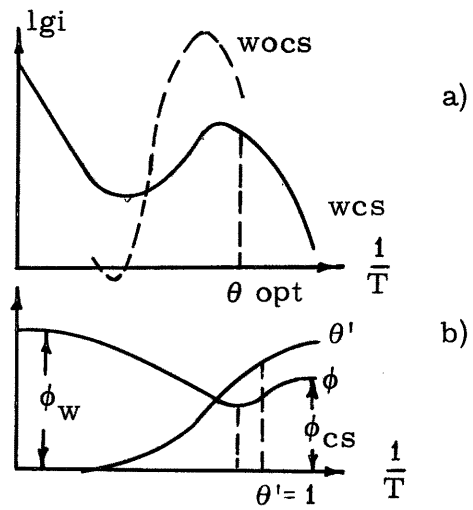

Fig. 51

while for tungsten at this temperature $j \sim 10^{-26} \frac{a}{cm^2}$. If this temperature is raised or lowered, the cesium vapor pressure remaining constant, the emission current decreases. The emission increases even more sharply, for oxidized tungsten in cesium vapor. For instance, for $t = 30^0$C and $T = 1000^0$K, the

emission current from oxidized tungsten is $j = 0.35 \frac{a}{cm^2}$, while the current from pure tungsten is $10^{-24} \frac{a}{cm^2}$, and that from oxidized tungsten not surrounded by cesium vapor is still lower.

The characteristic temperature curves of the thermionic emission for these cases are of the form of those in Fig. 31a. Their behaviour is explained as follows. For every temperature of the filament and every pressure of the cesium vapor, the coverage of the cathode with cesium atoms reaches a value which represents an equilibrium between the number of atoms absorbed on the surface of the filament from the cesium atmosphere and the number of atoms evaporated in the same time. The number of cesium atoms absorbed on the tungsten surface per sec per cm^2 is proportional to the number of atoms falling on the surface from the vapor. From the kinetic theory of gases, this number is known to be:

$$\frac{1}{4} n\bar{v} = \frac{p_{Cs}}{\sqrt{2\pi k m_{Cs} T_{Cs}}}$$

where p_{Cs} is the pressure and T_{Cs} the temperature of the cesium vapor, and m_{Cs} the mass of the cesium atom. The number of cesium atoms evaporated per sec per cm^2 is proportional to the coverage θ'_{Cs} of the tungsten by cesium and to the probability of evaporation. The probability increases with the temperature of the filament as $e^{-\lambda/kT}$, where λ is the heat of evaporation of cesium from a tungsten surface. Thus, the condition for equilibrium is of the form:

$$a \frac{p_{Cs}}{\sqrt{T_{Cs}}} = b \theta'_{Cs} e^{-\frac{\lambda}{kT}}$$

The probability of evaporation increases with the temperature of the cathode. As a result the equilibrium covering of the filament will decrease, the pressure of the cesium vapor remaining constant. At low temperatures, the cathode is covered with a relatively thick layer of cesium, ($\phi_{Cs} = 1.87$ ev.), but the emission from this cathode will be very weak because of the low temperature. As the temperature increases, the surplus cesium is evaporated, and a

monomolecular or less than monomolecular layer is established as the optimal covering. At the same time, the work function falls from ϕ_{Cs} to ϕ min (Fig. 51b). The decrease of the work function with the increase of the temperature leads to a rapid increase of the electron current. Further increases in the temperature of the tungsten and the resulting decreases in θ'_{Cs} increase the work function, which approaches the work function of pure tungsten as $\theta'_{Cs} \to 0$. At first, the temperatures at which this begins to increase have a stronger influence on the emission than the slight increase in ϕ near the minimum. The current still continues to increase, although at a slower rate than at lower temperatures. Soon however, the increase in the work function caused by the decreasing covering has a stronger effect, and the current begins to fall, despite the further increase in T. Finally, for $\theta_{CS} \approx 0$, the work function is almost constant and nearly equal to the work function for pure tungsten so that the emission current again begins to grow according to equation (6.8) for pure tungsten. The optimum coverage and maximum current of oxidized tungsten occur at a higher cathode temperature. The reason for this is that the work of evaporation of cesium atoms from oxidized tungsten is larger than from pure tungsten. Consequently, since the number of atoms falling on the filament from the vapor is unchanged, a given equilibrium covering for this number of atoms is established only at a higher temperature, when the probability of evaporation attains the value it had for pure tungsten at a lower temperature (See the dotted line in Fig. 51a.)

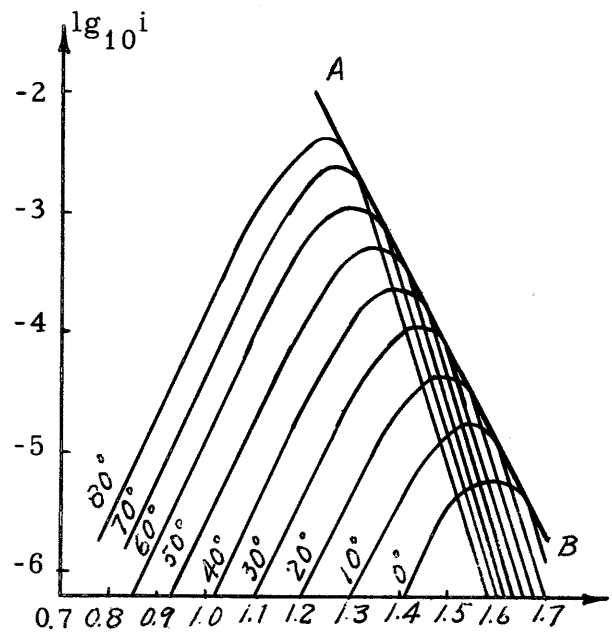

Fig. 52

If the density of the cesium vapor is raised , increasing the stream of atoms falling on the surface of the cathode, the tungsten temperature at which a given covering of cesium atoms is established will be higher. As a result, the optimal coverage and the maximum in the emission curve shift towards higher filament temperatures. Simultaneously, the magnitude of the maximum current grows, corresponding to the increase of the cathode temperature. For a given filament temperature T, as p_{Cs}, and consequently T_{Cs}, grow, the equilibrium coverage θ_{Cs} increases. For $\theta < \theta_{opt}$, the increase of the coverage results in the decrease of the work function. Therefore, the curve i(T) will extend higher for larger T_{Cs} than for smaller T_{Cs}. For $\theta > \theta_{opt}$ increases of the coverage are accompanied by increases of the work functions. Therefore, the maximum height of the curve i(T) decreases with increasing T_{Cs} for such coverings. In Fig. 52, the family of curves $\lg i = f(\frac{1}{T})$ is described for a number of different cesium vapor pressures determined by different T_{Cs}.

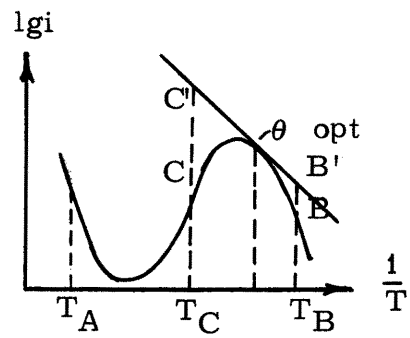

Fig. 53

We examine the methods of determining the thermionic constants of tungsten covered with cesium. Let a filament be rapidly cooled from a given, sufficiently high temperature T_A (Fig. 53) to a temperature T_B, corresponding to an equilibrium covering $\theta' > \theta_{opt}$. The covering will increase, approaching the equilibrium θ' corresponding $T = T_B$. As a result of absorption of cesium, the work function will decrease with time, reach a minimum for $\theta = \theta_{opt}$, and then increase again (Ref. 35). Simultaneously,

the electron current will grow with time, reaching a maximum (the point B') when the coverage is at its optimum value, and then decreases to a constant value (the point B) corresponding to an equilibrium covering $\theta' > \theta_{opt}$. If after this, the temperature is quickly raised to T_C, for which the equilibrium covering $\theta' < \theta_{opt}$ cesium will begin to evaporate, the current will grow with time, reaching a maximum value (the point C') when $\theta' = \theta_{opt}$ and then decreases to a constant equilibrium value (the point C). The points C' and B' represent the emission at temperatures T_C and T_B for the identical covering $\theta = \theta_{opt}$. By drawing Richardson's line through them, we can find ϕ_{min} and A_{opt}. It is evident that this line must touch the equilibrium characteristic temperature curve $\lg \frac{i}{T^2} = f(\frac{1}{T})$ at some point, for in the interval $T_C - T_B$, there is a point on the characteristic curve corresponding to the emission for the optimum covering, which is attained at some intermediate temperature.

The values of ϕ_{min} and A_{opt} can be determined in another way, by drawing a common tangent to the family of characteristic temperature curves of the electron current for different cesium vapor pressures (Ref. 41). Indeed, on each curve, there is a point representing the emission for the equilibrium optimum covering $\theta' = \theta_{opt}$. As shown above, each of these points occurs for a different filament temperature T. Therefore, the family of curves $\lg \frac{i}{T^2} = f(\frac{1}{T})$ must have a common tangent, which is identical with Richardson's line for $\theta' = \theta_{opt}$.

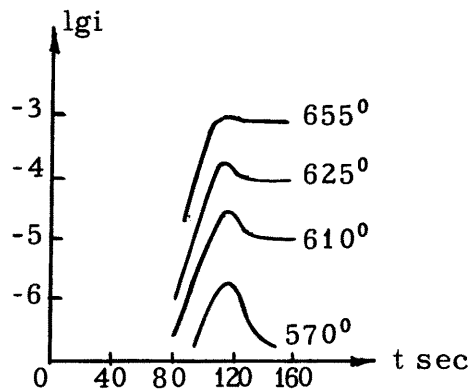

Fig. 54

Finally, a third method (Ref. 42) of determining ϕ_{min} and A_{opt} reduces to the following. A filament is cleaned from cesium by annealing at sufficiently high temperatures and is rapidly cooled to a temperature, at which the equilibrium θ' is larger than θ. This will cause θ' to increase with time, approaching an equilibrium value. At the same time, the electron current will also grow, passing through a maximum at $\theta' = \theta_{opt}$, and then decrease to an equilibrium value (Fig. 54).

By doing this experiment for a number of filament temperatures, we can construct Richardson's line through the points corresponding to the current maximums and thus find ϕ_{min} and A_{opt}. In these experiments, it was found that the time τ, in which the current reaches its maximum for a given pressure of the cesium vapor, does not depend on the temperature of the tungsten filament. This means that in the temperature range defined by $\theta' < \theta_{opt}$ all the cesium atoms falling on the surface of the filament are absorbed on it and practically none are evaporated in the period τ.

If the pressure and temperature of the cesium vapor and the time τ, in which θ_{opt} is reached, are known, the equations of the kinetic theory of gases yield the number of atoms n_{opt} absorbed in a time τ per cm^2 and corresponding to $\theta = \theta_{opt}$. By comparing this number with n_1, the number of cesium atoms in a monomolecular layer, one can find the true θ_{opt}. It was found that $\theta_{opt} = 0.67$.

The values of ϕ_{min} and A_{opt}, measured by different investigators using different methods, disagree conspicuously with one another. For tungsten covered with cesium:

$$\phi_{min} \sim 1,5 \; ; \quad A_{opt} \sim 3 \; a/cm^2 \cdot degree^2$$

For oxidized tungsten covered with cesium, there are two extremely different groups of results:

I) $A \approx 10^{-4}$ $a/cm^2 \cdot degree^2$; $\phi_{min} \sim 0,6$ v;

II) $A \approx 10^{7}$ $a/cm^2 \cdot degree^2$; $\phi_{min} \sim 2$v.

Effects analogous to the ones described above occur in rubidium and potassium vapors.

BIBLIOGRAPHY

Survey Articles

1. Bruining, H; Secondary Electron Emission, Pergammon Press (1954).

2. Dekker, A.J., Secondary Electron Emission, Solid State Physics, Academic Press (1958).

3. McKay, K.G., Secondary Electron Emission, Advances in Electronics, Academic Press (1948).

4. Hackenberg, O. and Brauer, W., Secondary Electron Emission from Solids; Advances in Electronics and Electron Physics, Academic Press (1959).

5. Dobretsov, L.N., Electron and Ion Emission, NASA Technical Translation, NASA TT F-73 (1963).

Independent Articles

6. Vyatskin, A. and Pilyankevich, A, Some Energy Characteristics of Electron Passage Through a Solid; Sov. Phy. - Sol. St. 5 1662 (1964).

7. Nakkodkin, N.G. and Melnik, P.V., Energy Distribution of Secondary Electrons and Photo Electrons. Excited by Soft X-Rays; Sov. Phys. - Sol. St. 5 1779 (1964).

8. Veksler, V.I., Investigation of Secondary Emission of Excited CS Atoms on the Bombardment of Mo with Positive Cs ions; Sov. Phys. - Sol. St. 5 410 2003 (1964).

9. Sawer, J.A., Calculation of High Energy Secondary Electron Emission; J. Appl. Phy. 35 1706 (1964)

10. Mastovskii, A.A., et al; Photo Electric and Secondary Emission Properties of Complex Photo Cathodes . Sov. Phy. - Sol. St. 5 2436 (1964).

11. Karicheva, I.R. and Barzdo, B.F., Deceleration and Inelastic Scattering of Electrons in Thin and Unsupported Films of Cu.; Sov. Phys.- Sol. St. 5 1870 (1964).

12. Bosch, S. and Kuskevics, G.; Kinetic Secondary Electron Ejection from Tungsten by Cs ions ; Phy. Rev. Vol. 134A no. 5A 1356 (1964).

13. Brophy, J.J.; Fluctuations in Hot Tungsten Filaments, J. Appl. Phys. 34 1890 (1963).

14. Schultz, A.A. and Pomerantz, M.A.; Secondary Electron Emission Produced by Relativistic Primary Electrons, Phys. Rev., 130 2135 (1963).

15. Shoshez, R.W. and Dekker, A.J.; Fine Structure of Secondary Emission as Angle of Incidence of the Primary Beam on Titanium Crystals. Phys. Rev. 121 1362(1961).

16. Kanter, H.; Energy Dissipation and Secondary Electron Emission in Solids, Phys. Rev. 121 677 (1961).

17. Kanter, H.; Contribution of Backscattered Electrons to Secondary Electron Formation; Phy. Rev. 121 681 (1961).

18. Dekker, A.J.; Variation of Secondary Electron Emission of Single Crystal with Angle of Incidence; Phys. Rev. Letters 4 55 (1960).

19. Whitten, N.R.; Primary Electron, Bull. Am. Phys. Soc. 5 347(A) (1960).

20. Sheppard, W.G.; Study of Elect. and Phys. Charact. of Secondary Emitting Surfaces. WADC TR. 59-473, PB61471 AF. Contract No. AF 33(616) 3325 (1959) (unavailable).

21. Hare, M.D.; The Effects of Initial Electron Velocities and Space Charge in Secondary Emission; Stanford Elect. Labs. Contract AF 33(616) 6207,

22. Waters, P.M., Kinetic Ejection of Electrons from Tungsten by Cesium Ions; Phys. Rev. 109 1466 (1958).

23. Barrington, R.E. and Anderson, S.M.; The Probability of Multiple Emissions of Secondary Electrons, Proc. Phys. Soc. 72 717 (1958).

24. Lye, R.G. and Dekker, A.J.; Theory of Secondary Emission; Phys. Rev. 107 977 (1957).

25. Van Der Ziel, A.; Estimate of the Time Constant of Secondary Emission; J. Appl. Phys. 28 1216 (1957).

26. Whitten, N.R. and Laponsky, A.B.;
Phys. Rev. 107 1521 (1957).

27. Halliday, J.E. and Sternglass, E.J.;
J. Appl. Phys. 28 1189 (1957).

28. Kollath, R.; Sekundarelektronen - Emission Lester Korper Handbuch d. Phys. 21 232 (1956).

29. Harrower, G. A.; Auger Electron Emission in the Energy Spectra of Secondary Electrons by M_o and W; Phys. Rev. 102 340 (1956).

30. Harrower, G. A.; Energy Spectra of Secondary Electrons from M_o and W for Low Primary Energies; Phys. Rev. 104 52 (1956).

31. Harrower, G. A.; Energy Spectra of Secondary Electrons from M_o and W; Phys. Rev. 99, 1650 CA (1955).

32. Shulman, A. R. and Dementyev, B. P.
J. Tech. Phys. (USSR) 25 2256 (1955).

33. Dekker, A. J.; Energy and Temperature Dependence of the Secondary Emission of MGO; Phys. Rev. 94 1179 (1954).

34. Wolff, P. A.; Theory of Electron Cascade in Metals; Phys. Rev. 93 981 (1954).

35. Barut, A. O.; The Mechanism of Secondary Electron Emission, Phys. Rev. 93 981 (1954).

36. Sternglass, E. J.; Energy Distribution of Secondary Electrons from Solids; Phys. Rev. 93 929A (1954).

37. Sternglass, E. J.; Temperature Dependence of Secondary Electron Emission from Tantalum, Platinum and Graphite; Phys. Rev. 90 380(A) (1953).

38. Van Der Ziel, A.; A Modified Theory of Production of Secondary Electrons in Solids; Phys. Rev. 92 35(1953).

39. Lander, J. J.; Auger Peaks in the Energy Spectra of Secondary Electrons from Various Metals; Phys. Rev. 91 1382 (1953).

40. Marshall, J. F.; The Theory of Secondary Emission; Phys. Rev. 88 416 (1952).

41. Dekker, A. J. and Van Der Ziel, A.; Theory of Production of Secondary Electrons in Solids; Phys. Rev. 86 755 (1952).

42. Jonker, J. L. H.; The Angular Distribution of Secondary Electrons from Nickel; Phys. Rev. 85 390A (1952).

43. Law, R. R.; Decay Time of Secondary Electron Emission; Phys. Rev. 85 291A (1952).

44. Dekker, A.J. and Van Der Ziel;
Phys. Rev. 85 391A (1952).

45. Johnson, J.B. and McKay, K.G.; Secondary Electron Emission from Germanium.

46. Jacobs, H. and Freely, J; The Mechanism of Field Dependent Secondary Emission; Phys. Rev. 88 492 (1952).

47. Jacobs, H. and Freely, J.; Field Dependent Secondary Emission. Phys. Rev. 86 585(A) (1952).

48. Brophy, J.J.; A Comparison of Theories of Secondary Emission; Phys. Rev. 82 757(L) (1951).

49. Jacobs.; Field Dependent Secondary Emission; Phys. Rev. 84 877 (1951).

50. Jonker, J.L.H.; The Angular Distribution of Secondary Electrons of N_i; Philips Res. Repts. 6 372 (1951).

51. Hine, G.J.; Backscattering of Secondary Electrons; Phys. Rev. 83 217(A) (1951).

52. Baroody, E.M.; A Theory of Secondary Emission from Metal; Phys. Rev. 78 780 (1950).

53. Brophy, J.J.; Secondary Emission of Electrons at Oblique Angles of Incidence; Phys. Rev. 78 643(A) (1950).

54. Sternglass, E.J.; Secondary Emission and Atomic Shell Structure; Phys. Rev. 80 925(L) (1950).

55. Sternglass, E.J.; An Interpretation of Secondary Emission Data for Homogeneous Solids; Phys. Rev. 76 189(A) (1949).

56. Trump, J.G. and Van de Graff, R.J.; Secondary Emission of High Energy Electrons; Phys. Rev. 75 44 (1949).

57. Johnson, J.B.; Secondary Electron Emission from Targets of Barium Strontium Oxide. Phys. Rev. 73 1058 (1948).

58. Kennedy, W.R. and Copeland, P.L.; The Temperature Coefficient of Secondary Emission and the Work Function of Molybdenum Targets Coated with Beryllium and Treated with HCℓ; Phys. Rev. 63 61(A) (1943).

59. McKay, K.G.; Primary Electrons; Phys. Rev. 61 708 (1942).

60. Woolridge, D. E.; Temperature Effects on the Secondary Emission from Pure Metals, Phys. Rev. 57 1080(A) (1940).

61. Kadyschevitsch, A. E.; Theory of Secondary Electron Emission from Metals; J. Phys. USSR 2 115 (1940).

62. Woolridge, D. E.; Theory of Secondary Emission; Phys. Rev. 56 562 (1939).

63. Coomes, E. A.
Phys. Rev. 55 519 (1939).

64. Woolridge, D. E.; The Secondary Emission from Evaporated Nickel and Cobalt; Phys. Rev. 56 562, 1062(L) (1939).

65. Copeland, P. L.; Secondary Emission of Electrons from N_a Films Contaminated by Gas; Phys. Rev. 55 1270(L) (1939).

66. Copeland, P. L.; Secondary Emission of Electrons from Sodium Films on Tantalum; Phys. Rev. 53 328(A) (1938).

67. Coomes, E. A.; Secondary Electron Emission from Thorium Coated Tungsten; Phys. Rev. 53 936(A) (1938).

68. Bruining, A. and de Boer, J. H.;
Physics 5 17, 901, 913 (1938).

69. Bruining, A. and de Boer, J. H.; Secondary Electron Emission; Physics 1 (1938).

70. Rudberg, E. and Slater, J. C.; Theory of Inelastic Scattering from Solids; Phys. Rev. 50 150 (1936).

71. Haworth, L. J.; The Energy Distribution of Electrons from Columbium; Phys. Rev. 50 216 (1936).

72. Haworth, L. J.; The Energy Distribution of Secondary Electrons from Molybdenum; Phys. Rev. 48 88 (1935).

73. Frohlich, H.;
Ann. d Physik 5 13 (1929).

74. Bethe, H.
Ann. d Physik 5, 5, 325 ((1930).

75. Young, J.R.; Penetration of Electrons and Ions in Aluminum; J. Appl. Phys. 27 1 (1956).

76. Young, J.R.; Penetration of Electrons in Aluminum Oxide Films; Phys. Rev. 103 292 (1956).

77. Lane, R.O. and Zaffarano, D.I.; Transmission of 0-40 kev Electrons by Thin Films with Application to Beta-Ray Spectroscopy; Phys. Rev. 94 960 (1954).

78. Faris, J.; Thesis (1950). (unpublished).

SECONDARY ELECTRON EMISSION

by

R. E. Bunney

ABSTRACT

The report reviews the available literature on secondary electron emission from metallic surfaces. The basic theories of secondary electron emission are considered in relation to one another. Special emphasis was placed on the quantum theories.